Finanziato dall'Unione europea NextGenerationEU | Ministero dell'Università e della Ricerca | Italiadomani PIANO NAZIONALE DI RIPRESA E RESILIENZA

multi-Risk sciEnce for resilienT commUnities undeR a changiNgclimate

Codice progetto MUR: **PE00000005** – CUP Lead Partner: F83C22001180002

Deliverable title: Assessment of remediation methodologies performance

Deliverable ID: DV 4.5.3

Due date: 31/03/2026

Submission date: 08/03/2026

AUTHORS

Daniele Di Trapani, Marco Capodici, Federica De Marines, Manuela Russo Tiesi, Giovanni Vinti, Gaspare Viviani (UNIPA); Carlo Punta, Laura Riva (POLIMI); Claudia Caltagirone, Giacomo Picci, Andrea Porcheddu, Angelo Frongia, Annalisa Vacca, Michele Mascia (UNICA); Claudio Lubello, Tommaso Lotti, Benedetta Pagliaccia (UNIFI); Armando Zarrelli, Fulvio De Paola, Gabriella Pinto, Marco Trifuoggi, Mauro Iuliano, Giancarlo Germano, Gaetano De Tommaso (UNINA); Gaetano Di Bella, Riccardo Campo, Enrico Licitra (UKE); S. A. Frisario, F. Villani (Eni Rewind), A. Conte (Eni); A. De Folly D'Auris (Eni), S. Ferro (INSTM), M. Vocciante (INSTM)

1. Technical references

Project Acronym	RETURN
Project Title	multi-Risk sciEnce for resilienT commUnities undeR a changiNg climate
Project Coordinator	Domenico Calcaterra UNIVERSITA DEGLI STUDI DI NAPOLI FEDERICO II domcalca@unina.it
Project Duration	December 2022 – November 2025 (36 months)

Deliverable No.	DV4.5.3
Dissemination level*	PP
Work Package	WP5 - WP Title: Prevention and remediation
Task	T4.5.1 - Task Title: Sensing and/or removal of contaminants with physical-chemical and electrochemical processes
Lead beneficiary	UNIPA & UNICA
Contributing beneficiary/ies	UNIPA, PoliMI, UNICA, UNIFI, UNINA, UKE, EniRewind

* PU = Public

PP = Restricted to other programme participants (including the Commission Services)

RE = Restricted to a group specified by the consortium (including the Commission Services)

CO = Confidential, only for members of the consortium (including the Commission Services)

Document history

Version	Date	Lead contributor	Description
0.1	21-02-2026	UNIPA, PoliMI, UNICA, UNIFI UNINA, UK and EniRewind	Individual contributions to the First draft
0.2	08-03-2026	Daniele Di Trapani (UNIPA) and Carlo Punta (PoliMI) – Task Coordinators	First draft
0.3	01/03/2026		Edits for approval
1.0			Final version

2. ABSTRACT

The present document reports the details of the results7products of the activities carried out until month 36 in the framework of Spoke VS4 ("Environmental Degradation"), Work Package 4.5 ("Prevention and Remediation"), T4.5.1("T 4.5.1 - Sensing and/or removal of heavy metals, organic pollutants and pathogens in water, soil and soil- water systems with physical-chemical, electrochemical, bio-electrochemical and photoelectrochemical processes) and addresses the growing environmental concern posed by organic and inorganic contaminants in the environmental matrices, including soil, sediments and water systems.
In compliance with the executive working plan of the whole project, T4.5.1 which main aim is to explore innovative procedures for contaminant tracking and remediation in the environmental matrices, including the assessment of microplastics removal in WWTP, adsorption kinetics and thermodynamics of different compound classes, application of innovative, cost-effective and user-friendly supramolecular materials, optical chemosensors, nanoparticles and inorganic/hybrid porous materials, electro-kinetic remediation technology and batch washing tests. While the assessment of nanoparticle tracking and microplastic removal have been the object of other documents (namely, DV 4.5.1 "Procedures for nanoparticle Tracking" and DV4.5.2 "Fate and removal of microplastics in wastewater treatment plants"), the present document deals with the assessment of innovative technologies for contaminated matrices remediation as well as contaminant detection in water and water-soil systems.
Target contaminants include both organic (e.g hydrocarbons) and inorganic (e.g. heavy metals) pollutants.
Tasl 4.5.1 can be seen as complementary to Task 4.5.2; indeed, while the activities of Task 4.5.1 mainly focused on physical-chemical processes for remediation of contaminated matrices, Task 4.5.2 was more devoted to the development of innovative remediation techniques based on biological processes. Both tasks, therefore, pose the basis to increase knowledge on innovative remediation processes, of both physical-chemical and biological nature.

In this light, the results obtained should be regarded to contribute jointly to the objectives and outputs of the RETURN project indicated in the following layout.
In particular, the investigation activities of T4.5.1 delivered as the final output of the project are grouped based on three main thematic areas, which were aimed at achieving the objectives of Spoke VS4 (indicated in parentheses):

1. Methods and protocols for the identification and quantification of environmental contaminants [O1, O3]
2. Development, application and validation of methods for advanced environmental monitoring [O1, O2]
3. Development, application and validation of processes for contaminant degradation [O4, O5]

Multiple activities were implemented during the project within the thematic areas outlined above, involving multiple competences, adopting various perspectives and approaches and yielding numerous results, as summarised below.

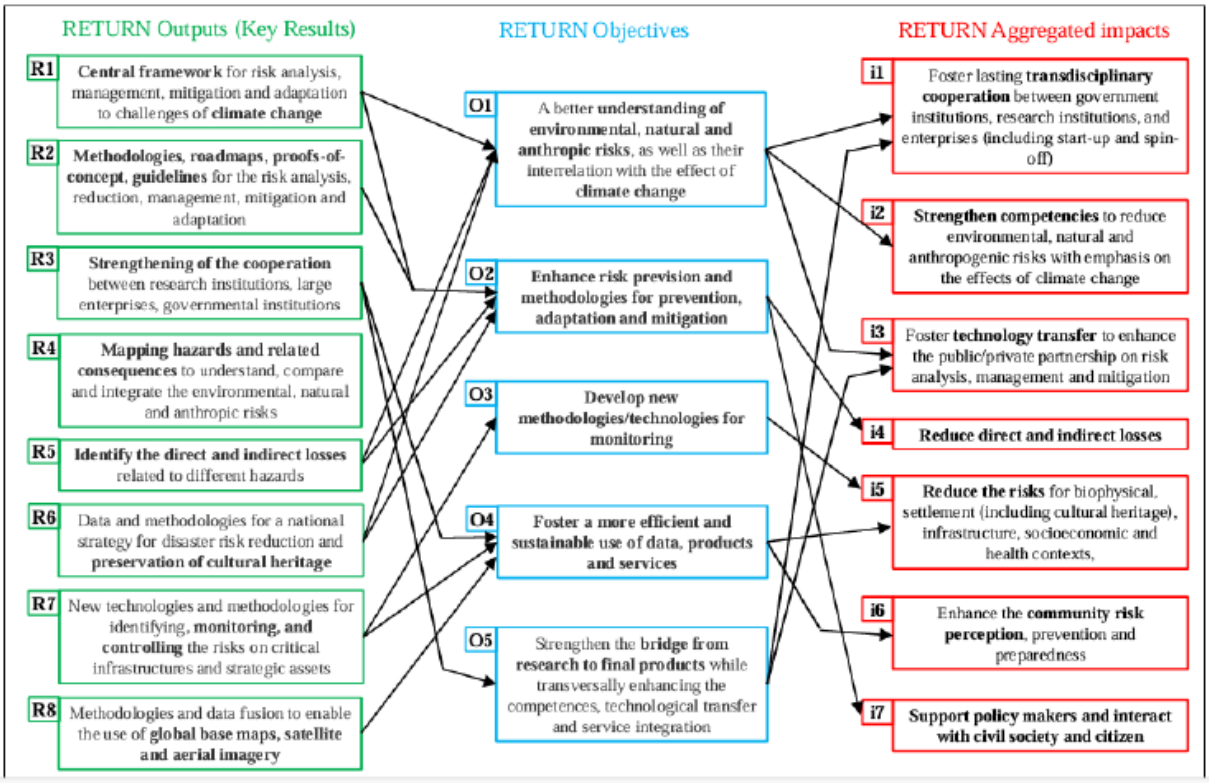

1. Development of methods and protocols for the identification and quantification of environmental contaminants:
   i. supramolecular materials, non-canonic aminoacids and natural biopolymers for sensing and remediation in environmental samples (UNICA) [R2]
   ii. performance evaluation of cellulose-based nanostructured materials for heavy metal removal and resource recovery (PoliMI) [R2]

2. Data analysis and modelling of transport, diffusion, transformation and degradation of contaminants:
   i. remediation of hydrocarbon contaminated soils by means of anionic and non-ionic surfactants: remediation efficiency and residual phytotoxicity (UNIPA), (UKE) [R2]
   ii. role of single and mixed surfactants for hydrocarbons removal from real marine sediments: removal efficiency and residual phytotoxicity after sediment washing treatment (UNIPA), (UKE) [R2]
   iii. oxidation of petroleum hydrocarbons in soil using potassium ferrate as new oxidizing agent: process optimization and benchmarking (UNIPA), (UKE) [R2]
   iv. petroleum hydrocarbons oxidation in marine sediments: first trials with potassium ferrate as a new chemical and comparison with potassium permanganate (UNIPA), (UKE) [R2]
   v. silver-decorated cellulose nanofibers for enhanced cadmium adsorption in water (PoliMI) [R2]
   vi. cellulose nanosponges for phosphorus recovery and leachate decontamination (PoliMI) [R2]

vii. remediation of polluted soils and wastewater using bioelectrochemical systems and the removal of microplastics with electrochemical and photoelectrochemical techniques (UNICA) [R2]
viii. supramolecular materials, non-canonic aminoacids and natural biopolymers for sensing and remediation in environmental samples (UNICA) [R2]
ix. development of novel adsorbent media based on extracellular polymeric substances (eps) extracted from wastewater treatment sludge for the removal of heavy metals (UNIFI) [R2]
x. removal of rare earth elements and organophosphorus pesticides from aqueous phases by adsorption onto natural and synthetic phases (UNINA) [R2]
xi. electro-Kinetic Remediation Technology for Soil contaminated by Heavy Metals (Eni Rewind) [R2]

Efforts were made to effectively combine the diverse expertise of participants in T4.5.1 — including chemistry, fluid mechanics, and civil and environmental engineering — to achieve the primary goal of WP4.5: the development of advanced methodologies and tools for comprehensive observation, modelling, and assessment of environmental degradation.

3. Table of contents

List of Tables

List of Figures

4. Assessment of remediation methodologies performance

4.1 Assessment of contaminated soils and sediments reclamation by means of physical-chemical treatments (UNIPA and UKE)

(Contributors: Daniele Di Trapani, Marco Capodici, Federica De Marines, Manuela Russo Tiesi, Giovanni Vinti, Gaspare Viviani for UNIPA; Gaetano Di Bella, Riccardo Campo and Enrico Licitra for UKE)

4.1.1 Remediation of hydrocarbon contaminated soils by means of anionic and non-ionic surfactants: remediation efficiency and residual phytotoxicity

4.1.1.1 Introduction

Soil and groundwater contamination caused by organic pollutants, particularly hydrocarbons, has become a global concern in recent decades, mainly due to the growing consumption of petroleum-derived products (Babaei and Copty, 2019; Huo et al., 2020). In addition, numerous human industrial activities — such as fossil fuel combustion and the production of coke and asphalt — lead to the release of Polycyclic Aromatic Hydrocarbons (PAHs) (Ailijiang et al., 2022).

Hydrocarbons pose significant risks because of their toxicity, chemical diversity, and persistence in soil environments, potentially threatening both human health and ecosystems (Mao et al., 2015). Once released into soil or water, PAHs tend to strongly associate with organic matter, which makes their removal particularly challenging. These compounds are highly persistent and may exhibit toxic, mutagenic, and carcinogenic effects.

Regarding petroleum-derived contaminants, they are typically characterized by high oil–water partition coefficients and low water solubility. As a result, they are likely to adsorb onto soil particles and may form non-aqueous phase liquids (NAPLs) within aquifers (Rogers and Logan, 2000). These trapped non-aqueous phases can gradually dissolve into groundwater, acting as long-term sources of contamination (Zhong et al., 2016).

Given the considerable risks to human health and ecological stability, remediation of hydrocarbon-contaminated soils is essential. Effective remediation requires the development of a dynamic conceptual site model, along with the assessment and selection of appropriate treatment technologies. However, remediation remains particularly challenging due to the strong sorption of hydrocarbons to soil matrices and their slow desorption rates (Cheng et al., 2017).

Furthermore, soil heterogeneity and composition significantly influence remediation effectiveness. Parameters such as particle size distribution (sand, silt, and clay) and organic matter content strongly affect the behavior of Total Petroleum Hydrocarbons (TPHs). For example, clay-rich soils with high organic matter content, characterized by hydrophobic properties and large surface areas, can reduce hydrocarbon bioavailability for microbial degradation and limit contaminant accessibility to treatment technologies. Additionally, since TPHs consist of complex mixtures of different compounds, each hydrocarbon exhibits distinct properties — including volatility, solubility, and degradability — which determine its environmental fate and transport behavior.

Among the different remediation technologies proposed in the recent years, the use of surfactants in soil washing/soil flushing applications (event at full scale) raised as one of the most promising (Karthick et al., 2019; Huang et al., 2021; Liu et al., 2021; Kumar et al., 2022). Surfactants are constituted by hydrophilic heads and hydrophobic tails. The hydrophobic groups bond with the organic compound while the hydrophilic group with the polar solvent, thus promoting its extraction from soil. Therefore, when surfactant-enhanced soil washing is performed, the organic pollutant can be desorbed from the soil surface and moved away. Surfactants can have either synthetic or natural origin and, depending on their hydrophilic head, they are classified as anionic, cationic, non-ionic or zwitterionic (Kumar et al., 2021). Nevertheless, the application of surfactants in polluted sites can be challenging, due to the potential environmental and health implications. Indeed, despite some biodegrade, they might be harmful to the environment, aquatic organisms and humans because of their bioaccumulation and persistence (Villarreal-Reyes et al., 2022). Moreover, surfactants can induce secondary pollution in soil due to the residual surfactant in soil after treatment (Zhong et al., 2016). The latter side effect should be avoided, especially when agronomic use of the treated soil is expected or when surfactant remediation should be coupled to phytoremediation (Sun et al., 2013). Indeed, despite anionic surfactants like Sodium Dodecyl Sulfate (SDS) and Sodium Dodecylbenzene-Sulfonate (SDBS) have been successfully used in subsurface remediation applications (Karthick et al., 2019; Sakhaei and Riazi, 2022), they might negatively impact soil features after treatment promoting secondary pollution, or adversely impacting the plants health by enhancing inhibitory effects on the living organisms in subsurface system also entailing phytotoxicity (Huo et al., 2020; Bolan et al., 2023).

Based on the above considerations, investigate the feasibility of surfactants application for the remediation of a quartz sand and real sandy soils, artificially contaminated with diesel-fuel. The role of surfactant concentration and flushing flow rate was assessed in terms of hydrocarbon solubilization effectiveness. Two different surfactants were tested, one anionic (SDBS) and one non-ionic (Tween 80), by simulating a soil flushing process carried out on a laboratory scale apparatus. Hydrocarbon removal from soil at different surfactant concentrations and flushing flow rates was assessed. Moreover, the suitability of treated soil for crop cultivation was elucidated by determining the germination index (GI) on Lepidium sativum seeds and by using remediated soil for Vicia Faba L. (faba bean) cultivation. The novelty of the present study is the elucidation of the relationship between surfactant concentration, flushing flow rate and flushing duration in the hydrocarbon extraction from a contaminated soil, providing useful operational insights in view of full-scale applications.

4.1.1.2 Materials and Methodologies

The experimental activities were divided into two different Experimental periods, namely Period 1 and Period 2, respectively, as better described below.

Period 1

In Period 1, the experimental activity was characterized by column batch tests aimed at simulating a soil flushing remediation process on a sandy soil artificially contaminated by diesel fuel. In particular, the hydrocarbon removal efficiency was evaluated in the case of (i) flushing tests with water and (ii) flushing tests with a solution of water and surfactant. In more detail, two different surfactants were tested, one anionic (SDBS) and one non-ionic (Tween 80). The experiments were divided into 3 phases (Phase1, Phase 2 and Phase 3, respectively). During Phase 1 short-term flushing tests were carried out with warm water only and represented the blank control. The flushing tests were carried out at different flow rates: 2 mL min^{-1}, 4 mL min^{-1}, 6 mL $min^{-1}$and 8 mL min^{-1}. In the Phase 2, the effect of both surfactants (SDBS and Tween 80) in the flushing solution was investigated in terms of surfactant concentration and flow rate, to assess the optimal condition for the remediation of the contaminated soil. For both surfactants, the behavior of four solutions at

different concentrations was evaluated: 0.1%, 0.2%, 0.3% and 0.4% (w/w). In addition, tests at different flow rates (2 mL min^{-1}, 4 mL min^{-1}, 6 mL min^{-1} and 8 mL min^{-1}) were also carried out for all the solutions. During Phase 3, basing on the best results obtained in the previous periods, "long-term" flushing tests were carried out at laboratory scale columns, in order to assess the effect of an "extended" flushing duration. In more details, for the short-term tests carried out in Phase 1 and Phase 2 a fixed volume of 1 liter was flushed, with a duration varying from 2 to 8 h depending on the flow rate with soil samples taken only at the end of each test; in contrast, in Phase 3 each test lasted 48 h and soil samples were taken after 24 h of washing and at the end of the test. Soil sample consisted of quartz sand spiked with a known volume of commercial diesel fuel; in detail, 0.6% (w/w) of diesel was added to 5 kg of sand to obtain an initial TPH concentration close to 6000 mg kg^{-1}_{SS}. Before the start-up of the experimental activity, the sample was manually mixed for several days to allow the volatilization of the most volatile components.

The experimental apparatus consisted of a Pyrex glass column (d = 2.1 cm, h = 13 cm), equipped with a special conical-shaped piece with dimensions of 29/32 mm. For each test, about 80 g of contaminated soil was introduced inside the column. The flushing solution was stored in a storage tank and flushed through the column by means of a peristaltic pump. Figure 1 shows a panoramic view (a) and a schematic layout (b) of the experimental system. In each test the washing solution was flushed through the contaminated soil sample in upward mode, alternatively with warm water and with a surfactant solution at different concentrations.

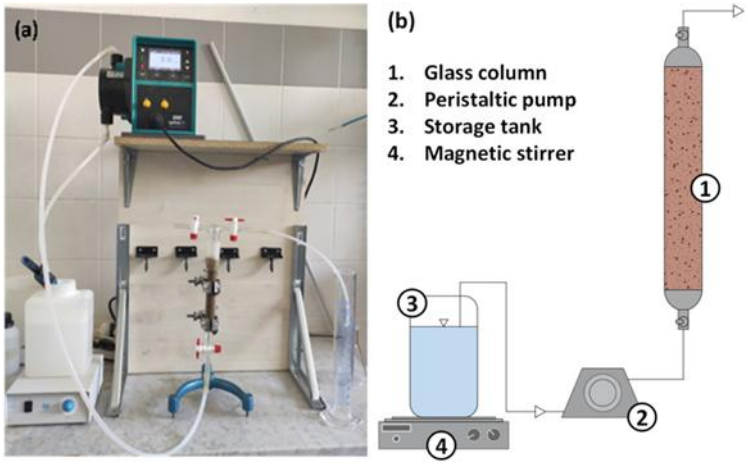

Figure 1: Panoramic view (a) and schematic layout (b) of the experimental apparatus (Di Trapani et al., 2023).

Period 2

In Period 2, the experimental campaign was divided into 2 phases (namely Phase 1 and Phase 2), lasting 2 months each. During Phase 1, an experimental apparatus was set up to simulate a soil flushing process by alternatively flushing water or a surfactant solution at different flow rates and concentrations, identical to that reported in Figure 1. Two different surfactants were tested: one anionic (SDBS) and one nonionic (Tween 80) surfactant. In more detail, a preliminary set of benchscale tests was carried out to assess the best operational conditions, as well as to confirm the results achieved in Period 1, but using a real sandy soil. For each test, three replicates were performed. Based on the results of these preliminary tests, a process scale-up was realized, and soil flushing experiments were carried out on a pilot-scale experimental apparatus. After each test, the soil's phytotoxic properties were determined by calculating the germination index (GI) on Lepidium sativum (garden cress) seeds. In Phase 2, the soil samples treated with the pilot-scale system as well as raw polluted soil samples were used for *Vicia Faba* (faba beans) cultivation in pots. The growth of *Vicia Faba* plants was

monitored and at the end of the growth period, the plants were uprooted and subjected to biometric and chemical analyses.

The soil used during the experimental campaign was collected in an olive orchard in the province of Palermo (Sicily, Italy). The soil was spiked with a known volume of commercial diesel fuel; in detail, 1 % (*w*/w) of diesel was added to 7.5 kg of soil to obtain an initial TPH concentration of 1600 mg kg_{SS}^{-1}. The aim was to obtain a TPH concentration that indicated potential soil contamination, slightly higher than the contamination threshold concentrations for commercial and industrial sites (750 mg kg_{SS}^{-1}) listed in column B, Table 1, part IV, Annex 5, Legislative Decree n. 152/06. After contamination and before the start of the experimental tests, the sample was manually mixed for 15 days to allow the volatilization of the volatile fractions.

In accordance with Period 1, the used surfactants were Sodium Dodecyl Benzensulphonate – SDBS and Polyoxyethylene (20) sorbitan monooleate – Tween 80; both surfactants were purchased from Sigma Aldrich (Milan, Italy). Surfactant solutions were prepared using tap water.

The bench scale apparatus consisted of a Pyrex glass column (d = 2.1 cm, h = 13 cm), with a special conical shaped piece of 29/32 mm at the bottom. For each test, the column was filled with approximately 80 g of diesel-contaminated soil, with an estimated pore volume (PV) value of 8.8 mL. One liter of solution (water, SDBS or Tween 80) was flushed through the column in upward mode by means of a peristaltic pump. Surfactant solutions were stored in a storage tank, maintained at a temperature of about 30°C and continuously mixed through a magnetic stirrer. Bench-scale flushing tests were carried out with water and surfactant solutions at washing flow rate of 6 and 8 mL min^{-1}. Moreover, two different concentrations were used for both surfactants, respectively, 0.05 % and 0.1 % by weight. In terms of CMC, these concentrations correspond approximately to 32 × CMC and 64 × CMC for Tween 80 and to 2.5 × CMC and 5 × CMC for SDBS, respectively. Basing on the best results obtained in the bench-scale tests, a system scale-up was made, and soil flushing experiments were carried out on a pilot-scale experimental apparatus. The pilot-scale apparatus consisted of a Pyrex glass column (d = 4.2 cm, h = 70 cm). For each test, the column was fed with 1.3 kg of contaminated soil, with an estimated PV value of 191.5 mL. The reference parameter used for the scale up of the system was the effective upward velocity through the column. Using this parameter and knowing the dimensions of the pilot-scale column, it was possible to determine the washing flow rates and the volumes of extracting solutions to be flushed through the pilot-scale system. For the washing tests with water and Tween 80, the optimal flow rate was 40 mL min^{-1}; concerning SDBS, the optimal flow rate was 30 mL min^{-1}. However, due to technical issues in the tests carried out at 40 mL min^{-1} with Tween 80, it was decided to decrease the flow rate at 30 mL min^{-1}.

In Phase 2, All soil samples (not contaminated, raw contaminated not treated and treated contaminated soil at pilot scale with water, SDBS, and Tween 80) were air-dried for approximately one week. Then, soil samples were mixed with 15 % by volume of perlite and amended with 5 % by weight of mature compost as organic fertilizer. Subsequently, the soil was used to fill polyethylene pots (h = 12 cm, d = 10 cm) where two seeds of faba bean per pot were sown (Fig. S2). Fava (*Vicia faba L.*) plants were selected for the experimental trial because they are a typical crop cultivated in semi-arid environments, such as Sicily in the same period during which the experiment was carried out (12 December – 13 February). Fava beans are also easy to grow in greenhouses and pots, and it responds well to changes in soil available P. The experiment was carried out in triplicate. After Fava beans were sown, pots were moved to a greenhouse. Pot irrigation was carried out at regular intervals of 3–4 days by adding an amount of tap water to maintain the soil at 50 % of its water holding capacity thus avoiding leaching. At the end of the growing period, plants were carefully extracted from the pots to avoid any damage to the roots. Subsequently, steams and roots were divided and oven-dried at 40°C until a constant weight (ca. after 72 h) and separately weighed. Dried roots and leaves were ground and kept in a plastic bottle at 4°C before further analysis. Also soil samples were collected to be analysed. Further details on the experiments can be found in De Marines et al. (2025).

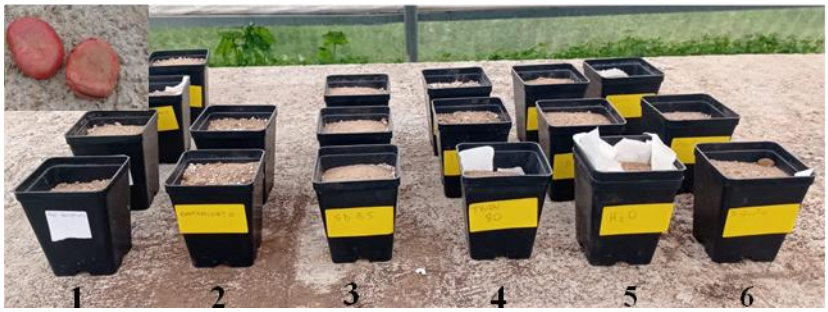

- Test 1: Clean soil
- Test 2: Raw contaminated soil
- Test 3: Washed with SDBS
- Test 4: Washed with Tween 80
- Test 5: Washed with water
- Test 6: Mixed soil

Figure 2: Panoramic view of the pots used for Vicia Faba cultivation, and a particular of the Fava beans seeds sown in the pots.

Analytical methods

Hydrocarbons residual concentration. The measurement of residual hydrocarbon concentration was performed on: (i) soil samples subjected to the flushing treatment, (ii) soil samples after Vicia Faba plant removal, and (iii) plant roots to assess hydrocarbons absorption by the root system. The determination of the residual concentration of TPHs was carried out by following "Procedure for the analysis of hydrocarbons C>12 in contaminated soils - Manuals and Guidelines 75/11" proposed by ISPRA (2011), which refers to ISO 16703 (2004) Specifically, TPHs concentration was determined by headspace gas chromatographic analysis using a gas chromatograph (Agilent 8890 GC System, purposely purchased for the activities of RETURN Project) equipped with a flame ionization detector (FID) and an Agilent 7693A injection system. Helium was used as the carrier gas; the oven temperature was set at 170°C and the injection temperature was 250°C.

Residual soil phytotoxicity. Potential phytotoxicity of soil samples (raw contaminated as well as after flushing) was detected using the germination index (GI) following tests on *Lepidium sativum* (Garden cress) seeds according to APAT (2004) procedure, which refers to USEPA (1988) protocol. Specifically, sample-sand percentages (w/w) of 25 %, 50 %, and 100 % were used, corresponding to a total amount of 10 g of dry mass for each test. In addition, the GI of Lepidium sativum was also evaluated on contaminated and untreated soil samples (positive control). The Petri dishes were incubated in a growth chamber at 27 ◦C for 72 h after being parafilm sealed to ensure closed-system models. At the end of incubation period, the number of germinated seeds was counted, and root length was measured. The Germination Index (GI) was calculated by multiplying the number of germinated seeds (G) and the root length (L). GI results were used to calculate the effect, expressed as percentage (GI %), with respect to the control.

Plant biometric properties and chemical analysis. The biometric properties of plants, such as shoot height, leaf length and width, and number of leaves were monitored every 4 days during the 2 months of cultivation. Moreover, for each plant, fresh and dry weight of both roots and shoots were determined. Dry weight was determined after drying the samples in an oven at 50 ◦C for one week. Starting from the knowledge of the dry weight, the shoot-to-root weight ratio (S/R ratio) was calculated. Total P on steams samples was determined, on mineralized plant samples, by acid (HNO_3 and 30 % H_2O_2) and the wet digestion procedure (Jones Jr. and Case, 1990) and by the Spectroquant® Phosphate test using a spectrophotometer (UVmini-1240, Shimadzu Italia srl, Milan Italy) after the formation of an orange-yellow complex.

4.1.1.3 Results and Discussion

Period 1

Figure 3a summarizes the TPH residual concentrations as well as removal rate obtained in the flushing tests carried out with warm water in Phase 1. From the observation of data reported in Figure 3a it is possible to appreciate the influence of the flushing flow rate, and consequently of the contact time, on the TPH extraction from soil. The contaminant solubilization was favored by the lower flushing flow rates corresponding to higher contact times. Results showed a reduction of removal efficiencies as the flushing flow rate increased, with a maximum removal efficiency of 25% for a flow rate of 2 mL min^{-1}, which decreased to 10% for a flow rate of 8 mL min^{-1}.

Referring to Phase 2, Figure 3b shows the removal rates achieved at different surfactant concentrations and flow rates for the flushing tests carried out with Tween 80. From the observation of data reported in Figure 3b, it is worth noting that the removal rates were generally higher than that observed with water, thus highlighting that Tween 80 provided an added value compared to what achievable with water flushing tests; this result is in accordance with the hydrophobic nature of these contaminants. In more detail, results showed that a significant increase of hydrocarbon removal can be achieved by increasing both the surfactant concentration and the flushing flow rate. This result is in line with previous findings. Indeed, Grasso et al. (2001) indicated that the concentrations of Tween 80 play a pivotal role in the removal of organic pollutants in soil washing processes and that the formation of Tween 80 micelles is essential for the solubilization of the sorbed pollutants. this increasing trend could be related to (i) an increase of pollutant solubility, due to the surfactant dosage at concentrations much higher than the CMC and (ii) an increase of the leaching effect of the contaminant, favored by the increase of the flow rate, corresponding to an increase of the upward fluid velocity, also enhanced by the presence of surfactant, contrarily to what observed in the tests carried out with water. Indeed, the presence of surfactant in the flushed solution reduces the interfacial tension between the hydrophobic compound and water and this behavior is emphasized by surfactant concentration.

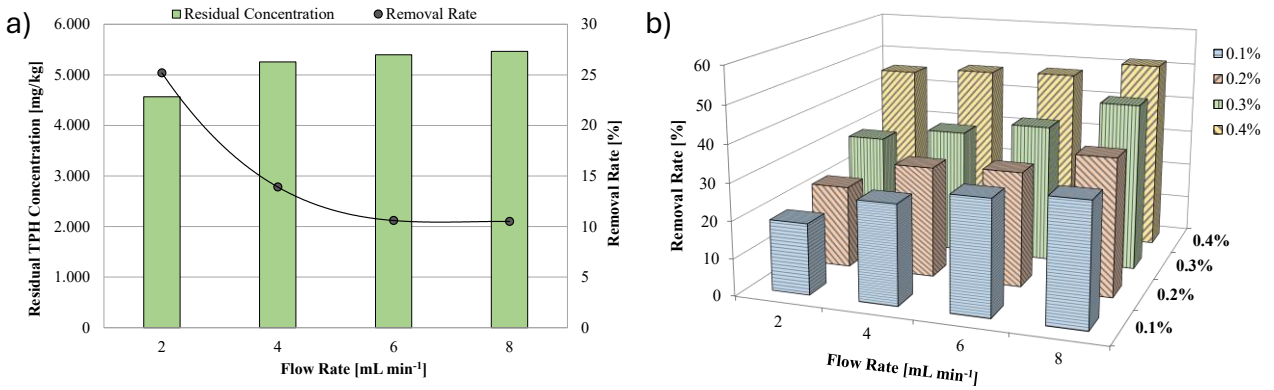

Figure 3: Residual concentration of TPH in soil samples and removal rate after water flushing (a) and TPH removal rate depending on Tween 80 concentration and flow rate (b) (Di Trapani et al., 2023).

data reported in Figure 3b highlighted that the higher efficiency (51.7%) was obtained with a Tween 80 concentration of 0.4% at a flushing flow rate of 8 mL min-1. The solubilization efficiency achieved in the present study was slight lower compared to what reported by Zhao et al. (2016) who achieved 81.5% removal of phenanthrene in 12 h in a soil flushing treatment with 4 g L-1 of Tween 80 solution. Nevertheless, the pollutant concentration used by Zhao and co-workers was slightly lower (100 mg kg^{-1}) compared to that of our study.

As an example, Figure 4 shows the chromatograms obtained from the GC analysis after the extraction and purification procedure for the raw contaminated soil (Figure 4a), the contaminated soil flushed with water at a flow rate of 4 mL min-1 (Fig. 4b) and the contaminated soil flushed with the Tween 80 solutions (0.1%, 0.2%, 0.3% and 0.4%) at a flow rate of 4 mL min^{-1} (Figure 4c-f). It is worth noting that the chromatograms related to the soil samples flushed with the surfactant solutions are more flattened (lowering of the peaks) and with the left side much more reduced than that related to the raw contaminated soil and that flushed with water. In the chromatogram relating to the soil sample flushed with Tween 80 at 0.4% (Fig. 4f), the lack of the most soluble and volatile part (far left chromatogram) is evident, representing the compounds more effectively mobilized and removed after flushing.

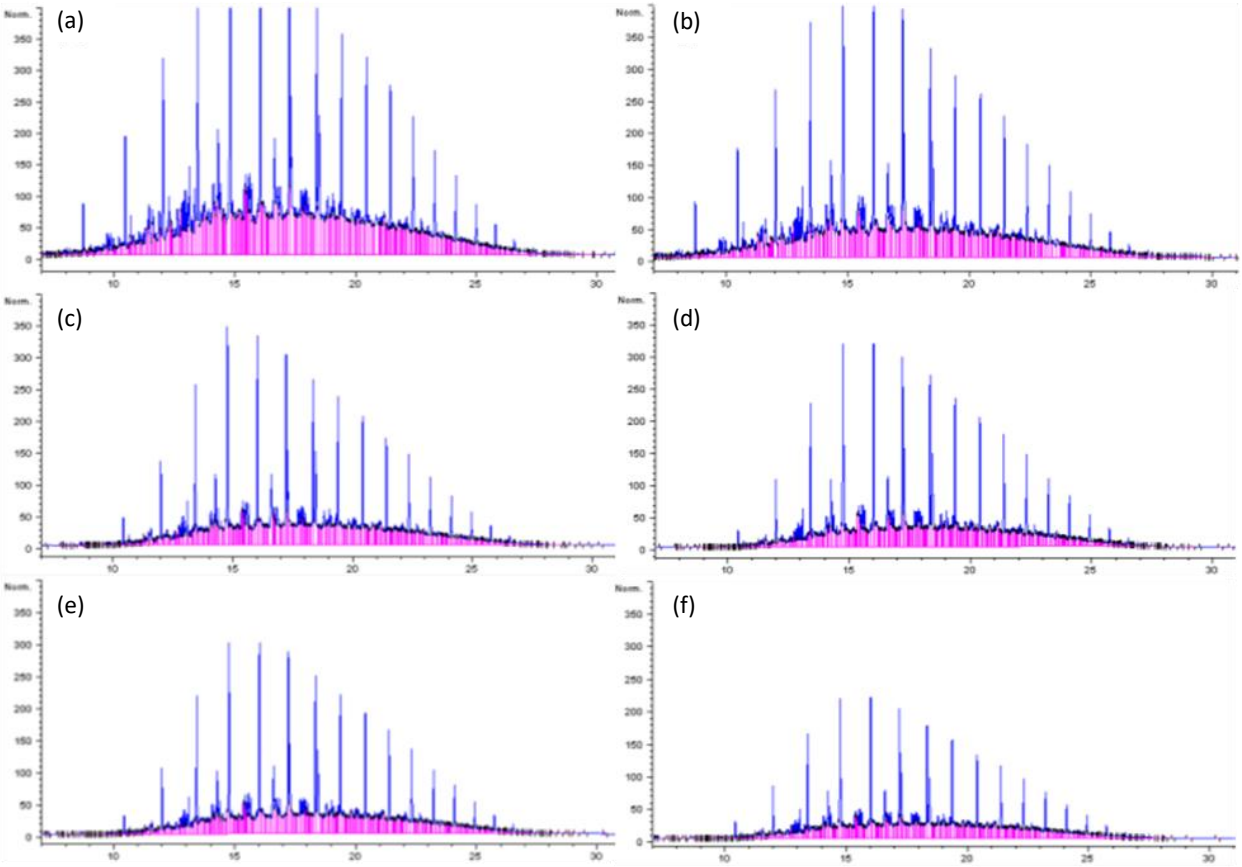

Figure 4: Chromatograms of raw contaminated soil (a), soil washed with only water (b), soil flushed with 0.1% (c), 0.2% (d), 0.3% (e) and 0.4% (f) of Tween 80 at a flow rate of 4 mL min^{-1}.

It is worth noting that the flushing tests with SDBS showed a different trend. In this case, indeed, the SDBS highlighted an opposite behavior in the hydrocarbon extraction efficiency compared to Tween 80, in terms of both flow rate and concentration. Referring to the same surfactant concentration, it was observed a general decrease of the extraction efficiency with the increase of the flow rate (Figure 5). In this case, the observed results suggested that the leaching effect was not predominant compared to the contact time. Morever, by increasing the surfactant concentration from 0.1% to 0.2%, for all four flow rates considered, the removal efficiency also increased significantly. Nevertheless, a further increase of surfactant concentration to 0.3% and then to 0.4% highlighted a slight decrease of the removal efficiency. Therefore, the results of the present study indicated the existence of a threshold value over which the extraction performance is reduced. In detail, the highest efficiency was obtained for a SDBS concentration of 0.2% and with a flushing flow rate of 2 mL min^{-1}; for such conditions, a removal of approximately 45% was achieved.

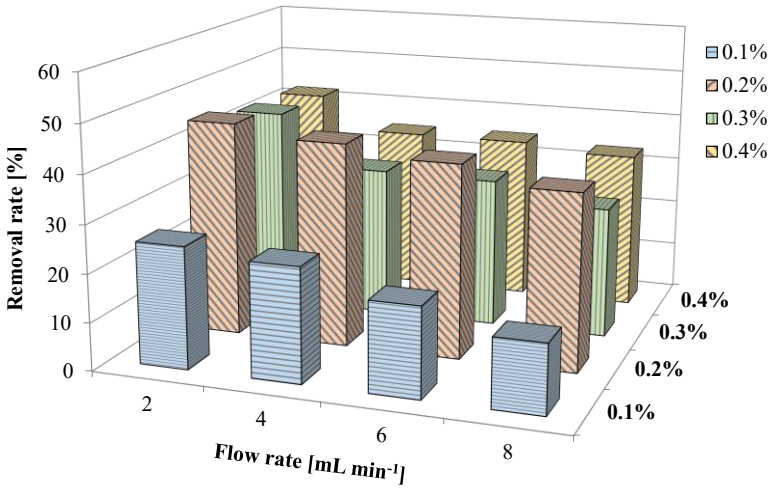

Figure 5: Trend of TPH removal rate depending on SDBS concentration and flow rate (Di Trapani et al., 2023).

This finding is consistent with earlier studies reported in the literature (Medjor et al., 2018), which identified the existence of an optimal surfactant concentration threshold beyond which removal efficiency declines. In principle, operating at concentrations above the CMC is expected to enhance removal performance; however, in certain cases (Zhao et al., 2014), exceeding the CMC has been shown to decrease contaminant solubilization. This reduction is attributed to an excessive number of micelles, which may limit the overall solubilization capacity.

As an example, Figure 6 shows the chromatograms obtained from the GC analysis after the extraction and purification procedure for the contaminated soil flushed with the different SDBS solutions (0.1%, 0.2%, 0.3% and 0.4%) at a flow rate of 2 mL min^{-1}.

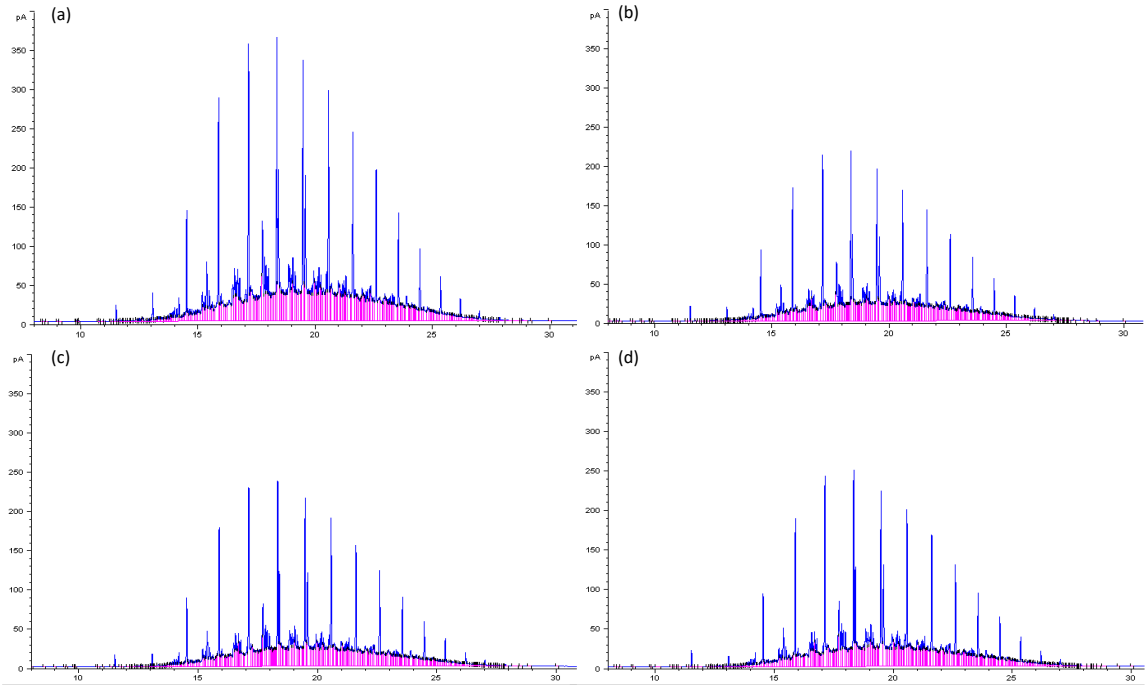

Figure 6: Chromatograms of soil flushed with 0.1% (a), 0.2% (b), 0.3% (c) and 0.4% (d) of SDBS at a flow rate of 2 mL min^{-1} (Di Trapani et al., 2023).

Even in this case, the chromatograms related to the soil samples flushed with the surfactant solutions (Figure 6a-d) are more flattened (lowering of the peaks) and with the left side much more reduced, compared to those related to the raw contaminated soil (Figure 4a) and that flushed with water (Figure 4b).

Based on the results obtained in Phase 1 and Phase 2, "long-term" experiments (48-hour duration) were conducted in Phase 3 using the same laboratory-scale setup under the following operating conditions: (i) flushing with warm water at a flow rate of 2 mL min^{-1}; (ii) flushing with 0.4% Tween 80 at 8 mL min^{-1}; and (iii) flushing with 0.2% SDBS at 2 mL min^{-1}. The results, presented in Figure 7, generally confirm the trends observed in the short-term tests.

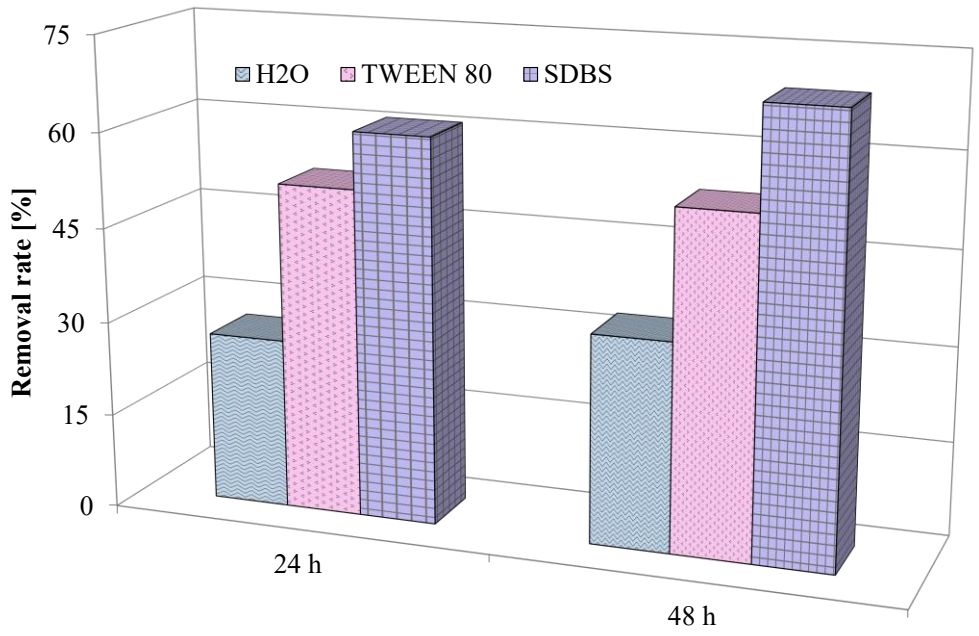

Figure 7: TPH removal rate after continuous flushing with water, Tween 80 and SDBS, respectively (Di Trapani et al., 2023).

As shown in Figure 7, flushing with water achieved an overall extraction efficiency of 32%, with a slight increase over time. This improvement is mainly attributable to the extended contact time between water and the contaminant, in agreement with the findings of Gautam et al. (2020), and supports the capability of water to mobilize a significant fraction of the adsorbed hydrocarbons. Long-term flushing with Tween 80 resulted in a 53% removal efficiency after 48 hours. The extraction efficiency remained nearly unchanged between 24 and 48 hours, suggesting that, in this case, contact time had a limited influence on the extraction process, whereas surfactant concentration likely played a more critical role. For SDBS, the highest removal efficiency—close to 70%—was achieved at the end of the flushing test. This result confirms that increasing the contact time between the surfactant and the contaminant enhances removal performance when using an SDBS solution. From a practical standpoint, these findings suggest that operating with lower SDBS concentrations over a longer flushing period may represent a more advantageous strategy.

The phytotoxicity tests, evaluated through the germination index (GI), indicated that both water and surfactant treatments affected the soil's phytotoxic properties in different ways. Figure 8, for instance, presents the GI values obtained in Phase 3, expressed as average values across the various dilutions tested.

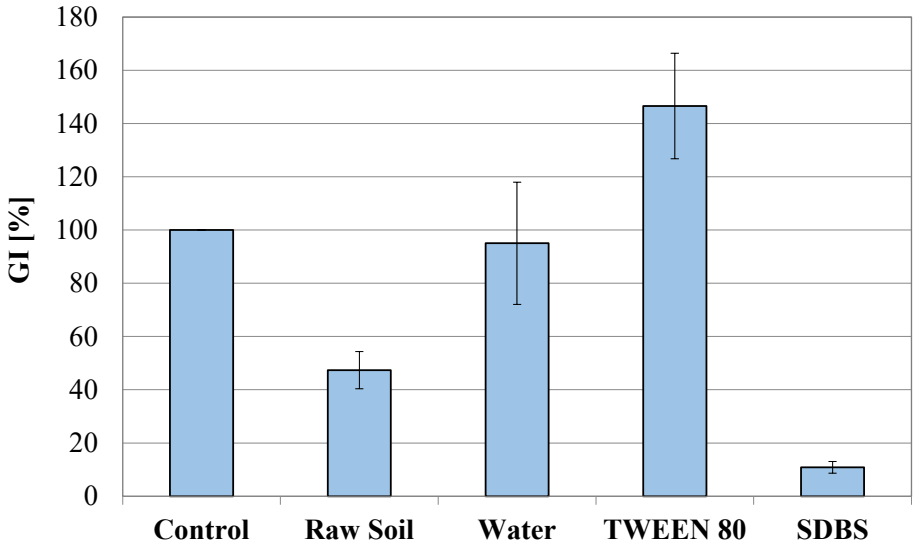

Figure 8: GI values (average ones) of soil samples after continuous flushing (Di Trapani et al., 2023).

Soil samples washed with water exhibited a germination index comparable to that of the blank control. In contrast, samples treated with SDBS showed a markedly lower GI (10.88%) relative to both the control and the untreated soil. This effect was also reflected in the reduced growth of Lepidium sativum seeds (Figure 9). Although the flushing process significantly decreased the hydrocarbon concentration in the soil, the residual presence of SDBS likely induced phytotoxic effects.

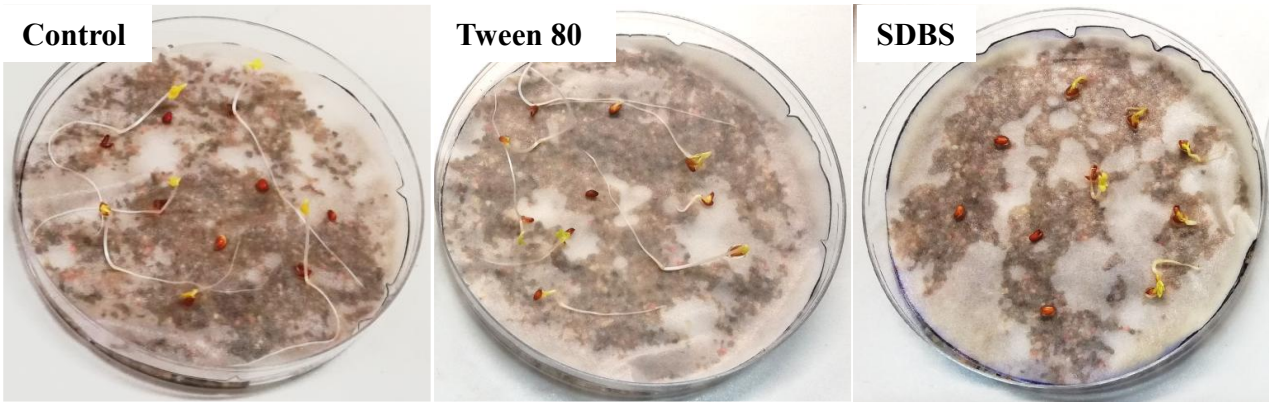

Figure 9: View of Lepidium Sativum seeds germination on control, soil treated with Tween 80 and SDBS respectively (Di Trapani et al., 2023).

These findings are consistent with the studies by Chen et al. (2001) and Singh and John (2013), which reported SDBS as toxic and poorly biodegradable (approximately 20%). Conversely, residual Tween 80 appeared to promote seed growth (Figure 9), with a GI value significantly higher than the control (146.61%). This enhancement may be attributed to the carbon content of Tween 80, which is potentially bioavailable and may increase root permeability, thereby improving nutrient uptake from the soil (Cheng et al., 2017).

Overall, these results suggest that the application of Tween 80 in soil flushing treatments, particularly for soils intended for agricultural use, would not adversely affect soil phytotoxicity characteristics.

Period 2

Figure 10 presents the residual TPH concentrations and removal efficiencies obtained from the bench-scale flushing tests. Water flushing resulted in limited removal, with a maximum efficiency of about 20% at 8 mL min^{-1}, confirming that water alone can mobilize only a small fraction of hydrocarbons (Yan et al., 2016). Slightly lower efficiencies reported in a previous study (Di Trapani et al., 2023) were likely due to differences in initial contamination levels and soil characteristics, highlighting the influence of these factors on process performance. Overall, both studies confirm the limited effectiveness of water as a standalone flushing agent.

In contrast, surfactant application significantly enhanced TPH removal. For SDBS, efficiencies increased from approximately 30% at 0.05% concentration to about 40% at 0.1%. In both cases, the highest removal was achieved at the lowest flow rate (6 mL min^{-1}), indicating that contact time plays a more important role than increased leaching. These findings are consistent with previous results, although higher efficiencies in the present study further emphasize the role of initial contamination and soil properties.

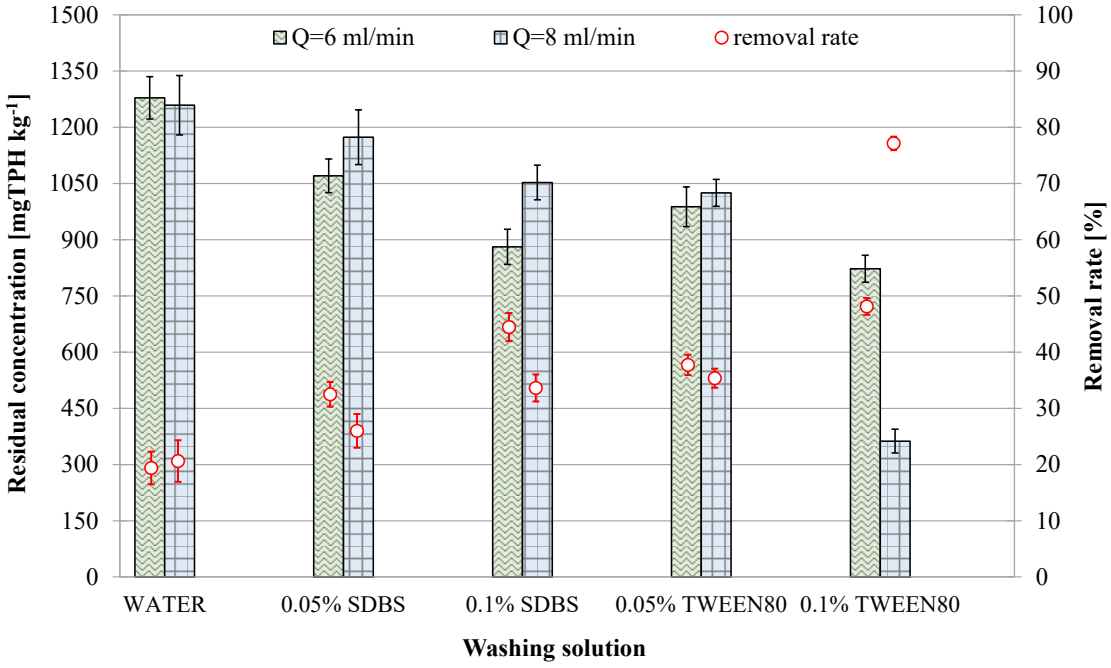

Figure 10: Residual concentration of TPHs in soil samples and removal rate after bench-scale water flushing (De Marines et al., 2025).

Tween 80 showed superior performance compared to SDBS. Increasing its concentration from 0.05% to 0.1% led to an average 30% rise in extraction efficiency, and the highest removal (77%) was achieved at 0.1% and 8 mL min^{-1}. This suggests that Tween 80 efficiency benefits from both higher concentration and flow rate, in agreement with Guo et al. (2009). The better performance of Tween 80 compared to SDBS is attributable to its much lower critical micelle concentration (CMC), which promotes hydrocarbon desorption at lower doses. Non-ionic surfactants such as Tween 80 form micelles more easily, whereas anionic surfactants like SDBS

require higher concentrations due to electrostatic repulsion between charged head groups (Ji et al., 2021). Surfactant adsorption onto soil was found to have a limited impact on removal efficiency.

Finally, surfactant effectiveness strongly depends on soil characteristics, including texture and organic matter content (Huo et al., 2020). While Tween 80 generally performs well across different soil types, its efficiency may decrease in soils rich in organic matter. Conversely, anionic surfactants such as SDBS tend to perform better in sandy soils and less effectively in soils with high silt and clay content. These aspects warrant further investigation.

Depending on the results obtained with the bench-scale flushing tests, pilot-scale tests were carried out by imposing the following operational conditions: flushing tests with water (flow rate of 40 mL min^{-1}) and flushing tests with 0.1% Tween 80 or 0.1% SDBS (flow rate of 30 mL min^{-1}). Results of the pilot-scale flushing test are depicted in Figure 11.

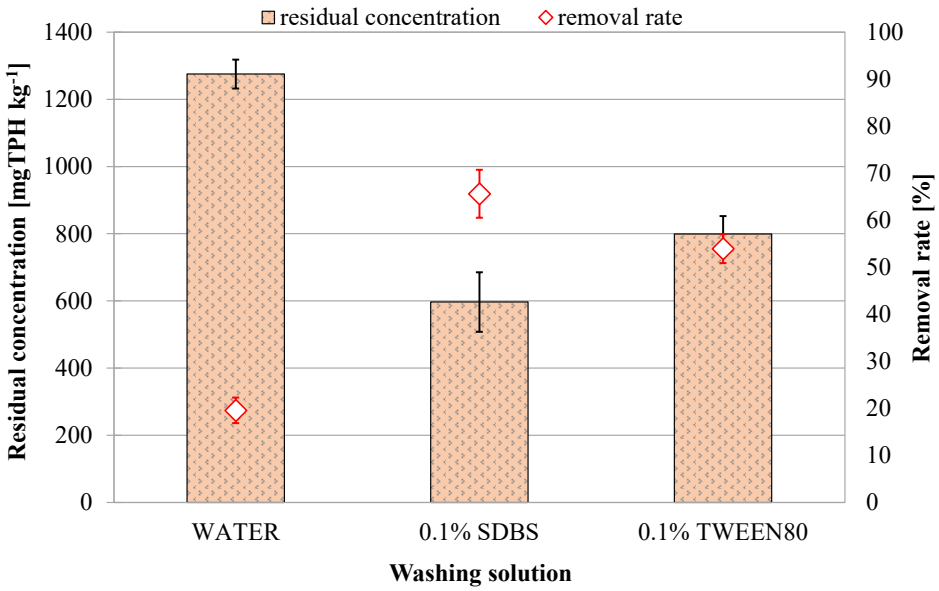

Figure 11: Residual concentration of TPHs in the soil samples as well as removal rate after pilot-scale water flushing (De Marines et al., 2025).

The results obtained with the pilot-scale flushing tests confirmed that surfactants are more effective than water in extracting TPH. Precisely, the average removal rates were 19.6%, 53.9%, and 65.6% respectively for water, Tween 80 and SDBS. However, contrarily to what observed in the bench-scale flushing tests, the extraction efficiency was higher for SDBS compared to Tween 80. The decrease of Tween 80 extraction efficiency could be due to the technical issues outlined above that hampered the regular development of the test. As a result, the lower flushing flow rate may have negatively impacted the final extraction rate. Nonetheless, this result supports the findings of Period 1 where it emerged that for Tween 80, the leaching effect due to the higher flow rate plays a key role in TPHs removal, prevailing on the contact time between the contaminant and the surfactant.

Table 1 summarizes the GI values obtained for the 25%, 50%, and 100% dilutions, respectively, on soil samples subjected to flushing with water as well as with SDBS and Tween 80 solutions, related to the bench-scale tests. Flushing with water or with the two surfactants had significantly different effects on the potential phytotoxicity of soil. Indeed, higher GI were observed in soil flushed with water and Tween 80 compared to the negative control (GI=100%). Conversely, soil flushed with SDBS showed lower GI values as well as low

growth of Lepidium Sativum seeds. Such results are consistent with studies carried out by Zheng et al. (2007), Ni et al. (2014) and Di Trapani et al. (2023), which demonstrated that Tween 80 does not exhibit any inhibitory effect on plant growth in aqueous solutions: indeed, referring to its molecular structure and the consequent interactions with soil particles, it is worth noting that Tween 80 olds carbon potentially bioavailable, which increases the root permeability, leading to a more efficient absorption of nutrients from soil (Cheng et al., 2017). Also, the toxicity and inhibitory effect of SDBS are supported by studies conducted by Garon et al. (2002) and Singh and John (2013), who identified SDBS as toxic and poorly biodegradable (20%).

Table 1: Average values of GI of soil samples after bench-scale water flushing (in brackets the standard deviation) (De Marines et al., 2025).

	DILUTIONS		
	25%	50%	100%
Water	154.7 (±28.7)	120.3 (±11.0)	104.7 (±2.2)
0.05% SDBS	25.7 (±5.5)	12.5 (±4.4)	7.8 (±2.2)
0.1% SDBS	18.7 (±4.4)	10.9 (±3.1)	6.3 (±5.3)
0.05% Tween 80	159.4 (±13.3)	143.8 (±26.5)	114.1 (±6.6)
0.1% Tween 80	206.3 (±26.5)	165.6 (±8.8)	132.8 (±37.6)

Results obtained from the germination tests conducted on soil samples after the pilot-scale experiments (Figure 12) confirmed those obtained from the bench-scale tests, underlining the negative impact exerted by SDBS on soil residual phytotoxicity compared to Tween 80, and confirming the hypothesis of higher toxicity of SDBS.

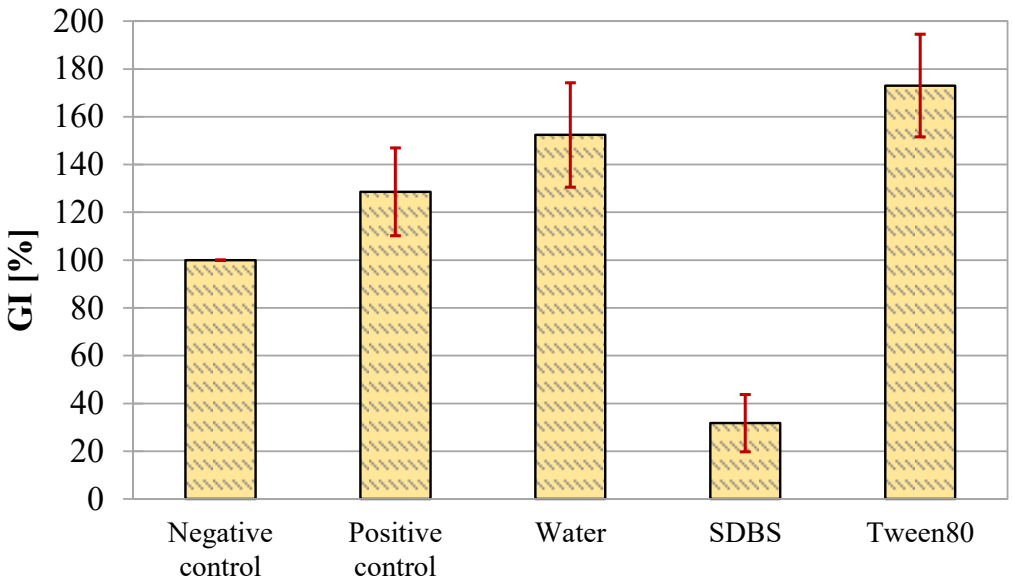

Figure 12: Average GI values of soil samples after pilot-scale water flushing (De Marines et al., 2025).

Anionic surfactants, including SDBS, are generally more toxic than non-ionic ones, like Tween 80. In particular, the highest GI value (173%) was achieved for soil samples treated with Tween 80, while the lowest GI (31.7%) was observed in the test carried out with soil treated with SDBS, thus confirming its toxic effect

on seeds germination. The phytotoxic effect exerted by SDBS was more significant compared to that caused by hydrocarbons, which, in contrast, showed less or no negative influence on seeds germination and this could impact the biological and physicochemical properties of soil in the long-term.

Concerning the results achieved in Phase 2, it is worth noting that contamination with TPH did not affect the amount of available phosphorus (P), showing the same value as the control soil (Figure 13). Conversely, treatment with water and Tween 80 reduced the available P content. On the other hand, the SDBS-treated soil showed an available P increase of about 20% compared to the control. The decrease of available P in Tween 80 and water-treated soils can be ascribed to the effect of the treatment (i.e. soil flushing) that leached soil available P, or to a greater P uptake by plants. Considering that P uptake did not show significant differences among treatments, the lower available P in Tween 80 and water treatments compared to the control can be ascribed to soil P leaching.

On the other hand, the increase of available P in SDBS-treated soil is probably due to the supply of P through the surfactant which holds 5.1 mg P g^{-1}. However, an increase of available P already held by soil following the treatment with SDBS cannot be excluded. Indeed, following TPH and SDBS treatment, soil pH decreased from 7.6 to 7.0, thus increasing the solubility and availability of P. Penn and Camberato (2019) reported that the highest amount of available P usually occurs at soil pH between 6.5-7. Furthermore, the sulphate group of SDBS may substitute the phosphate group on soil colloids thus further increasing the availability of soil P. Such an increase, if on the one hand could promote plant growth, on the other hand might contribute to eutrophication of surface waters.

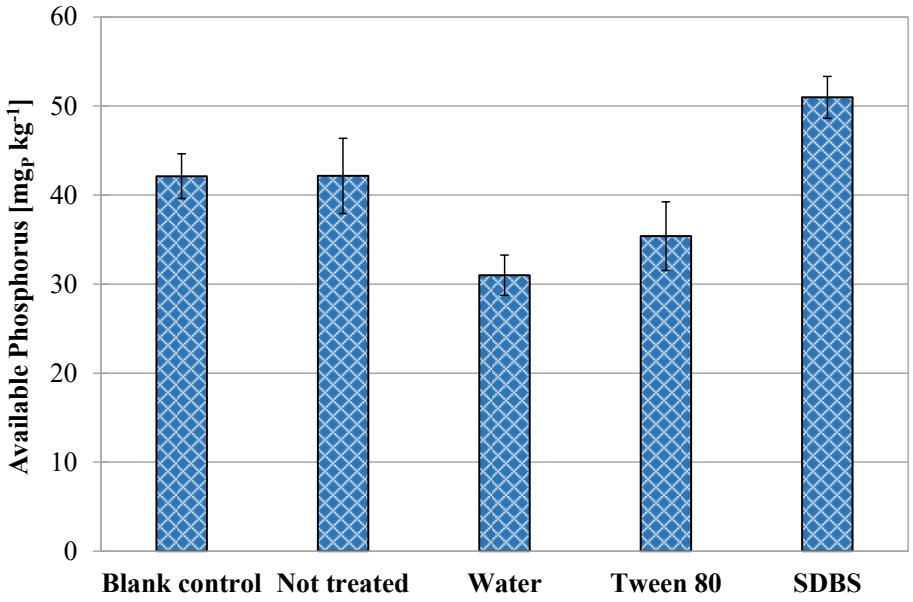

Figure 13: Average GI values of soil samples after pilot-scale water flushing (De Marines et al., 2025).

Fava plants started to sprout after 15 days from sowing, and the first measurements were taken after an additional 10 days.

Fava grew well in all soil samples (Figure 14). Specifically, plants grown in the blank control and in the soil treated with Tween 80 reached the same average height thus suggesting that this surfactant does not inhibit plant growth. On the contrary, the lowest plant growth occurred in the soils treated with SDBS that suggesting

its negative impact on plant growth. This result is in accordance with findings reported by Garon et al. (2002), who showed that the presence of the anionic surfactant inhibited the growth of fungal strains, negatively impacting the nutrients cycles thus resulting in reduced plant growth.

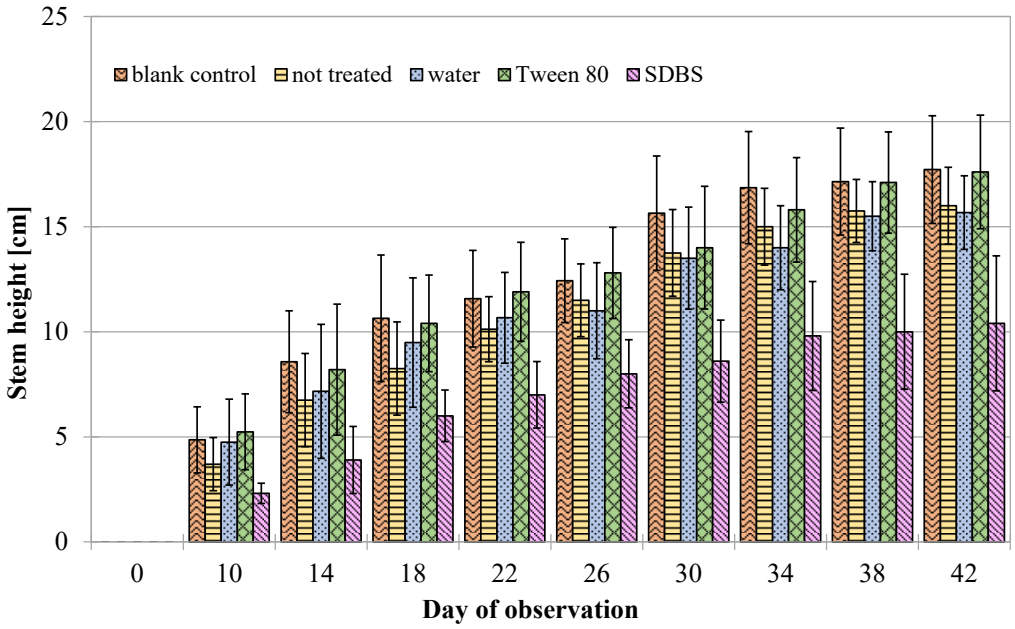

Figure 14: Average stem height of Vicia Faba during Phase 2 (De Marines et al., 2025).

On the contrary, in the not treated soil and in the one treated with only water, a modest growth was observed, indicating that the presence of hydrocarbons does not negatively influence plant development. Table 2 reports the final average stem heights and the average leaf sizes.

Table 2: Final average stem heights, number and average sizes of leaf (in brackets the standard deviation) (De Marines et al., 2025).

Sample	Final stem height [cm]	Number of leaves [-]	Leaf length [cm]	Leaf width [cm]
Blank control	17.7 (± 2.6)	7 (± 2.0)	6 (± 0.2)	4 (± 0.2)
Not treated	16.0 (± 1.8)	7 (± 1.5)	5 (± 0.2)	3 (± 0.4)
Water	15.7 (± 1.7)	7 (± 2.5)	4.5 (± 0.3)	3.5 (± 0.2)
Tween 80	17.6 (± 2.7)	7 (± 1.5)	6 (± 0.3)	5 (± 0.3)
SDBS	10.4 (± 3.2)	6 (± 1.4)	3 (± 0.3)	2.5 (± 0.4)

Figure 15 provides a comparison of plant growth and roots development after their eradication. From the observation of Figure 15, it can be seen that all plants exhibited comparable stem growth and root development (Figure 15a-d), excepting those grown in the soil treated with SDBS (Figure 15e). This difference was also corroborated by the weights of the plants (Table S4). In fact, the plants grown in the soils treated with SDBS

exhibited the lowest weight values compared to those cultivated in the blank control and in the other treatments. In addition, the analysis of stem/root ratio showed no significant differences from the control, except for plants grown in soils treated with water and SDBS, where the highest stem/root ratios were recorded. These results suggest that the two treatments caused the root system to develop less than the stem. These results confirm that the residue of TPHs and presence of SDBS in the soil may have had a toxic or growth-inhibiting effect on Vicia Faba plants.

Figure 15: Comparison of roots and plants growth: blank control (a), not treated (b), water (c), Tween 80 (d) and SDBS (e) (De Marines et al., 2025).

4.1.1.4 Main conclusions of the study

Period 1

The application of both surfactants in the washing solution resulted in substantial hydrocarbon removal from the contaminated soil, with extraction efficiencies markedly higher than those achieved through flushing with water alone. This confirms the key role of surfactants in the remediation of hydrocarbon-polluted soils.

In short-term tests with Tween 80, the highest removal efficiency (51.7%) was achieved using a 0.4% concentration at a flushing flow rate of 8 mL min^{-1}. For SDBS, the best performance in short-term conditions (45%) was obtained at a concentration of 0.2% and a flow rate of 2 mL min^{-1}. Chromatographic analyses after flushing with both surfactants showed flattened profiles, characterized by lower peak intensities and a marked

reduction on the left side of the chromatogram, indicating the removal of the more soluble and volatile hydrocarbon fractions.

Under long-term conditions, removal efficiencies reached 53% for Tween 80 and 70% for SDBS, highlighting that SDBS performance improved with longer contact time. Despite the higher long-term removal achieved with SDBS, the two surfactants showed significant differences in terms of residual soil phytotoxicity. Specifically, the germination index values (10.9% for SDBS and 146.6% for Tween 80) revealed that soils treated with SDBS exhibited much greater phytotoxicity compared to those treated with Tween 80.

Overall, these findings indicate that Tween 80 may represent a more suitable option when the objective is to restore treated soils for agricultural use.

Period 2

The tested surfactants proved more effective than water in removing hydrocarbons from contaminated soil. Plants grown in soils treated with surfactants showed the lowest hydrocarbon accumulation in their roots. However, the two surfactants exhibited different behaviors depending on the flushing rate: Tween 80 achieved better performance at the highest flow rate, whereas SDBS was more effective at the lowest flow rate, indicating that it requires longer contact time to enhance removal efficiency.

The potential phytotoxicity of contaminated soils treated with water or surfactants was evaluated through germination tests and by cultivating Vicia faba plants, along with assessing hydrocarbon accumulation in plant roots. Germination index results showed greater phytotoxicity in soils treated with SDBS compared to Tween 80 (31.7% vs 173%, respectively). These findings were supported by the growth response of Vicia faba L., which exhibited reduced height and biomass in SDBS-treated soils, suggesting an inhibitory effect of this surfactant on plant development.

Consistent with the reduced plant growth, total phosphorus uptake was lowest in plants grown in SDBS-treated soils, despite a 20% increase in soil available phosphorus. This increase may be attributed to the phosphorus content of the surfactant (5 mg P g^{-1}) and the associated decrease in soil pH.

From a practical standpoint, these results provide useful guidance for selecting surfactants and defining operational conditions in view of potential scale-up applications.

4.1.2 Role of single and mixed surfactants for hydrocarbons removal from real marine sediments: removal efficiency and residual phytotoxicity after sediment washing treatment

4.1.2.1 Introduction

Chemical pollution represents a global concern, resulting from the intentional or accidental release of contaminants into the environment, with annual emissions estimated between 120,000 and 220,000 million tonnes (Naidu et al., 2021). Among the main contributors are petroleum-related industrial activities—such as transportation, drilling, storage, exploration, refining, and processing—which are major sources of hydrocarbon spills and environmental contamination (Ambaye et al., 2024). In this framework, the contamination of marine sediments linked to anthropogenic activities is one of the most critical environmental issues, particularly in areas heavily impacted by decades of uncontrolled industrial operations, including cement and steel production, fertilizer manufacturing, chlor-alkali plants, and crude oil refining (Proietto et al., 2024). Sediments act as the principal repository for both organic and inorganic pollutants entering aquatic systems, including heavy metals, polychlorinated biphenyls (PCBs), polycyclic aromatic hydrocarbons (PAHs), and petroleum hydrocarbons (HCs), which are primarily introduced through industrial and human activities (Chen et al., 2020). Owing to the dynamic exchange between sediments and the overlying water, contaminants may either accumulate in or be released from sediments, making them both a sink and a secondary source of pollution (Zhang et al., 2021). Due to their hydrophobic character and low water solubility, hydrocarbons (HCs) preferentially associate with organic matter and consequently accumulate in sediments. For this reason, environmental policies and management strategies have increasingly focused on improving environmental quality, making the remediation of contaminated sediments a key priority for protecting both ecosystems and human health. Over recent years, various techniques have been developed to remove HCs from sediments. These approaches can be categorized by type—thermal, physicochemical, chemical, or biological—or by application mode, namely in situ or ex situ. Among them, surfactant-enhanced washing has gained attention because it generally exhibits lower toxicity and greater biodegradability than organic solvents (Befkadu and Chen et al., 2018). Surfactants are classified according to their origin as natural (e.g., rhamnolipids, commonly referred to as biosurfactants) or synthetic. Most biosurfactants are anionic or neutral, while cationic forms typically contain amine groups (Azevedo et al., 2024). Rhamnolipids, in particular, are anionic due to the presence of carboxylic groups and are produced through microbial metabolism (Ma et al., 2024). Their aqueous solubility increases as pH rises from 5 to 8, owing to the enhanced negative charge on the polar head group (Abdel-Mawgoud et al., 2009).Synthetic surfactants, on the other hand, are divided into four categories—cationic, anionic, nonionic, and zwitterionic—based on the charge of their hydrophilic head group (Shih et al., 2020). In general, biosurfactants are considered more environmentally compatible, as they typically show higher surface activity, lower toxicity, and improved biodegradability compared with synthetic surfactants (Pekdemir et al., 2005). This aspect is particularly relevant because surfactants may sometimes alter soil or sediment properties after treatment, potentially leading to secondary contamination or inhibitory effects on subsurface organisms, including phytotoxicity (Huo et al., 2020; Bolan et al., 2023). Several studies have also highlighted the advantages of using surfactant mixtures, especially combinations of anionic and nonionic types. Mixing surfactants in aqueous solutions can promote the formation of mixed micelles—most commonly ionic–nonionic systems—which often exhibit enhanced performance (Parekh et al., 2011). Certain combinations display synergistic effects, leading to improved solubilization capacity and reductions in both surface tension and critical micelle concentration (CMC) (Rosen and Kunjappu, 2012; Liu et al., 2021). The interactions between different surfactants adsorbed at interfaces are described by the interaction parameter β, which reflects both the strength and nature of these interactions (Rosen and Kunjappu, 2012). In ionic–nonionic mixtures, where strong electrostatic attractions are not typically expected, negative β values are often attributed to a decrease in the electrostatic self-repulsion of the ionic surfactant when diluted with the nonionic component—essentially a dilution effect (Zhou and Rosen, 2003). Previous research has demonstrated promising synergistic behavior in nonionic–anionic systems, attributed to the formation of mixed micelles stabilized by ion–dipole interactions between distinct hydrophilic head groups. These interactions reduce both

electrostatic and steric repulsion among similar surfactant molecules, thereby enhancing overall performance (Liu et al., 2021; Rosen and Kunjappu, 2012).

Despite surfactant-washing seems promising for the remediation of polluted marine sediments, only few applications on real sediments have been reported so far. Most studies in the literature have focused on soils instead. Although sediments and soils share several common characteristics, however important distinctions exist. Marine sediments, for example, are constantly submerged, thus leading to a high redox potential. This means they have a strong tendency to gain electrons and become reduced, a characteristic that makes them particularly prone to adsorbing contaminants (Kalev and Toor, 2018). To the best of our knowledge, there is a clear gap in the current literature regarding the application of mixed surfactant systems for the remediation of real marine sediments contaminated by HCs. While several studies have examined surfactant-enhanced remediation in soils or synthetic sediments, most have focused on single surfactants.

Within this framework, the present study aimed to evaluate the feasibility of surfactant-enhanced washing as a remediation strategy for marine sediments heavily contaminated with total petroleum hydrocarbons (TPH). Two synthetic surfactants—sodium dodecyl benzene sulphonate (SDBS) and polysorbate 80 (Tween 80)—and one natural surfactant—rhamnolipids produced by Pseudomonas aeruginosa—were tested at different concentrations. Process performance was assessed in terms of TPH removal efficiency and residual phytotoxicity, with particular attention to the influence of surfactant concentration and the use of either single surfactants or their mixtures in the washing solutions. The innovative aspect of this work lies in the evaluation of both individual and combined surfactants for contaminant removal from real marine sediments, while also examining the phytotoxic characteristics of sediments after treatment. By integrating remediation effectiveness with ecological compatibility, the study provides a meaningful contribution to the development of more sustainable strategies for marine sediment management. The results offer practical insights to support the selection of suitable surfactant combinations and operating conditions, paving the way for future research and potential full-scale applications.

4.1.2.2 Materials and methodologies

Sampling site and sediment features. The sediments used during the experiments were dredged from the Bay of Augusta (Italy), a contaminated site of national interest. The Augusta-Priolo industrial zone is one of the largest petrochemical areas in both Italy and Europe, characterized by the presence of numerous industrial plants whose pollution has a significant impact on the Rada of Augusta (commonly referred to simply as the "Rada"), causing substantial contamination of marine sediments. Since the 1950s, the Rada of Augusta has hosted several chemical and petrochemical facilities, some of which are now decommissioned, as well as power plants, cement factories, military bases, and a commercial port, all of which have affected the quality of the marine environment.

Table 3 summarizes the main features of the investigated marine sediments, reporting in the last column the references to the methodology adopted for the analysis of each parameter. Sediment was artificially contaminated with diesel fuel to achieve a higher level of TPHs contamination, according to the aim of the study taking previous studies on spiking organic chemicals onto sediments as a reference (Picone et al., 2022). It must be noted that previous studies highlighted that TPH concentration can significantly influence the extraction efficiency of the process. and very few studies addressing soil and sediment with TPH contamination levels exceeding 10,000 mg/kg has emerged from the literature (Lai et al., 2009; Saxena et al., 2023). Commercial diesel fuel (density ≈ 0.83 kg/L) was added to the raw sediment at a 1:10 volume-to-weight (v/w) ratio, corresponding to 100 mL of diesel per 1 kg of sediment. The contaminated sediment underwent daily manual mixing for 15 days, to enhance contaminant homogenization and promote the volatilization of the most

volatile TPHs fractions. Subsequently, the drying phase was completed by placing the sample in an oven at 40°C for 72 hours, ensuring a uniformly contaminated sediment for the subsequent washing tests. The subsequent pretreatment phases focused on crushing and sieving the dried sediment, with the aim of isolating the fine fraction. This choice was driven by the fact that the concentration of hydrocarbons adsorbed onto the solid matrix usually is closely related to the specific surface area, becoming higher as the particle size decreases (Rajabi et al., 2018). Specifically, the dried sample was first crushed using a mortar and pestle to reduce particle size and then subjected to sieving. The sieving process was performed using a two-stage sieve system with mesh sizes of 2 mm and 63 µm. The sediments before artificial contamination had a pH of 9, a Total Organic Carbon (TOC) value of 2.2 g/kg and a 53.5% residue at 105°C. The concentration of hydrocarbons C<12 and C>12 was below the regulation limits and respectively equal to <0.3 mg/kg$_{DS}$ and 130 mg/kg$_{DS}$; instead, the concentration of mercury was equal to 16 mg/kgDS. Table 3 shows the characterization of the sediments used and the initial level of hydrocarbons before artificial contamination and pretreatment. After the artificial contamination, the sediment fraction < 63 µm was characterized by a TPH concentration equal to 61109 mg/kg$_{DS}$ (±8361 mg/kg$_{DS}$), which simulates a severe TPH contamination.

Table 3: Main features of the sediments before contamination (Russo Tiesi et al., 2025).

Parameter	Units.	Value
Residue at 105°C	%	53.5
pH	-	9
EC	mS/cm	2.6
TOC	g/kg	2.2
TC	mg/L	27.8
IC	mg/L	15.8
OC	mg/L	11.9
Mercury	mg/kg$_{DS}$	16
Hydrocarbons C<12	mg/kg$_{DS}$	<0.3
Hydrocarbons C>12	mg/kg$_{DS}$	130

Surfactants used. The surfactants used (SDBS, Tween 80, and Rhamnolipids produced by *P. aeruginosa*) were purchased from Sigma Aldrich. Surfactant solutions were prepared using distilled water. The above surfactants were selected due to the different chemical composition (nonionic, anionic and natural) but also because they were thoroughly applied in previous remediation applications (Paria, 2008; Lai et al., 2009; Bolan et al., 2023), even if mostly on soils; therefore, further research is needed for sediment washing. The above surfactants have different environmental behaviour. Indeed, SDBS is potentially toxic and persistent; Tween 80 is considered to be more environmentally friendly, due to its higher biodegradability (Zhang et al., 2024); despite this, among the three surfactants used, Rhamnolipids are the most environmentally friendly because they do not accumulate in the environment, are non-toxic and are naturally produced by bacteria, making them a sustainable choice compared to synthetic surfactants (Ambaye et al., 2021). The different surfactants used are characterized by

different CMCs: SDBS has a CMC of 212.57 mg/L, Tween 80, a CMC of 13.1 mg/L, instead, Rhamnolipids from *P. aeruginosa* have a CMC of 31 mg/L (Lai et al., 2009; Di Trapani et al., 2023).

Description of the experimental campaign. All three surfactants were tested both individually and in combination to form mixed micelles. Each experiment was conducted in duplicate to enhance the reliability of the results. The effect of surfactant concentration in the washing solution was evaluated in terms of hydrocarbon removal efficiency from the sediments and the residual phytotoxicity of the treated material. The experimental plan included several variants based on the surfactant or combination of surfactants applied. Preliminary washing trials were carried out using tap water as a blank control (Test A). Subsequently, five additional test series were performed at different surfactant concentrations. Test B involved the exclusive use of Tween 80, while Test C employed only SDBS. Test D examined the combined application of SDBS and Tween 80 to promote the formation of mixed micelles. Test E evaluated rhamnolipids alone, and Test F investigated the combined use of Tween 80 and rhamnolipids. The mixed-surfactant experiments (Tests D and F) were designed to assess TPH mobilization and removal efficiency when combining anionic surfactants (SDBS and rhamnolipids) with non-ionic surfactants (Tween 80 and rhamnolipids). In all cases, the selected concentrations exceeded the critical micelle concentration (CMC) of each surfactant and were maintained constant within each test series to allow proper comparison among treatments. Table 4 summarizes the experimental conditions and the corresponding surfactant concentrations for each test. All experiments were performed in duplicate to ensure the robustness and reproducibility of the results.

Table 4: Summary of the experimental tests carried out at different surfactants concentration (Russo Tiesi et al., 2025).

Test	H_2O	Tween80			SDBS			Rhamnolipids		
% by weight		0.2	0.4	0.6	0.2	0.4	0.6	0.2	0.4	0.6
A	X									
B		X								
			X							
				X						
C					X					
						X				
							X			
D		X			X					
		X				X				
			X		X					
E								X		
									X	
										X
F		X						X		
		X							X	
			X					X		

For all washing experiments, an orbital shaker was employed to enhance the interaction between the solid matrix and the washing solution. Specifically, 10 g of sediment were mixed with 40 mL of solution (solid-to-liquid ratio 1:4) in Pyrex glass bottles. The bottles were agitated on the orbital shaker at 100 rpm for 24 hours. Each test was conducted in duplicate to improve the reliability of the results. At the end of the washing period, the samples were allowed to settle for 2 hours. The supernatant was then removed, and the solid fraction was air-dried at room temperature. The three surfactants were applied at different concentrations in the washing solutions (Table S2, Supplementary Material). When used individually, the tested weight concentrations were 0.2%, 0.4%, and 0.6%. For SDBS, these values corresponded to approximately 10, 20, and 30 times its critical micelle concentration (CMC). In the case of Tween 80, the concentrations were about 150, 300, and 450 times the CMC, while for rhamnolipids they were approximately 65, 130, and 195 times the CMC. When surfactants were combined to promote mixed micelle formation (Tween 80–SDBS and Tween 80–rhamnolipids), the weight concentration pairs tested were 0.2%–0.2%, 0.2%–0.4%, and 0.4%–0.2%. Based on previous studies (Mirzaee and Sartaj, 2022; Di Trapani et al., 2023), concentrations were defined in terms of weight percentage. Furthermore, determining the CMC of mixed micelles would have required specific experimental procedures (Rosen and Kunjappu, 2012), involving additional laboratory equipment that was not available for this study.

Analytical Methods. The measurement of TPHs concentration in the solid phase as well as the residual phytotoxicity after the washing tests, were evaluated according to what already discussed in the previous section.

4.1.2.3 Results and discussion

TPH mobilization removal efficiency with water and individual surfactants. Figure 16 shows the TPH extraction efficiencies achieved using water and the specific surfactants at varying weight concentrations in the washing solution. The results showed that surfactants-enhanced washing significantly improved TPH extraction compared to water alone ($\eta \approx 15\%$). Furthermore, the performance of each surfactant varied, indicating their distinct mechanisms of action. These findings underscore the strategic importance of surfactants in augmenting pollutant mobilization removal as discussed below. Indeed, surfactants are applied in soil washing because they also can significantly enhance the solubility of TPHs, thereby improving remediation efficiency (Qiu et al., 2019). Pollutants are mobilized by solubilization or chemical interactions (Mao et al., 2015). However, the mobilization removal efficiency achieved with water is consistent with previous studies on TPH-contaminated soils, where it was observed that washing with water alone led to the mobilization and subsequent removal of a non-negligible portion of TPH from the soil (Lai et al., 2009; Di Trapani et al., 2023).

Overall, as shown in Figure 16, the lowest efficiency in the case of individual surfactant was obtained for Rhamnolipids at 0.2%, with TPH removal rate of $\eta \approx 21\%$. In contrast, the efficiency significantly increased with Tween 80 and SDBS at 0.2%, with removal rate of $\eta \approx 44\%$ and $\eta \approx 42\%$, respectively.

The TPH extraction yield improvement obtained by using Tween 80, compared to the washing tests carried out with only water can be attributable to Tween 80's ability to solubilize and disperse hydrocarbons due to its amphiphilic structure, which allows effective interaction with hydrophobic hydrocarbon molecules (Kopanichuk et al., 2018).

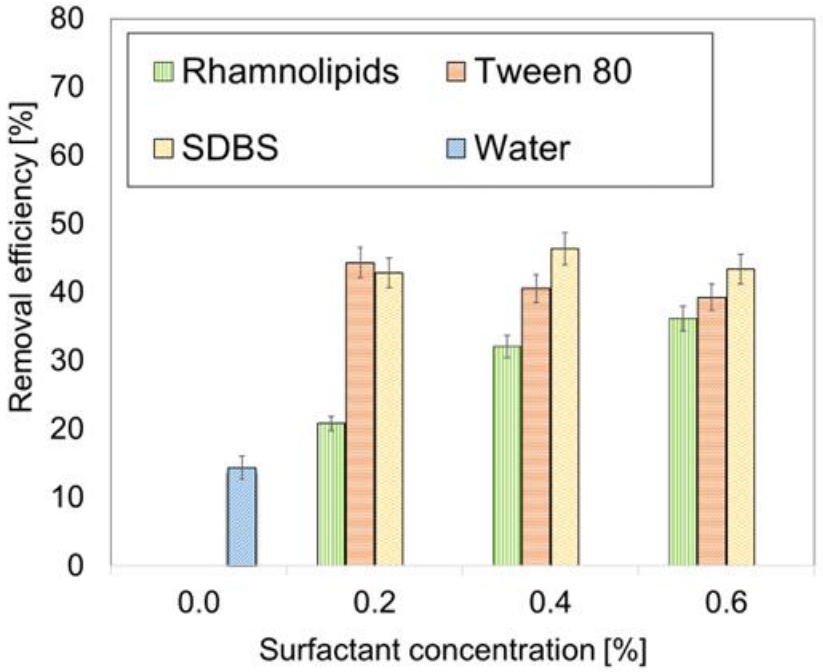

Figure 16: Average values of TPH removal efficiency from sediments using water and individual surfactants individually at 0.2%, 0.4% and 0.6%, with standard deviations (Russo Tiesi et al., 2025).

However, as illustrated in Figure 16, increasing Tween 80 concentration to 0.4% and 0.6% w/w did not result in further improvement in extraction efficiency. On the contrary, the yield decreased by approximately 5%, suggesting that beyond a certain threshold the effectiveness of the surfactant slightly declined, at least for marine sediments characterized by such high TPH concentrations. This observation indicates the existence of an optimal concentration range for Tween 80, above which hydrocarbon mobilization and removal efficiency may decrease. The order of magnitude of TPH mobilization removal obtained in this study is comparable to that reported by Caetano et al. (2024), who investigated similar contact times using Tween 80 at 100 times its CMC. In their work, contact times ranging from a few hours up to three days were examined, and TPH removal efficiency was found to stabilize after approximately 24–36 hours. The non-ionic nature of Tween 80 may explain this behavior. Indeed, due to the absence of electrostatic repulsion, Tween 80 tends to adsorb onto the soil matrix, temporarily reducing the amount of active surfactant available for hydrocarbon solubilization. Prolonged and vigorous mixing can promote its desorption back into the aqueous phase, although this is a time-dependent process. In contrast to our findings, Caetano et al. (2024) observed that increasing Tween 80 concentration up to 700 CMC led to mobilization removal efficiencies exceeding 80%. Nevertheless, washing performance is strongly influenced by the physicochemical characteristics of the treated medium (Saxena et al., 2023). In their study, soils with particle size < 2 mm were used, whereas the present research employed a finer sediment fraction (< 0.063 mm), which may significantly affect TPH extraction efficiency. Therefore, further investigations are needed to better elucidate the relationship between marine sediment properties, surfactant concentration, and extraction performance. Since the adsorption of Tween 80 onto the solid matrix plays a key role in hydrocarbon desorption and solubilization, the combined use of SDBS and Tween 80 could represent a promising strategy (Cheng et al., 2017), potentially enhancing pollutant solubilization through synergistic effects (see Section 3.2).

The use of SDBS significantly improved hydrocarbon solubilization from contaminated sediment (Figure 21). Overall, extraction yields were slightly higher than those achieved with Tween 80 at equivalent concentrations, except at 0.2%. The highest removal efficiency (approximately 46%) was obtained at 0.4% w/w SDBS, while

a further increase to 0.6% resulted in a moderate decline in performance. Although higher surfactant concentrations often enhance TPH removal (Liu et al., 2021), several studies have reported reduced efficiency at excessive concentrations. This effect may be attributed to excessive micelle formation, which can hinder rather than promote hydrocarbon solubilization. Zhao et al. (2014) observed that concentrations exceeding the CMC may reduce contaminant solubilization due to micelle overabundance. Similarly, Urum and Pekdemir (2004) found that increasing concentrations of surfactants such as lecithin, aescin, and tannin reduced TPH removal efficiency in soil washing applications. The results obtained with SDBS are consistent with those reported by Di Trapani et al. (2023), who identified a threshold concentration beyond which extraction efficiency declined. In their soil flushing experiments (0.1–0.4% w/w SDBS), the highest removal was achieved at 0.2%. Although the optimal concentration in the present study was 0.4%, the initial TPH concentration strongly influences the outcome (Lai et al., 2009; Saxena et al., 2023). Notably, the initial TPH level in Di Trapani et al. (2023) was approximately one order of magnitude lower (≈6000 mgTPH/kgDS) than that considered here. Comparable trends were reported by Salehian et al. (2012), who used the anionic surfactant SDS in soil flushing of diesel-contaminated soils (10,000 and 20,000 mg/kg). The best efficiencies were achieved at intermediate concentrations (0.3% SDS for 10,000 mg/kg and 0.1% SDS for 20,000 mg/kg), whereas higher concentrations reduced performance. The authors suggested that excessive surfactant may promote interactions with soil particles, leading to gel-like structures that hinder diesel separation.

Additional explanation may be drawn from Zoghi and Mafigholami (2023), who highlighted that high surfactant concentrations can induce excessive foaming or precipitation. Excessive foaming limits contact between washing solution and sediment particles, while precipitation may occur due to interactions with other compounds, reducing surfactant solubility. These findings emphasize the importance of optimizing surfactant dosage to maximize washing efficiency while avoiding adverse effects.

Beyond the CMC, absolute surfactant concentration appeared to play a more decisive role than the number of times the CMC was exceeded (Perinelli et al., 2020). Although the CMC of SDBS is about one order of magnitude higher than that of Tween 80, both surfactants exhibited similar mobilization removal efficiency at 0.2%. At 0.4% and 0.6%, SDBS slightly outperformed Tween 80 despite the lower CMC of the latter. Anionic surfactants may be more effective due to reduced adsorption onto negatively charged soil particles, as electrostatic repulsion limits their retention (Li et al., 2019). Furthermore, Tween 80 performance may be negatively influenced by high organic matter content (Chen et al., 2017).

Previous studies support these findings. Niu et al. (2020) reported that SDBS (1%) achieved removal efficiencies above 50%, outperforming Tween 80 (<40%) in highly contaminated soils. Ritoré et al. (2022) similarly observed better TPH removal with SDBS across soils of different textures, with efficiency increasing from finer to coarser materials. However, Di Trapani et al. (2023) reported better performance of Tween 80 compared to SDBS in soil flushing, although under significantly lower initial TPH concentrations. These discrepancies may be attributed to differences between soils and marine sediments, as well as to grain size and contaminant concentration. Further studies should therefore assess performance under varying TPH levels and granulometric fractions (e.g., <2 mm).

Only one study was identified addressing marine sediment washing with SDBS (Shih et al., 2020). In that work, focusing on PAHs, approximately 45% removal efficiency was achieved at 100 CMC—comparable to the present findings—although initial PAH concentrations were three orders of magnitude lower.

Regarding rhamnolipids, Figure 16 shows a consistent increase in TPH mobilization removal with rising concentration. Efficiencies of 21%, 32%, and 36% were obtained at 0.2%, 0.4%, and 0.6%, respectively. A similar trend was reported by Lai et al. (2009), who observed improved removal with increasing rhamnolipid concentrations in contaminated soils.

Nevertheless, rhamnolipid performance remained lower than that of SDBS and Tween 80. This contrasts with some soil-based studies (Liu et al., 2021) reporting superior performance of rhamnolipids compared to Tween 80. The discrepancy may be related to sediment-specific characteristics (Kalev and Toor, 2018), as well as to grain size and TPH concentration. Moscatelli et al. (2024) investigated PAH removal from marine sediments using individual surfactants, including rhamnolipids, reporting efficiencies below 10%. However, their initial PAH concentrations (≈3500 mg/kg) were much lower than those considered here, and experimental conditions differed substantially (solid-to-liquid ratio 1:42; 48 h mixing). Overall, since most available studies focus on soils, further research on real marine sediment washing is essential to deepen understanding of the mechanisms governing hydrocarbon removal in washing processes.

TPH mobilization removal efficiency with mixed surfactants. Figure 17 summarizes the TPH mobilization removal efficiency with mixed SDBS-Tween 80 (Figure 17a) and Rhamnolipids-Tween 80 (Figure 17b), respectively.

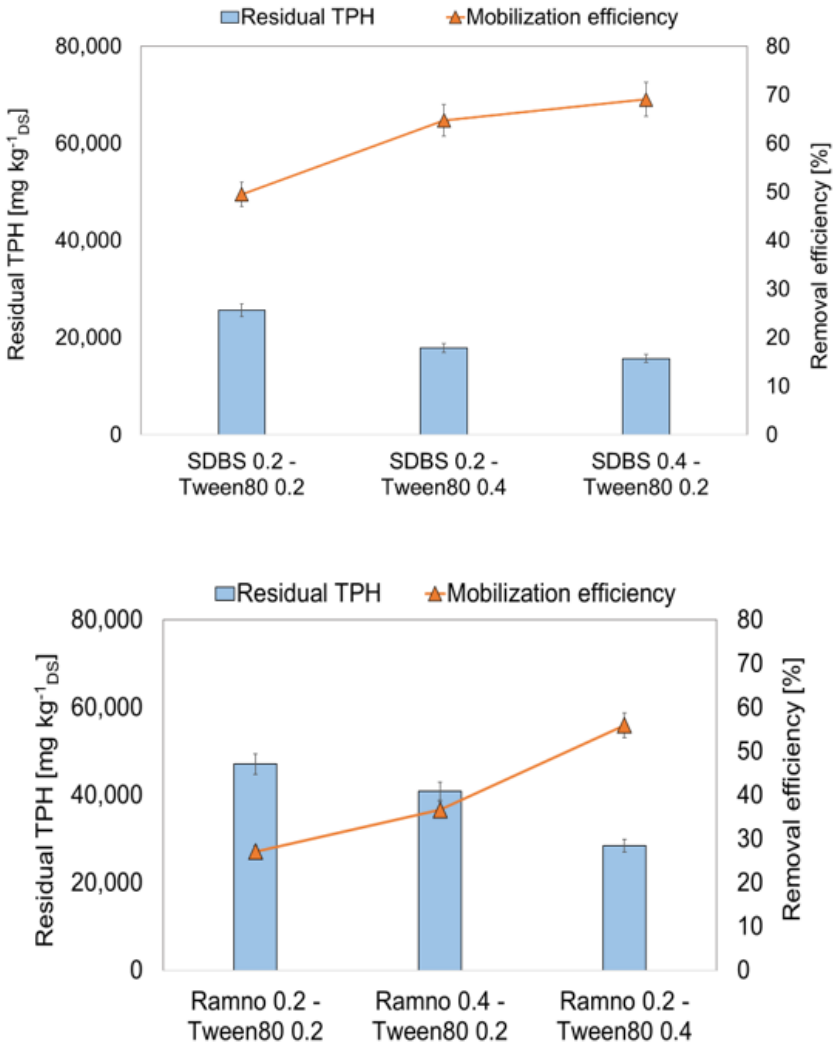

Figure 17: Average values of TPH residual concentration and removal efficiency from sediments using SDBS and Tween 80 (a) and Rhamnolipids and Tween 80 (b) as mixed surfactants, with standard deviation (Russo Tiesi et al., 2025).

From the observation of data reported in Figure 17, it is worth noting that the mobilization removal efficiency of TPH from sediment led to substantial increase in the mobilization removal yield of TPH for SDBS and

Tween 80 as mixed micelles (Figure 17a). In particular, the best results (η ≈ 69%) were achieved with SDBS at 0.4% and Tween 80 at 0.2%. Similarly, SDBS at 0.2% and Tween 80 at 0.4% reached a mobilization removal yield of about 65%. Finally, SDBS and Tween 80 both at 0.2% led to a mobilization removal yield of about 50%, slightly higher compared with the results achieved for each individual surfactant at a concentration of 0.4% (Figure 17). It is important to note that the other combination of mixed surfactants (i.e., Tween 80 and Rhamnolipids) started with a lower mobilization removal efficiency, even below that of Tween 80 or SDBS alone. Interestingly, as shown in Figure 17b, Rhamnolipids at 0.2% and Tween 80 at 0.4% led to a significant increase of the TPH mobilization removal yield, allowing to reach the third best result of all (η≈56%). Furthermore, when using Rhamnolipids at 0.4% and Tween 80 at 0.2%, a mobilization removal efficiency of 37% was achieved, i.e. above all the experiments with Rhamnolipids alone.

Additionally, the observed increase in rhamnolipid concentration corroborated the corresponding improvement in TPH removal efficiency previously reported when rhamnolipids are applied alone (Lai et al., 2009). Therefore, future research should evaluate the potential enhancement in TPH removal yields by employing Tween 80 at concentrations of 0.2% or 0.4% while further increasing rhamnolipid concentrations beyond 0.4%. Overall, the present findings confirm that combining anionic and nonionic surfactants to generate mixed micelles is a highly promising strategy, yielding the greatest removal efficiencies. As previously reported, the interaction between anionic and nonionic surfactants produces synergistic effects. Mixed micelles are formed through ion–dipole interactions between different hydrophilic groups, which mitigate both electrostatic and steric repulsion among surfactants of the same class. Consequently, nonionic molecules integrate into anionic micelles, decreasing electrostatic repulsion among hydrophilic head groups, facilitating micelle formation, and reducing the critical micelle concentration (Wu et al., 2024). This combination is characterized by a lower CMC, minimized adsorption and precipitation losses, and greater tolerance to fluctuations in temperature, salinity, pH, and other environmental parameters (Liu et al., 2021). Furthermore, previous studies have shown that incorporating nonionic surfactants into anionic surfactant solutions can limit precipitation induced by multivalent cations such as Ca^{2+} and Mg^{2+}, thereby reducing the loss of anionic surfactants to soil matrices (Zhao et al., 2005; Yang et al., 2006). Conversely, anionic surfactants may decrease the sorption of nonionic surfactants by weakening electrostatic attractions, promoting micelle formation and ultimately enhancing contaminant removal (Paria and Khilar, 2004; Guo et al., 2009; Yang et al., 2006). The results obtained in this study are consistent with those reported by Wu et al. (2024), who applied mixed micelles for the removal of benzo(a)pyrene from contaminated soil. Specifically, the authors employed an environmentally friendly and biodegradable anionic surfactant (MES) in combination with a nonionic surfactant (APG), achieving encouraging outcomes. Considering the limited number of studies addressing the use of diverse surfactants to form mixed micelles for soil and sediment washing in TPH-contaminated environments, the present work represents a meaningful contribution to the existing literature. These findings underscore the importance of further research aimed at optimizing surfactant combinations in mixed micelle systems to maximize remediation performance.

Phytotoxicity features of sediments after washing. Phytotoxicity tests based on the germination index (GI) indicated that sediment washing with different surfactants exerted distinct effects on sediment phytotoxicity. Figure 18 presents the mean GI values for all treatments, including standard deviations, together with the average removal efficiencies achieved with each surfactant. The elevated hydrocarbon concentrations in the contaminated sediment severely impaired its phytotoxic properties. In the untreated contaminated sample, germination of *L. sativum* seeds was nearly absent, with a very low GI value (2.24%) compared to the uncontaminated clay soil used as negative control.

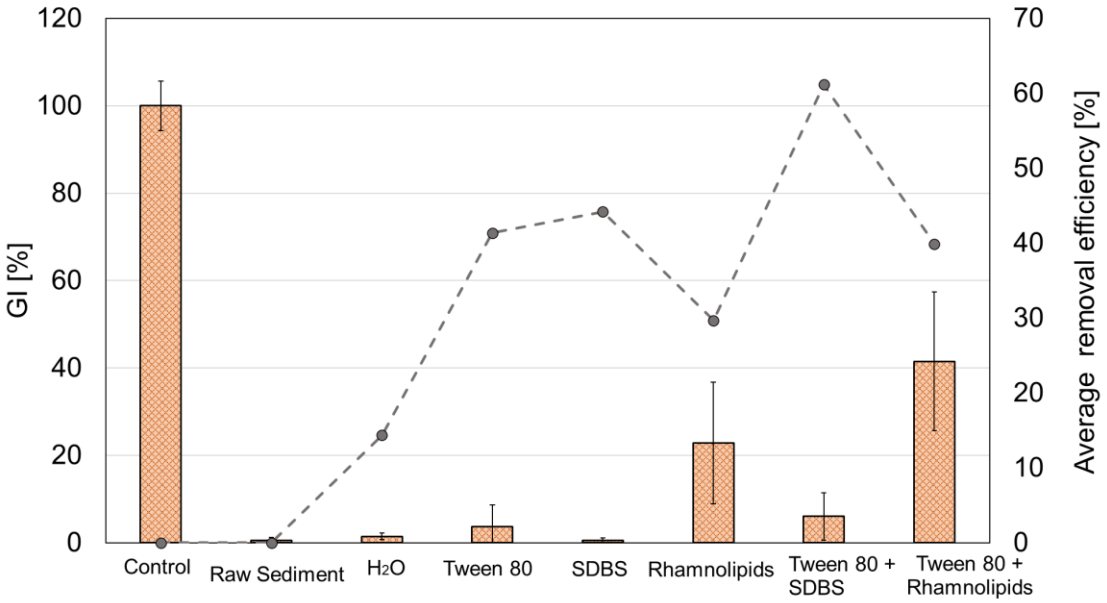

Figure 18: Average values of the germination index for the different samples with standard deviations and average values of removal efficiency (Russo Tiesi et al., 2025).

The results clearly demonstrate that the surfactants played different roles. Treatment with Tween 80 resulted in a GI of 3.7%, markedly higher than that observed with SDBS (0.54%), whose pronounced phytotoxicity has already been documented in the literature (De Marines et al., 2025). A similar pattern was observed for the Tween 80/SDBS mixture, which achieved a GI of 6.07%. This finding further supports the potential of combined Tween 80/SDBS solutions in sediment washing, not only to enhance hydrocarbon removal but also to mitigate residual phytotoxicity. The beneficial effect may be associated with the bioavailable organic carbon in Tween 80, which appears to enhance root permeability and thus promote nutrient uptake from the soil (Cheng et al., 2017). The application of rhamnolipids led to a substantial increase in GI (22.8%) compared to untreated sediment, highlighting the capability of these biosurfactants to attenuate contaminant-induced toxicity. This improvement can be attributed to the surfactant properties of rhamnolipids, which facilitate biodegradation and the removal of toxic compounds. When combined with Tween 80, rhamnolipids produced an even greater enhancement in GI (41.5%) relative to rhamnolipids alone, suggesting a synergistic interaction. This synergy is likely due to Tween 80's ability to increase contaminant solubility, thereby lowering toxicity and supporting plant recovery. Additionally, the higher GI may also be linked to improved nutrient solubility in the sediment, increasing nutrient availability to plants (Ferrans et al., 2022). The environmental compatibility of rhamnolipids is further evidenced by their use in agriculture for pathogen control and soil quality improvement (Eras-Muñoz et al., 2022). Overall, the improved germination of L. sativum appears to result from both the effective pollutant removal achieved with mixed surfactants—leading to lower residual TPH concentrations—and the reduced toxicity of the surfactants themselves, particularly Rhamnolipids. The higher toxicity of SDBS relative to the other tested surfactants has already been reported (Liu et al., 2021). Although widely used as a detergent and commonly discharged with greywater, its excessive use may pose risks to human health and the environment. SDBS can cause irritation and toxicity in aquatic systems, compromising water quality, and its limited biodegradability may lead to environmental persistence (Feng et al., 2022). Therefore, despite achieving high TPH removal rates—either alone or in combination with Tween 80—its application may conflict with the objectives of sustainable sediment remediation due to the risk of secondary contamination (Wu et al., 2024). Moreover, as illustrated in Figure 18, no clear correlation can be established between pollutant removal efficiency and residual phytotoxicity. Future studies should therefore

assess the potential benefits of an additional water-washing step following surfactant treatment to eliminate residual surfactants. Such an approach could mitigate adverse effects associated with surfactant residues and potentially enhance TPH removal if TPH–surfactant complexes remain in the sediment. In contrast, Rhamnolipids represent a promising class of biosurfactants that are increasingly attracting attention due to their eco-friendly profile and lower toxicity compared with synthetic surfactants such as SDBS and Tween 80 (Ambaye et al., 2021; Liu et al., 2021). This strategy aligns with the recent Directive 2025/2360 of the European Parliament on soil monitoring and resilience, which emphasizes the need to remediate contaminated soils using approaches that preserve soil ecosystem integrity. The directive explicitly states that remediation measures should avoid secondary pollution and prevent additional ecotoxic effects.

4.1.2.4 Main conclusion of the study

This study offers new evidence on the application of single and mixed surfactant systems for the remediation of heavily hydrocarbon-contaminated marine sediments. By investigating a complex real sediment matrix, it evaluated both TPH removal efficiency and the residual phytotoxicity of treated sediments. The results confirmed the feasibility of using mixed surfactants, showing a significant enhancement in TPH removal compared to single-surfactant systems, likely due to mixed micelle formation. The highest removal efficiency (approximately 70%) was achieved with the anionic/nonionic combination of SDBS and Tween 80. However, substantial differences emerged in terms of residual phytotoxicity: SDBS-treated sediments exhibited pronounced phytotoxic effects, whereas treatments with Tween 80 and/or rhamnolipids resulted in lower residual toxicity, despite somewhat lower extraction efficiencies. This behavior highlights the more environmentally compatible profile of biodegradable or less toxic surfactants, in line with sustainable remediation objectives and the proposed Directive on soil quality. For severely contaminated sediments, future research should investigate higher concentrations of natural or biodegradable surfactants, assess sediment washing as a pretreatment step within integrated treatment trains, and explore strategies to remove residual surfactants in order to prevent secondary contamination. Overall, these findings contribute to the development of eco-efficient and scalable sediment remediation approaches consistent with emerging soil protection policies.

4.1.3 Oxidation of petroleum hydrocarbons in soil using potassium ferrate as new oxidizing agent: process optimization and benchmarking

4.1.3.1 Introduction

Environmental contamination remains a major concern due to its impacts on human health, and the environment (Islam et al., 2017). Soil contamination by petroleum hydrocarbons (PHC) poses a serious risks owing their mutagenic, carcinogenic, and toxic properties (ITRC, 2014; U.S.EPA, 2015). The health and environmental risks of PHC are further influenced by the chemical composition of hydrocarbons, the exposure duration, and the pathways (U.S.EPA, 2022). Thus, the development of effective and sustainable treatment strategies is critical. In recent years, several physical, chemical or biological methods have been developed and tested (Gautam et al., 2020; Ritoré et al., 2023, Zhang et al., 2024). Among them, chemical oxidation, especially advanced oxidation processes (AOPs), has emerged as a promising approach for the degradation of organic pollutants (Fang et al., 2013). Widely used in water treatment, AOPs can also be adapted for subsurface applications, such as in situ chemical oxidation (ISCO) of soils and groundwater (Han et al., 2015; Feng et al., 2017). Surfactant-enhanced ISCO (S-ISCO) improves the solubility of hydrophobic contaminants, facilitating oxidation, but concerns remain regarding the toxicity of residuals and byproducts formed during treatment (Besha et al., 2018; Zhao et al., 2025). This highlights the need for oxidation techniques that are not only efficient and cost-effective but also minimise the formation of toxic byproducts. Ferrate (Fe(VI)) is a high-potential oxidant with combined oxidative and coagulative properties (2.20 V in acidic and 0.78 V in alkaline conditions), producing non-toxic Fe(III) end products (Wang et al., 2020; Acosta-Rangel et al., 2020),. While effective in degrading pharmaceuticals, personal care products (PPCPs), phenols, bisphenols, benzophenones, and halogenated flame retardants (Luo et al., 2021), its application for soil remediation, particularly for hydrocarbon-contaminated matrices, remains underexplored (Rai et al., 2018; Liu et al., 2022). Potassium ferrate (K_2FeO_4), or more broadly ferrate (VI), thus presents a relatively novel option for soil treatment, with additional potential to exploit natural organic matter, such as humic substances, for in situ activation, and reducing the need for synthetic surfactants.

This study provides one of the first systematic investigations of potassium ferrate (K_2FeO_4) for the remediation of a diesel-contaminated soil, including optimization of its dosing strategy and interaction with surfactants and natural organic matter. Unlike prior studies focused on water treatments, this work evaluates complex soil matrices. The study further demonstrates the capability of in situ humic substances to enhance Fe(VI) activation, reducing the need for synthetic surfactants. The findings aim to support the development of effective Fe(VI)-based oxidation strategies for hydrocarbon-contaminated soils by providing novel and useful insights for full-scale applications.

4.1.3.2 Materials and Methodologies

Two different soils (P1 and P2) were used in this study. Their physical and chemical properties are summarised in Table 5. Both soils were artificially contaminated with diesel fuel at a concentration of 1% (w/w). To ensure homogeneous contamination, diesel fuel was added to the soils during continuous mixing, followed by an additional 15 minutes of mixing. The spiked soils were then manually mixed and aged for 15 days to allow partial volatilisation of light hydrocarbons. To assess the potential loss of total petroleum hydrocarbons (TPH) due to volatilisation during the ageing period, a 48-hour test was conducted. Contaminated soil samples were mixed with tap water under gentle agitation, and TPH levels in both solid and liquid phases were measured.

Results showed that the TPH mass measured after 48 hours (in both solid and liquid phases) differed from the initial TPH content by 9.9% for Soil 1 and 12.6% for Soil 2, indicating that volatilisation contributed negligibly to the overall TPH loss.

Table 5: Summary of the experimental tests carried out at different

Soil	Sand [%]	Silt [%]	Clay [%]	pH	TOC [g/kg]	TPH [mg/kg]
P1	91,6	6.2	2.2	7.6	8.3	2260 ± 237
P2	63	22	15	7.8	31.4	4510 ± 226

The oxidants used were potassium ferrate (K_2FeO_4) and potassium permanganate ($KMnO_4$), and the anionic surfactant sodium dodecylbenzenesulfonate (SDBS) was used to enhance TPH solubilisation. The main characteristics of the chemicals are provided in Table 6.

Table 6: Characteristics of SDBS and Fe(VI)

Chemical nomenclature	CAS number	Chemical formula	Ionic Nature	Purity	Molecular weight [g/mol]	CMC* [mM]
Sodium Dodecyl Benzene-Sulfonate	25155-30-0	$C_{18}H_{29}NaO_3S$	anionic	90%	348.48	0.612
Potassium ferrate	39469-86-8	K_2FeO_4	-	99%	198.04	-
Potassium permanganate	7722-64-7	$KMnO_4$	-	97%	158.3	-

*Critical Micelle Concentration

Experimental procedure and oxidant use. All experiments were carried out in slurry mode using 100 g of diesel contaminated soil mixed with 500 mL of tap water. A standard jar test apparatus was used for mixing, involving three sequential steps: (i) rapid mixing at 200 rpm for 5 minutes; (ii) slow mixing at 40 rpm for 48 hours and (iii) Settling for 30 minutes. The experimental set-up was conducted in two phases, namely Phase 1 and Phase 2. In Phase 1, the objective was to optimise the treatment protocol for diesel contaminated soil using K_2FeO_4 in combination with SDBS, using soil P1. Two application strategies were tested as follows: Strategy 1 (S1) where SDBS and K_2FeO_4 were added simultaneously at the onset the treatment. Four conditions were evaluated (Table 3). The second strategy (S2) consisted of adding SDBS first and mixed gently for 24 hours to pre-solubilise diesel components. K_2FeO_4 was added afterwards, followed by the same mixing and settling steps as in S1. This strategy was designed to enhance TPH bioavailability by allowing sufficient surfactant interaction prior to oxidation (Ritoré et al., 2022; Zhang et al., 2024).

In Phase 2, a comparative evaluation of K_2FeO_4 and potassium permanganate ($KMnO_4$) was carried out using soil P2, which was freshly spiked with diesel fuel using S2 strategy. The investigated conditions are summarized in Table 7.

Table 7: Overview of the experimental conditions evaluated in Phase 1 and Phase 2

Phase		Condition	[oxidant] (% w/w)	[SDBS] (% w/w)	CMC multiple*
1	1	K_2FeO_4 alone (Control)	0.5/ 1.0 / 1.5	0	0
	2	K_2FeO_4 + low SDBS	0.5/ 1.0 / 1.5	0.1	5×
	3	K_2FeO_4 + medium SDBS	0.5/ 1.0 / 1.5	0.2	10×
	4	K_2FeO_4 + high SDBS	0.5/ 1.0 / 1.5	0.4	20×
2	1	$KMnO_4$ alone (Control)	0.5/ 1.0 / 1.5	0	0
	2	$KMnO_4$+ low SDBS	0.5/ 1.0 / 1.5	0.1	5×
	3	$KMnO_4$+ medium SDBS	0.5/ 1.0 / 1.5	0.2	10×
	4	$KMnO_4$+ high SDBS	0.5/ 1.0 / 1.5	0.4	20×

*SDBS concentrations were selected to represent 5×, 10×, and 20× the critical micelle concentration (CMC) to promote desorption and solubilisation of hydrophobic contaminants into the aqueous phase (Li et al., 2019; Qiu et al., 2019).

Analytical Methods. TPH in soils were measured according to the "Procedure for the analysis of hydrocarbons >C12 in contaminated soils - Manuals and Guidelines 75/11" (ISPRA, 2011), which is based on the ISO 16703 (2004). The method includes solid-phase extraction, purification on Florisil, and subsequent analysis using an Agilent 8890N Network gas chromatography system equipped with a flame ionisation detector and an Agilent 7693 autoinjector tower, purchased in the frame of RETURN Project (Figure 19). TPH in the aqueous phase were measured using the "Oil Index" method (UNI EN ISO 9377-2:2002).

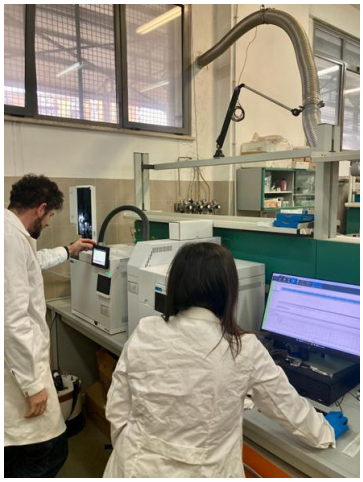

Figure 19: View of the Agilent 8890N Network gas chromatography system during TPH analysis

Ferrate concentration was determined spectrophotometrically at 510 nm using a UV-Vis spectrophotometer (Beckman Coulter DU 720). Two calibration curves (0–1 g/L and 1-5 g/L) were established with commercial potassium ferrate (99% purity) as the standard. Prior to analysis, all samples were filtered through 0.45 µm cellulose membranes to remove particulate matter.

Residual soil phytotoxicity was assessed using the germination index (GI) following the procedure outlined by APAT (2004) and using Lepidium sativum (garden cress) as the test species. Seeds were placed in 90 mm Petri dishes lined with filter paper sheet as support (Avona et al., 2022).

4.1.3.3 Results and discussion

Effect of Fe(VI) dosing strategy on TPH removal. Figure 20 compares TPH removal efficiencies in Phase 1 under the two dosing strategies.

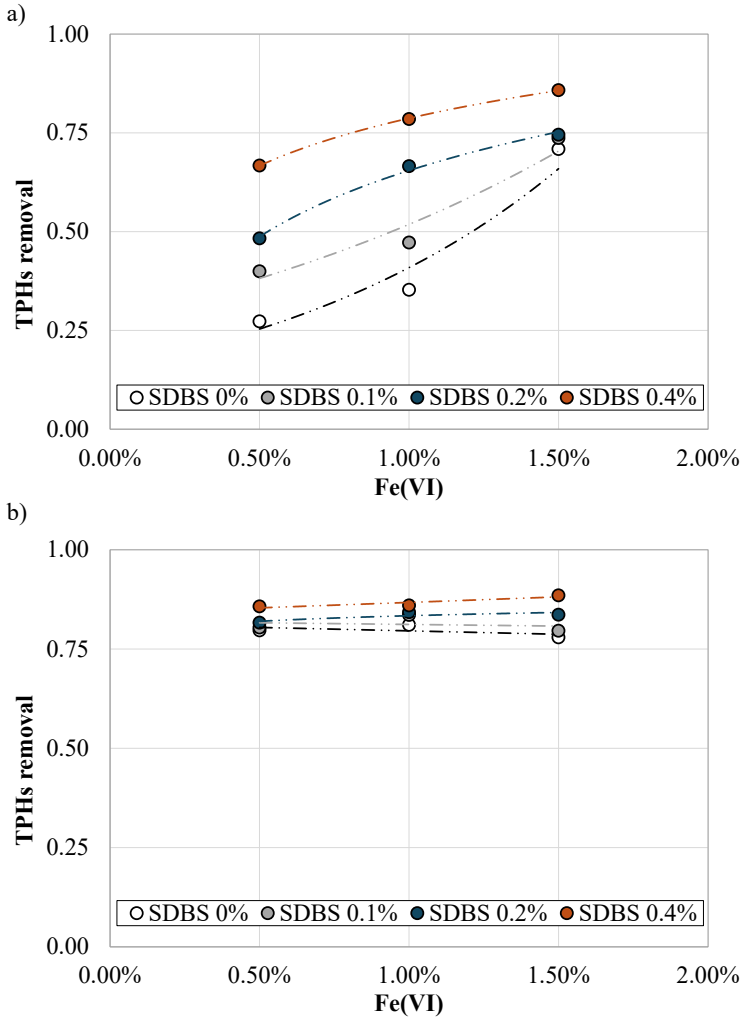

Figure 20: TPHs removal efficiencies in Phase 1 S1 (simultaneous spiking) (a) and in Phase 1 S2 (24 hours delayed Fe(VI) spiking) (b).

Simultaneous addition of SDBS and Fe(VI) (S1) showed a dose-dependent increase in TPH removal, reaching 83% at 1.5% Fe(VI) and 0.4% SDBS. Fe(VI) alone was significantly less effective, highlighting the importance

of surfactant-facilitated solubilization. which is in good agreement with previous studies (Li et al., 2019; Qiu et al., 2019; Ritoré et al., 2022). In contrast, the delayed Fe(VI) dosing (S2) consistently yielded high TPH removal (78–89%) across all tested concentrations even without SDBS (Figure 1b). Delaying Fe(VI) dosing likely allowed for greater desorption of TPH into the aqueous phase and reduced competition for oxidant (Deng et al., 2018; Wang et al., 2022). This suggests that allowing a 24-hour pre-contact period enhances TPH desorption into the aqueous phase and reduces oxidant competition, while natural humic substances in the soil may act as in situ Fe(VI) activators (Guigue et al., 2015; Barışçı, 2017). Together, these findings explain the higher TPH removal observed under delayed dosing conditions, highlighting the importance of both contaminant availability and intrinsic soil-mediated oxidant activation.

TPH mass balance in solid and liquid phases. In S1, the residual TPH decreased with increasing Fe(VI) doses, but maximum efficiency was only achieved when both Fe(VI) and SDBS were used (Figure 21a). In S2, significantly lower residual TPH in solids was achieved, even without SDBS, confirming the enhanced Fe(VI) activation via prolonged soil-water contact (Figure 21c) (Cui et al., 2024).

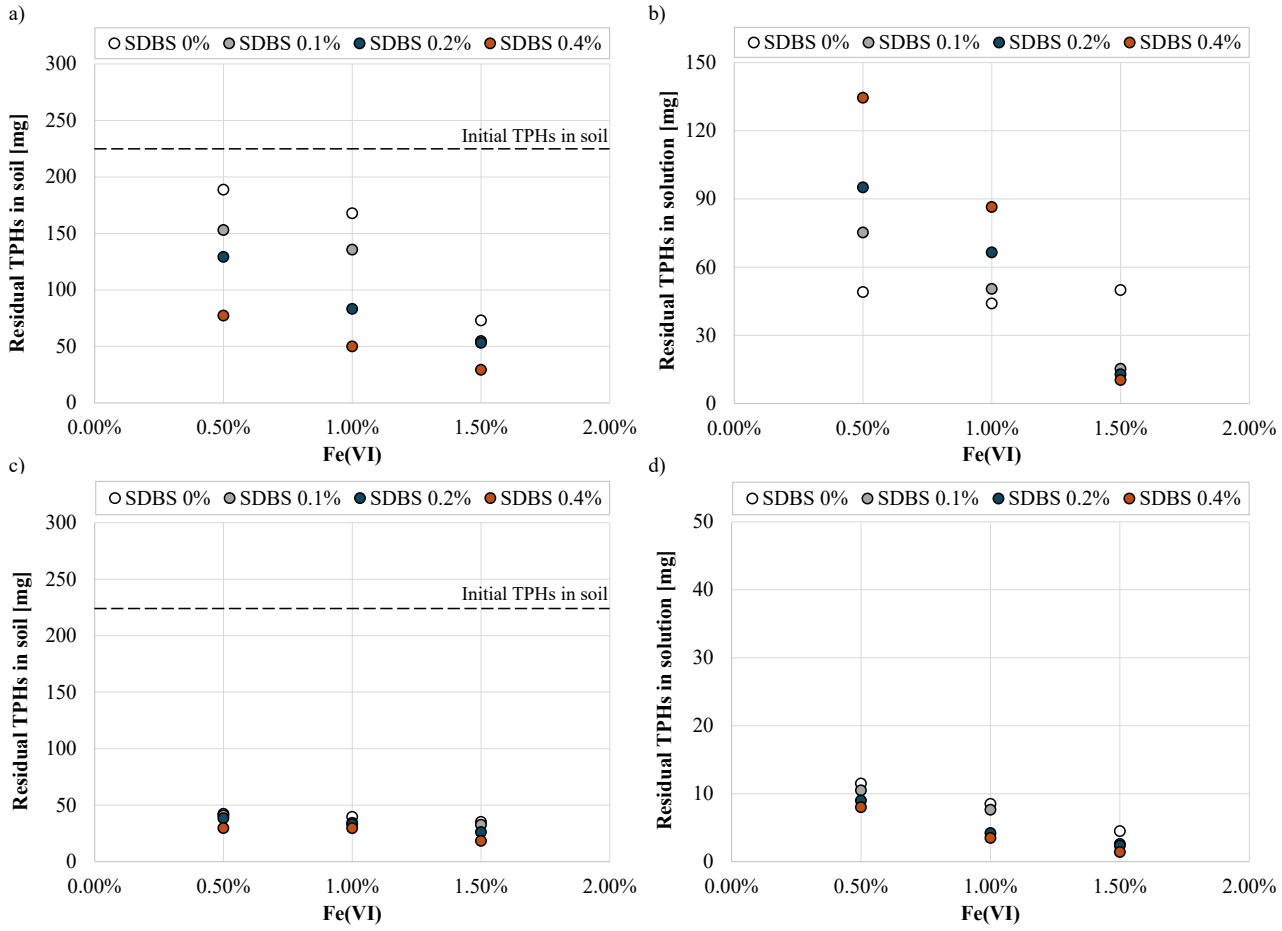

Figure 21: Residual TPHs in P1 S1 in soil (a) and in liquid (b) after treatment with simultaneous dosage of both Fe(VI) and SDBS; residual TPHs in P1 S2 in soil (c) and in liquid (d) after treatment with Fe(VI) dosed 24 hours later than SDBS.

The absence of TPH accumulation in the aqueous phase confirms that removal was predominantly due to oxidative degradation. The mass balance results confirm that TPH removal is predominantly attributable to oxidative degradation rather than physical partitioning or volatilization. This is supported by the minimal TPH accumulation in the aqueous phase across all scenarios (Figure 2b and 2d), indicating that solubilized hydrocarbons were effectively oxidized. This has important implications for field application, as it suggests a reduced risk of contaminant mobilization and potential groundwater contamination (Liu et al., 2021; Wei et al., 2022). Results also provide indirect evidence that Fe(VI) can penetrate the soil matrix and oxidize sorbed-phase hydrocarbons, a key performance barrier in soil remediation efforts (Mohinuzzaman et al., 2020).

Comparison with permanganate oxidation efficiencies. Phase 2 results (Figure 22) show that K_2FeO_4 achieved >90% TPH removal under all tested conditions. The best performance (96%) occurred with high doses of both chemicals.

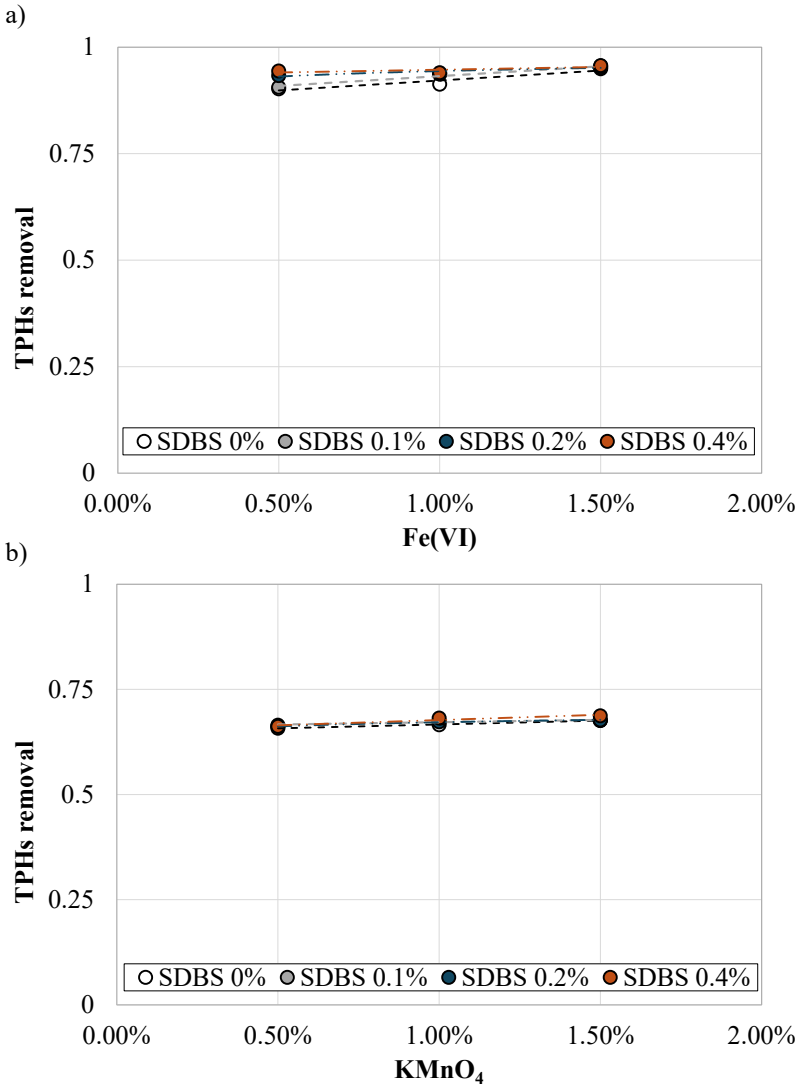

Figure 22: TPHs removal efficiencies in Period 2: Potassium Ferrate (a) and Potassium Permanganate (b).

These results align with previous findings where Fe(VI) effectiveness increased after humic acid release (Guigue et al., 2015; Deng et al., 2018; Wang et al., 2022). Compared to $KMnO_4$, Fe(VI) achieved a 27% higher removal efficiency under equivalent dosing conditions. More precisely, $KMnO_4$ removal efficiencies ranged between 66% and 69% (Figure 3b), corroborating findings by Yen et al. (2011), Johansson et al. (2020),

and Ritoré et al. (2023). The lower $KMnO_4$ performance is attributed to competitive consumption by soil organic matter, which limits its oxidising capacity. The results of the present study confirm the general behaviour of both oxidants, in the case of soils contaminated by petroleum hydrocarbons; it was highlighted the beneficial role of organic matter in soil oxidation with Fe(VI), while, at the same time, the performance of $KMnO_4$ were reduced by the presence of organics. These results could provide useful information in view of treatment scale-up for field applications.

Figure 23 confirms that residual TPH in solids was an order of magnitude lower with K_2FeO_4 compared to $KMnO_4$. However, $KMnO_4$ exhibited relatively higher TPH removal in the aqueous phase. However, $KMnO_4$ exhibited relatively higher TPH removal in the aqueous phase.The side-by-side comparison (Figure 23) with potassium permanganate ($KMnO_4$) highlights the superior performance of Fe(VI). Indeed, residual TPH in solids was an order of magnitude lower with K_2FeO_4 compared to $KMnO_4$ (Figure 23a vs. 234c). This aligns with literature describing the limitations of permanganate in soils with high organic matter content, where oxidant demand from natural substrates can significantly reduce efficiency (Yen et al., 2011; Johansson et al., 2020).

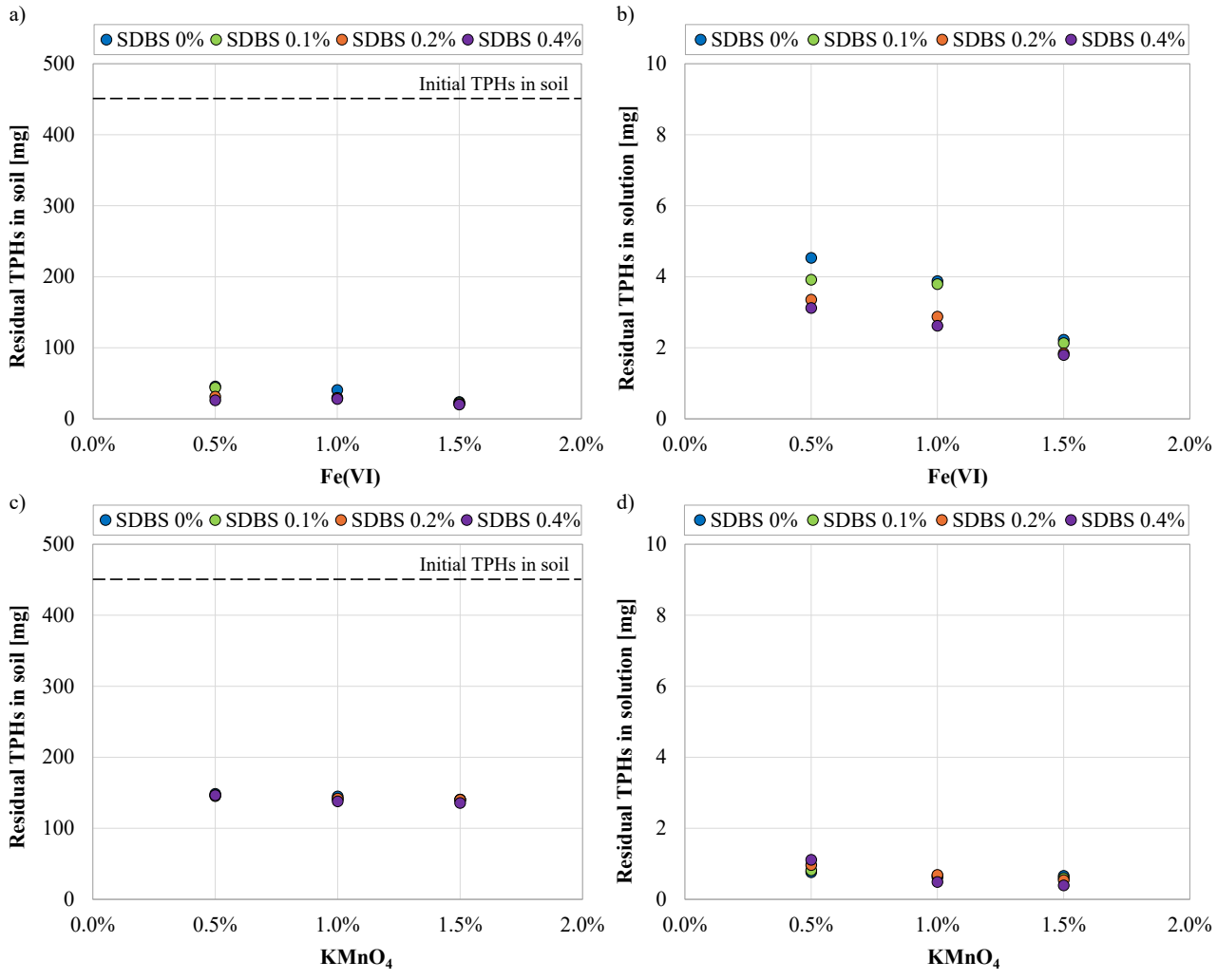

Figure 23: TPHs removal efficiencies in Period 2: Potassium Ferrate (a) and Potassium Permanganate (b).

In contrast, Fe(VI) appears to maintain high oxidative capacity even in organic-rich matrices; additionally, the stronger performance of Fe(VI) in the solid phase reinforces its suitability for source zone treatment, where

contaminants are often tightly bound to soil particles. However, $KMnO_4$ exhibited relatively higher TPH removal in the aqueous phase. Overall, these results demonstrate the unique advantage of Fe(VI) for treating tightly bound contaminants and reinforces its potential for environmentally efficient, surfactant-minimized strategies.

Residual phytotoxicity. Despite the promising contaminant removal results, all treatments resulted in significant phytotoxicity, with germination index (GI) values remaining below 45% (Figure 24). This suggests that chemical oxidation alone may not be sufficient to restore ecological functionality without further soil conditioning. All treatments showed GI values <45%, indicating phytotoxicity. The untreated soil (positive control) had a GI of 63.6 ± 6.8%, confirming minimal diesel toxicity on germination (Smith et al., 2005; Smith et al., 2006; Sirguey et al., 2008; De Marines et al., 2025). SDBS was the main contributor to toxicity due to its poor biodegradability (~20%) and inherent phytotoxic effects (Garon et al., 2002; Singh and John, 2013; Han et al., 2019; Masoudian et al., 2020; Di Trapani et al., 2023). Interestingly, Fe(VI) treatments also induced phytotoxicity, likely due to the alkaline environment it induces (pH >13) and was more phytotoxic than $KMnO_4$. These findings are consistent with Sirguey et al. (2008), who observed negative impacts of $KMnO_4$ on ryegrass. However, this finding reinforces the need for post-treatment stabilization measures, such as pH neutralization or organic amendments, particularly in scenarios targeting land reuse or revegetation. These insights emphasize the value of integrating chemical performance with ecotoxicological criteria in remediation treatments, a practice that is still not widely implemented in soil oxidation studies.

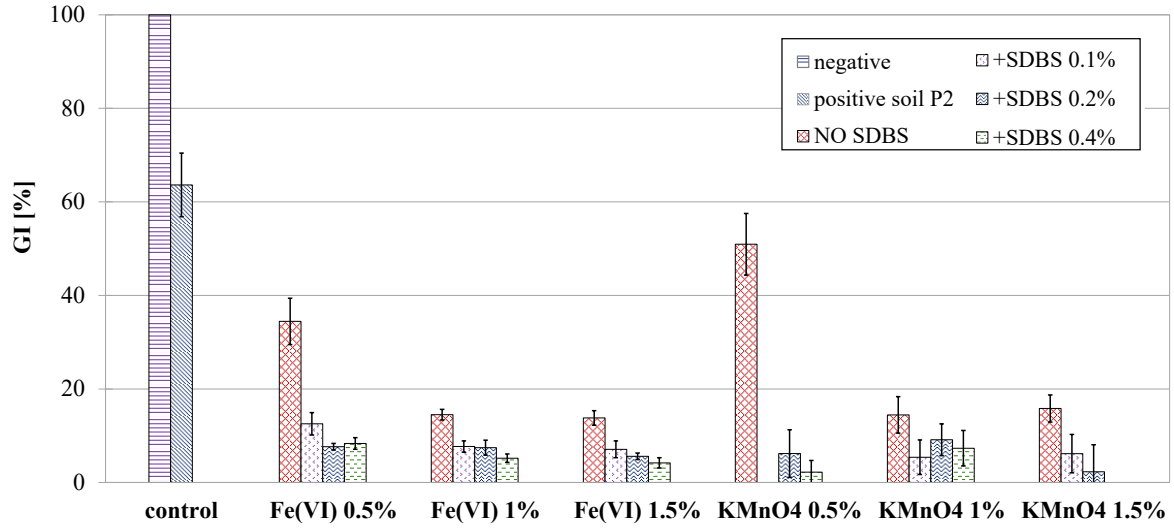

Figure 24: Germination Index in soil before and after treatment in Period 2.

4.1.3.4 Main conclusions of the study

This study demonstrates that ferrate (VI) is a highly effective oxidant for the remediation of diesel-contaminated soils, particularly when applied using a delayed dosing strategy. Allowing the surfactant to interact with the soil prior to oxidant addition significantly enhanced TPH desorption and removal, indicating the importance of optimising the sequence of reagent application in chemical oxidation treatments. A noteworthy outcome is the high removal efficiency achieved even in the absence of added surfactant, suggesting that natural soil constituents such as humic and fulvic acids can facilitate ferrate activation. This finding highlights the potential of exploiting in situ activation mechanisms to reduce the reliance on synthetic

additives, offering a more sustainable approach to remediation. Further to this, the comparative experiments with potassium permanganate confirmed the superior performance of ferrate, particularly in the solid phase, where it consistently achieved higher TPH removal. Nevertheless, all treatments involving ferrate and SDBS resulted in measurable phytotoxicity, highlighting the need for post-treatment strategies to mitigate ecological risks, especially where land reuse or revegetation is intended. Overall, the findings contribute to a better understanding of ferrate chemistry in complex environmental matrices and provide a practical basis for refining in situ chemical oxidation approaches. By coupling contaminant removal with phytotoxicity assessment, the study demonstrates the importance of integrating chemical effectiveness with environmental compatibility in the design of remediation technologies.

4.1.4 Petroleum hydrocarbons oxidation in marine sediments: first trials with potassium ferrate as a new chemical and comparison with potassium permanganate

4.1.4.1 Introduction

Chemical pollution represents a major global concern due to the intentional and accidental release of contaminants into the environment, with estimated annual emissions ranging between 120,000 and 220,000 million tonnes (Naidu et al., 2021). Among the primary contributors to this issue are petroleum-related industrial activities, such as transportation, drilling, storage, exploration, refining, and processing, which are responsible for substantial releases of petroleum hydrocarbons into the environment (Ambaye et al., 2024). In particular, the contamination of marine sediments associated with anthropogenic activities constitutes one of the most pressing environmental challenges, especially in regions subjected to decades of unregulated industrial operations, including cement and steel manufacturing, fertilizer production, chlor-alkali plants, and crude oil refining (Proietto et al., 2024). Marine sediments function as the principal repository for both organic and inorganic contaminants introduced into aquatic systems, including heavy metals, polychlorinated biphenyls (PCBs), polycyclic aromatic hydrocarbons (PAHs), and petroleum hydrocarbons (HCs), largely originating from industrial and human activities (Chen et al., 2020). Owing to the dynamic interactions between sediments and overlying waters, sediments can act not only as sinks but also as secondary sources of pollutants through processes of adsorption and release (Zhang et al., 2021). Compared to terrestrial soils, marine sediments pose additional challenges due to their elevated organic matter content, which promotes contaminant adsorption and persistence. This characteristic enhances pollutant mobility within aquatic environments, facilitating their transfer into the food web and ultimately posing risks to human health through seafood consumption (Meric et al., 2012). Petroleum hydrocarbons are of particular concern, as certain fractions exhibit mutagenic, carcinogenic, and teratogenic properties, and may impair reproductive functions in marine organisms (Zhou et al., 2014). Their hydrophobic nature and low water solubility favor their accumulation in organic-rich sediments. Consequently, increasing attention has been directed toward the implementation of environmental regulations and management strategies aimed at improving environmental quality. In this context, the remediation of contaminated sediments has emerged as a critical priority for the protection of ecosystems and human health. In recent years, several physical, chemical or biological methods have been developed and tested (Gautam et al., 2020; Ritoré et al., 2023, Zhang et al., 2024); among these remediation techniques, chemical oxidation and surfactant washing have gained particular attention. In this study, the potential of surfactant-enhanced oxidation for HCs removal from contaminated marine sediments was investigated. The anionic surfactant sodium dodecylbenzene sulfonate (SDBS) was used to improve to improve the solubility and availability of HCs, thus facilitating oxidation (Besha et al., 2018; Herzog et al., 2023). The oxidation efficiency of a new advanced oxidant, Fe(VI), was compared with potassium permanganate (KMnO4), a conventional oxidant used in chemical sediment remediation. Parameters evaluated include (i) Fe(VI), KMnO4 and surfactant concentration dose, (ii) the influence of NOM content and (iii) residual phytotoxicity after treatment.

4.1.4.2 Materials and Methodologies

Marine sediments characteristics and diesel fuel contamination. The sediment used during the experiments was dredged from Augusta Bay (Italy), a contaminated site of national interest. Table 8 summarizes the main features of the investigated marine sediments. Since the HCs concentration was below the regulatory limit (750 mg/kg), the sediments were artificially contaminated with diesel fuel to achieve a higher level of HCs contamination.

Table 8: Main features of the sediments before contamination

Parameter	Units	Value
Residue at 105°C	%	53.5
pH	-	9
EC	mS/cm	2.6
TOC	g/kg	2.2
Mercury	mg/kg_{DS}	16
Hydrocarbons C<12	mg/kg_{DS}	<0.3
Hydrocarbons C>12	mg/kg_{DS}	130

Commercial diesel fuel was added to the raw sediment at a concentration of 1% (w/w). To ensure homogeneous contamination, diesel fuel was added to the sediment during continuous mixing, followed by an additional 15 minutes of mixing. The spiked soils were then manually mixed and aged for 15 days to allow partial volatilisation of light hydrocarbons. Subsequently, the drying phase was completed by placing the sample in an oven at 40°C for 72 hours, ensuring a uniformly contaminated sediment for the subsequent washing tests. The subsequent pretreatment phases focused on crushing and sieving the dried sediment, with the aim of isolating the fine fraction. This choice was driven by the fact that the concentration of hydrocarbons adsorbed onto the solid matrix usually is closely related to the specific surface area, becoming higher as the particle size decreases (Rajabi et al., 2018). Specifically, the dried sample was first crushed using a mortar and pestle to reduce particle size and then subjected to sieving. The sieving process was performed using a two-stage sieve system with mesh sizes of 2 mm and 63 µm. After the artificial contamination, the sediment fraction < 63 µm was characterized by a HC concentration equal to 6090 mg/kg (±836 mg/kg).

Chemicals and reagent characteristic. The oxidants used were potassium ferrate (K_2FeO_4) and potassium permanganate ($KMnO_4$), and the anionic surfactant sodium dodecylbenzenesulfonate (SDBS) was used to enhance TPH solubilisation. The main characteristics of the chemicals are provided in Table 9.

Table 9: Characteristics of SDBS, Fe(VI) and KMnO4

Chemical nomenclature	CAS number	Chemical formula	Ionic Nature	Purity	Molecular weight [g/mol]	CMC* [mM]
Sodium Dodecyl Benzene-Sulfonate	25155-30-0	$C_{18}H_{29}NaO_3S$	anionic	90%	348.48	0.612
Potassiumferrate	39469-86-8	K_2FeO_4	-	99%	198.04	-
Potassium permanganate	7722-64-7	$KMnO_4$	-	97%	158..3	-

Experimental procedure and oxidant use. All experiments were carried out in slurry mode using 100 g of diesel contaminated sediment mixed with 500 mL of tap water. A standard jar test apparatus (Figure 25) was used for mixing, involving three sequential steps: (i) rapid mixing at 200 rpm for 5 minutes; (ii) slow mixing at 40 rpm for 48 hours and (iii) settling for 30 minutes. The experimental set-up was conducted in two phases. In phase 1, the objective was evaluating the treatment protocol for diesel contaminated sediment using K_2FeO_4 in combination with SDBS; instead, in the second phase, the efficiency of permanganate was evaluated. In both phases SDBS was first added to the solution and mixed gently for 24 hours to pre-solubilise diesel components. The oxidant was added afterwards, followed by the mixing and settling steps. This strategy was designed to enhance HC bioavailability by allowing sufficient surfactant interaction prior to oxidation (Ritoré et al., 2022; Zhang et al., 2024). Moreover, to assess the potential loss of HCs due to volatilisation during the ageing period, a 48-hour test was conducted, and sediment samples were mixed with tap water under gentle agitation. The investigated conditions are summarized in Table 10.

Figure 25: Jar test apparatus used for the batch tests

Table 10: Overview of the experimental conditions

Phase	Condition		[oxidant] (% w/w)	[SDBS] (% w/w)	CMC multiple*
Water			0	0	0
1	1	K_2FeO_4 alone (Control)	0.5 / 1.0 / 1.5	0	0
	2	K_2FeO_4 + low SDBS	0.5 / 1.0 / 1.5	0.1	5×
	3	K_2FeO_4 + medium SDBS	0.5 / 1.0 / 1.5	0.2	10×
	4	K_2FeO_4 + high SDBS	0.5 / 1.0 / 1.5	0.4	20×
2	1	$KMnO_4$ alone (Control)	0.5 / 1.0 / 1.5	0	0
	2	$KMnO_4$+ low SDBS	0.5 / 1.0 / 1.5	0.1	5×
	3	$KMnO_4$+ medium SDBS	0.5 / 1.0 / 1.5	0.2	10×
	4	$KMnO_4$+ high SDBS	0.5 / 1.0 / 1.5	0.4	20×

*SDBS concentrations were selected to represent 5×, 10×, and 20× the CMC to promote desorption and solubilisation of hydrophobic contaminants into the aqueous phase (Li et al., 2019; Qiu et al., 2019).

Analytical methods. The measurement of TPHs concentration in the solid phase as well as the residual phytotoxicity after the washing tests, were evaluated according to what already discussed in the previous section. The analysis of mercury before and after oxidation treatment was performed through an ICP-MS analyser (Inductively Coupled Plasma Mass Spectrometry), purchased in the frame of RETURN Project. In the following Figure 26, some details of the ICP-MS are shown.

Figure 26: Panoramic view of the ICP-MS analyser used during experiments.

4.1.4.3 Results and discussion

Petroleum hydrocarbon removal efficiency. Figure 27 illustrates the HC removal efficiencies achieved with $KMnO_4$ and Fe(VI) at different oxidant dosages and SDBS concentrations.

$KMnO_4$ treatments (Figure 27a) resulted in relatively high HC removal efficiencies (~35–55%) under all tested conditions. The good performance observed even at the lowest oxidant dosage (0.5%) is consistent with literature reporting that low organic matter content reduces non-specific oxidant consumption and competitive scavenging reactions, thereby improving permanganate efficiency (Johansson et al., 2020; Ritoré et al., 2023). In sediments with limited natural organic matter, a greater fraction of $KMnO_4$ remains available for target contaminant oxidation.

Increasing $KMnO_4$ concentration beyond 0.5% did not result in substantial additional removal. Under low NOM conditions, oxidant demand from the matrix is reduced, and contaminant accessibility may become the limiting factor rather than oxidant availability. Furthermore, the possible MnO2 precipitation formed during permanganate reduction may partially hinder oxidant transport within sediment pores, limiting further improvements at higher dosages (Xu et al., 2022). In contrast, Fe(VI) treatments (Figure 27b) showed lower efficiencies at 0.5% and 1% dosages, with a marked improvement only at 1.5%. Ferrate(VI) oxidation involves reduction to Fe(III), often through highly reactive intermediate species such as Fe(V) and Fe(IV), which contribute to contaminant degradation (Barışçı, 2017; Sharma, 2013).

Importantly, recent studies have demonstrated that natural organic matter, particularly humic and fulvic substances, may enhance ferrate oxidation by promoting electron transfer processes and facilitating the formation of reactive intermediates (Sun et al., 2019). Given the low NOM content of the investigated sediment, this activation pathway is likely limited, which may explain the comparatively lower removal efficiencies observed at lower Fe(VI) dosages. Only at 1.5% Fe(VI) does direct oxidation appear sufficient to achieve HC removal approaching that of $KMnO_4$. These findings align with recent evidence highlighting the dependence of ferrate efficiency on sediment composition and the presence of organic activators (Barışçı,

2017; Sharma et al., 2022; Sun et al., 2019). Lastly, for both oxidants, HC removal increased progressively with rising SDBS concentration. This confirms that contaminant desorption and mass transfer limitations are key controlling factors in low NOM sediment, where hydrocarbons are likely associated predominantly with mineral surfaces.

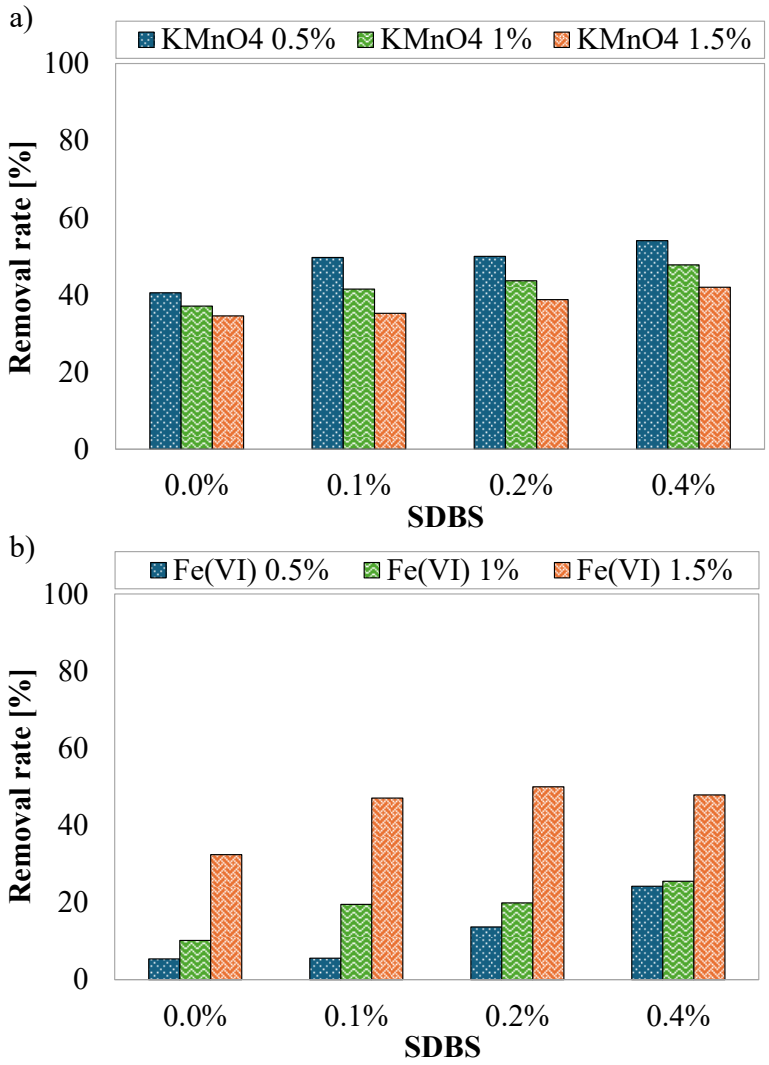

Figure 27: HC removal rate from sediment after treatment with KMnO4 (a) and Fe(VI) (b)

Residual mercury after treatment. Residual mercury concentrations obtained after treatment are presented in Figure 28. Overall, both oxidants were able to partially reduce Hg concentrations in the contaminated sediment; however, different trends were observed depending on the oxidant type and dosage. In the case of $KMnO_4$ (Figure 28a), mercury removal remained relatively limited under the investigated conditions, with residual concentrations generally remaining above the regulatory threshold. Increasing oxidant dosage produced only moderate improvements, suggesting that permanganate oxidation alone was not sufficient to significantly enhance mercury removal. This behaviour is consistent with the fact that permanganate primarily acts as an oxidizing agent for organic contaminants, while its capacity to oxidize mercury is relatively limited (Crimi and Siegrist, 2004; Ritoré et al., 2023).

Ferrate-based treatments (Figure 28b) exhibited comparatively higher mercury removal efficiencies, particularly at increased oxidant dosages.

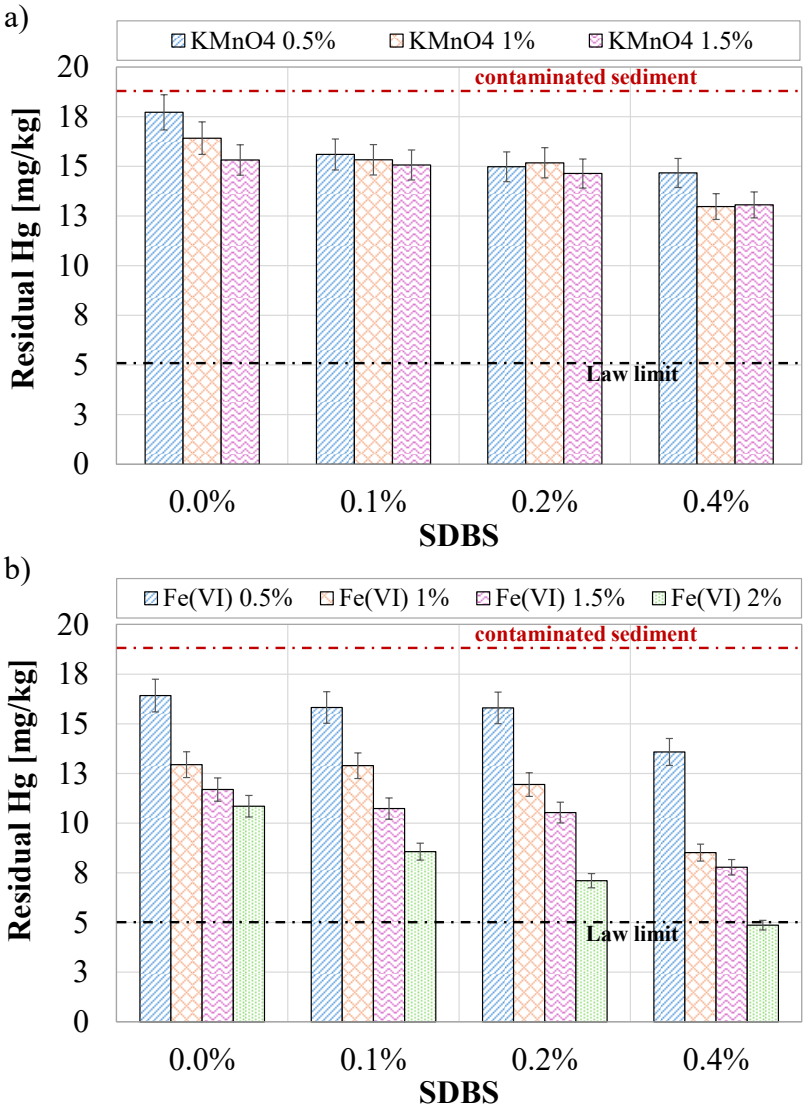

Figure 28: Residual Hg concentration in sediment after treatment with KMnO4 (a) and Fe(VI) (b)

Residual phytotoxicity after treatment. The germination index (GI) of Lepidium sativum was employed to evaluate the residual phytotoxicity of HC-contaminated sediments (Figure 29). The contaminated sediment treated with water alone showed a substantial reduction in GI (~ 45%), indicating persistent toxicity associated with residual hydrocarbons. Oxidation with potassium ferrate in the absence of surfactant (no SDBS) significantly enhanced the GI (~ 65%), suggesting an effective reduction in phytotoxic compounds and partial reclamation of sediment quality. This improvement can be attributed to the oxidative capacity of ferrate, which likely promoted the degradation of toxic hydrocarbon fractions and reduced their bioavailability. However, the addition of SDBS altered this trend. At 0.1% SDBS, the GI slightly decreased (~ 55%) compared to ferrate alone, while at 0.2% SDBS a pronounced decline was observed (~ 30%). This concentration-dependent reduction indicates that the surfactant exerted additional phytotoxic effects, counteracting the benefits of oxidation. Given that SDBS is a known toxic surfactant (De Marines et al., 2025; Feng et al., 2022; Liu et al., 2021), its residual presence in the sediment and/or the increased mobilization of hydrocarbons due to enhanced solubilization may have contributed to greater exposure of seeds to harmful compounds.

Treatments based on potassium permanganate resulted in generally lower GI values compared to ferrate-based systems. Permanganate combined with 0.1% SDBS achieved very low germination (~ 15%), suggesting considerable residual phytotoxicity. This outcome may be related to the formation of potentially toxic oxidation by-products, and the combined toxic effect of residual permanganate species and SDBS. The comparatively poorer performance of permanganate indicates that, under the tested conditions, ferrate was more effective in mitigating phytotoxicity in HC-contaminated sediments.

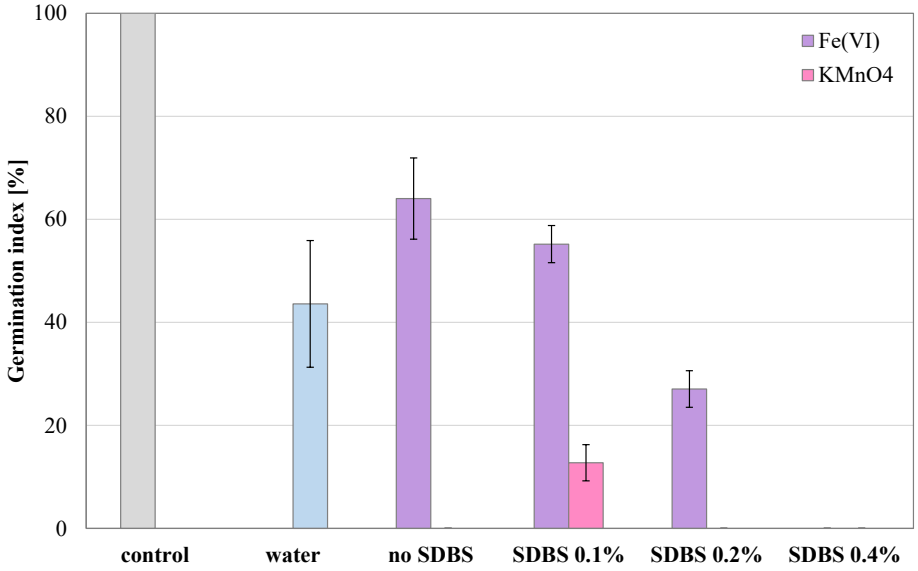

Figure 29: Germination Index in sediment after treatment

4.1.4.4 Main conclusions of the study

Overall, the present results demonstrate that sediment composition critically influences oxidant performance and ecological outcomes. In low-organic-matter sediments, permanganate benefits from reduced background oxidant demand, resulting in relatively high and stable HC removal efficiencies. Conversely, ferrate oxidation appears more sensitive to oxidant dosage and to the presence of organic activators, which are limited in such matrices. Although surfactant addition enhances hydrocarbon removal by improving contaminant accessibility, increased chemical efficiency does not necessarily correspond to improved biological quality due to the intrinsic toxicity of SDBS. Therefore, successful sediment remediation strategies must balance oxidant selection, dosage optimization, and surfactant use to achieve both effective contaminant degradation and measurable ecological recovery.

4.1.5 Scientific products and dissemination

Peer Reviewed Journals

Di Trapani, D., De Marines, F., Greco Lucchina, P., Viviani, G. 2023. Surfactant-enhanced mobilization of hydrocarbons from soil: comparison between anionic and nonionic surfactants in terms of remediation efficiency and residual phytotoxicity. Process Safety and Environmental Pollution, 180, 1-9. https://doi.org/10.1016/j.psep.2023.09.071.

De Marines, F. Di Bella, G., Laudicina, V.A., Paliaga, S., Di Trapani, D. 2025. Remediation of a diesel contaminated soil by means of anionic and non-ionic surfactants: effect on soil phosphorus availability and Vicia Faba L. growth. Science of The Total Environment, 958, 177999. https://doi.org/10.1016/j.scitotenv.2024.177999.

Russo Tiesi, M., Di Bella, G., Licitra, E., Oleszczuk, P., Vinti, G., Di Trapani, D. 2025. Role of mixed surfactants for hydrocarbons removal from real marine sediments: Removal efficiency and residual phytotoxicity after sediment washing treatment. Journal of Environmental Chemical Engineering, 13(6), 119873. https://doi.org/10.1016/j.jece.2025.119873.

De Marines F., Di Trapani D. vivani, G. Utilizzo di surfattanti per il risanamento di suoli contaminati da idrocarburi. Ingegneria dell'Ambiente Vol. 10 n. 3/2023. dx.doi.org/10.32024/ida.v10i3.471 (in Italian).

De Marines F., Capodici M., Coulon F., Di Bella G., Licitra E., Di Trapani D. Oxidation of petroleum hydrocarbons in soil using potassium ferrate as new oxidizing agent: process optimization and benchmarking (submitted to Journal of Hazardous Materials).

Conference Proceedings

De Marines, F., Capodici, M., Di Bella, G., Di Trapani, D., Torregrossa, M., Viviani, G. Utilizzo combinato di ferrato di potassio e tensioattivo per il risanamento di suoli contaminati da idrocarburi. In: Siti Contaminati: Esperienze negli interventi di risanamento, Taormina, 8-10 February 2024. ISBN: 978-88-7850-028-0.

Di Trapani, D., De Marines, F., Di Bella, G., Laudicina, V.A., Paliaga, S., Viviani, G. Utilizzo di tensioattivo per la bonifica di un contaminato da diesel: potenziale di risanamento e effetto fitotossico sulla crescita di Vicia Faba. In: Siti Contaminati: Esperienze negli interventi di risanamento, Taormina, 8-10 February 2024. ISBN: 978-88-7850-028-0.

Russo Tiesi M., Di Bella G., Licitra, E., Vinti, G., Viviani, G. Di Trapani, D. (2024). Surfactant enhanced remediation of marine sediments using anionic, non-ionic and mixed surfactants: role of operational conditions. SIDISA 2024 XII International Symposium on Environmental Engineering Palermo, Italy, October 1 – 4, 2024.

De Marines, F., Capodici, M., Di Bella, G., Licitra, E., Viviani, G., Di Trapani, D. Chemical enhanced oxidation with surfactants: a comparison of the effectiveness of two oxidants for the remediation of hydrocarbon-contaminated soils. SIDISA 2024 XII International Symposium on Environmental Engineering Palermo, Italy, October 1 – 4, 2024.

De Marines F., Capodici M., Di Bella G., Licitra E., Catania V., M. Russo Tiesi, Vinti G., Di Trapani D. (2025) Ossidazione chimica di suoli e sedimenti contaminati con Ferrato(VI) di potassio potenziato da tensioattivo:

valutazione delle performance e confronto con Permanganato di potassio. In: Siti Contaminati: Esperienze negli interventi di risanamento. Brescia (Italia). 12-14 February 2025. ISBN: 978-88-7850-029-7.

Russo Tiesi M., Di Bella G., Castiglione G.M., Vinti G., Vivani G., Di Trapani D. (2025) Bonifica dei sedimenti marini contaminati mediante l'uso di tensioattivi singoli e misti: efficienze di rimozione e fitotossicità residua. In: Siti Contaminati. Esperienze negli interventi di risanamento. Brescia (Italia), 12-14 February 2025. ISBN: 978-88-7850-029-7

De Marines, F., Capodici, M., Coulon, F., Di Bella, G., Licitra, E., Russo Tiesi, M., Vinti, G., Viviani, G., Di Trapani, D. Ferrate(VI) chemical oxidation enhanced with surfactant: a comparison on the effectiveness between soil and marine sediment. AcquaConSoil 2025, Liège, Belgium, 16-20 June 2025.

4.2 Performance Evaluation of Cellulose-Based Nanostructured Materials for Heavy Metal Removal and Resource Recovery (PoliMI)

(Contributors: Carlo Punta, Laura Riva)

In this section, we assess the performance of innovative cellulose-based remediation strategies developed within our research activities, focusing on both water decontamination and resource recovery. Specifically, we describe and critically analyze the outcomes of two complementary studies in which we designed, synthesized, and tested sustainable nanostructured materials for pollutant removal from aqueous systems.

In the first study (Riva et al., 2024), we developed silver-decorated TEMPO-oxidized cellulose nanofibers (TOCNFs) and evaluated their performance in cadmium adsorption from water. We demonstrated that the incorporation of silver nanoparticles significantly enhances the adsorption capacity of the cellulose matrix. Through advanced spectroscopic analyses, we discovered that silver does not directly bind cadmium; instead, it promotes greater exposure of negatively charged carboxylic groups on the cellulose surface, which act as the main active sites for cation uptake. This work provided mechanistic insight into the synergistic interaction between metallic nanoparticles and bio-based nanofibers, leading to improved remediation efficiency.

In the second study (Boniardi et al., 2024), we addressed phosphorus recovery from sewage sludge ash within a circular economy framework. We synthesized cellulose-based nanosponges via thermal cross-linking and applied them as selective adsorbents for the removal of heavy metals from acidic leachates generated during phosphorus extraction. We demonstrated that these bio-derived materials effectively remove interfering metal ions such as iron and aluminium, enabling the production of a phosphorus-rich precipitate compliant with European safety standards.

Together, these studies illustrate how we designed and validated high-performance, sustainable remediation methodologies based on renewable cellulose platforms, capable of addressing both contaminant removal and resource valorization.

4.2.1 Silver-Decorated Cellulose Nanofibers for Enhanced Cadmium Adsorption in Water

4.2.1.1 Introduction

Nanotechnology emerged as a critical tool for environmental remediation, particularly for the removal of toxic heavy metals from water. Although manufactured nanomaterials (MNMs) offered high surface area and strong chemical affinity toward pollutants, their potential ecotoxicity and mobility raised significant environmental concerns (Corsi et al., 2018; Esposito et al., 2021). To address these issues, we adopted an eco-design strategy based on sustainable, biobased building blocks, selecting nanocellulose as the structural platform.

We focused on TEMPO-oxidized cellulose nanofibers (TOCNF), which are characterized by negatively charged carboxylic groups capable of capturing heavy metal ions through electrostatic and chelating interactions (Fiol et al., 2019; Si et al., 2022; Yu et al., 2021). While silver nanoparticles (AgNPs) have been widely recognized for their effectiveness in water treatment, their intrinsic toxicity has limited their direct use (Rasheed et al., 2023). We hypothesized that immobilizing AgNPs onto a TOCNF support could reduce their mobility while enhancing overall decontamination performance (Ali et al., 2018).

We therefore synthesized a novel nanocomposite through the *in situ* deposition of AgNPs onto TOCNF and selected Cd^{2+} as a model contaminant. We demonstrated that the AgNP-decorated composite significantly outperformed pristine TOCNF, increasing the sorption capacity from 78 mg/g to 116 mg/g.

The main contribution of this work was the elucidation of the synergistic interaction mechanism between silver nanoparticles and the cellulose matrix. Through advanced spectroscopic analyses, including XPS and XAS, we demonstrated that AgNPs did not directly interact with Cd^{2+} ions. Instead, we discovered that the presence of silver nanoparticles enhanced the surface exposure of carboxylic groups on the cellulose nanofibers. As a result, the cellulose remained the active sorbent phase, while AgNPs acted as structural promoters that improved the accessibility of functional groups responsible for ion capture. This mechanistic insight advanced our understanding of how supported metal nanoparticles could enhance the performance of biobased sorbents for environmental remediation.

4.2.1.2 Materials and Methods

The methodology employed in this study focuses on the synthesis of TOCNF and their functionalization with AgNPs for heavy metal adsorption.

Materials and Sample Preparation

The primary raw material was long-fiber spruce-derived paper. The researchers produced TEMPO-oxidized cellulose (TOC) by treating the paper with a TEMPO/NaClO/KBr system at a stable pH of 10.5–11.0 for 18 hours. The resulting TOC was then converted into TOCNFs through ultrasonication for 5 minutes in an ice bath to prevent overheating.

To synthesize the TOC-Ag and TOCNF-Ag nanocomposites, AgNPs were generated *in situ* (Figure 30). The cellulose materials were suspended in an $AgNO_3$ solution, where the cellulosic support itself acted as a reducing agent. Sodium hydroxide (NaOH) was added to accelerate the process kinetically, leading to the deposition of metallic silver onto the fibers.

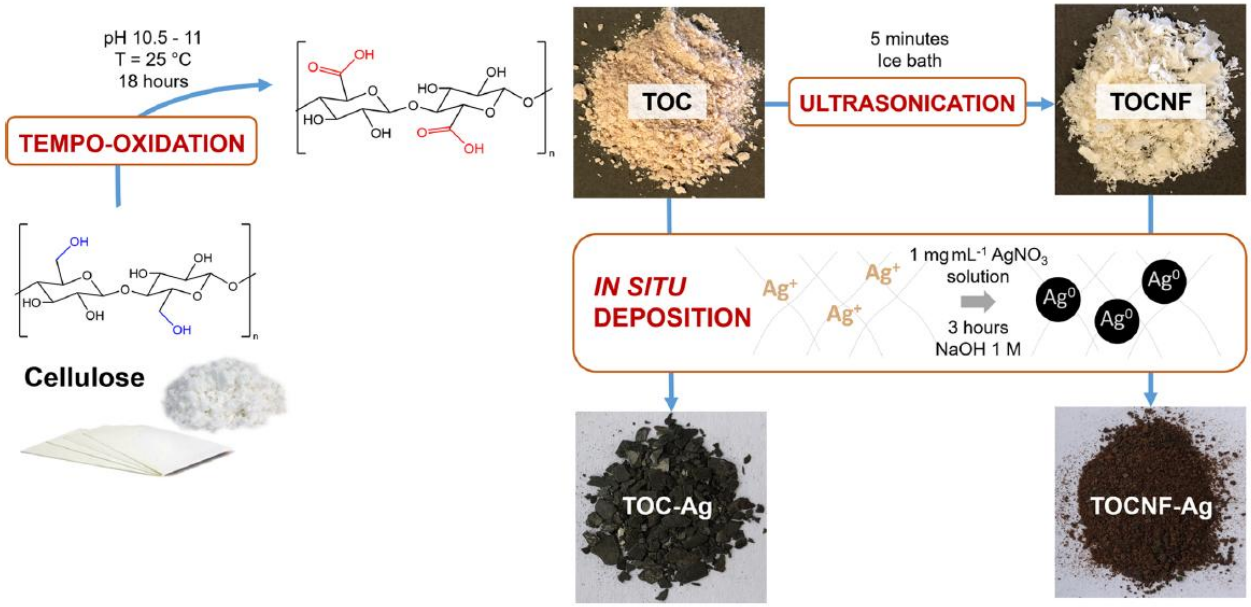

Figure 30: Graphical Description of Synthetic Steps Used for TOC-Ag and TOCNF-Ag Batch Production. (Riva et al., 2024)

Additionally, alkaline-conditioned versions of these materials (e.g., $TOCNF_b$) were prepared by treating the neutral powders with 0.1 M NaOH to ensure the carboxylic groups were fully deprotonated.

Characterization Techniques

A multi-physics analytical approach was used to analyze the composites:

- **Spectroscopy**: FTIR-ATR confirmed the conversion of alcoholic groups to carboxylic moieties, while ICP-OES quantified the silver loading and cadmium concentrations.
- **Microscopy**: SEM-EDS and FE-SEM provided elemental mapping and surface morphology, while TEM confirmed the deposition of AgNPs (5–10 nm) on the nanofibers.
- **Surface Charge**: ζ-potential measurements were used to track changes in surface charge after AgNPs loading and Cd^{2+} adsorption.
- **Advanced Interaction Analysis**: XPS was used to study the electronic structure and functional group exposure, while XAS (Ag-K and Cd-K edges) investigated the local coordination environment to determine if direct Ag-Cd interactions occurred.

Sorption Experiments

Batch adsorption tests were conducted using Cd^{2+} solutions (150 mg/L). Sorbents were shaken with the solutions for 24 to 72 hours at room temperature. Finally, the researchers tested the materials' selectivity by

introducing interfering ions, specifically Na^+ and Ca^{2+}, to evaluate the impact of competitive cations on Cd^{2+} capture.

4.2.1.3 Results

We synthesized a novel nanocomposite by depositing AgNPs in situ onto TOCNF. We used the reducing efficiency of the cellulosic support itself to generate the AgNPs, though we added NaOH to kinetically accelerate the process by promoting intermediate silver oxides.

Through TEM and FE-SEM imaging (Figure 31), we observed that the AgNPs (5–10 nm) were homogeneously distributed on the nanofibers without significant aggregation. We confirmed the successful conversion of alcoholic groups to carboxylic moieties via FTIR-ATR, noting that the OH stretching bands disappeared after silver loading, which indicates these groups are heavily involved in fixing the nanoparticles to the cellulose. Interestingly, we measured a decrease in the ζ-potential after loading the AgNPs, suggesting that we increased the density of negative charges on the composite surface.

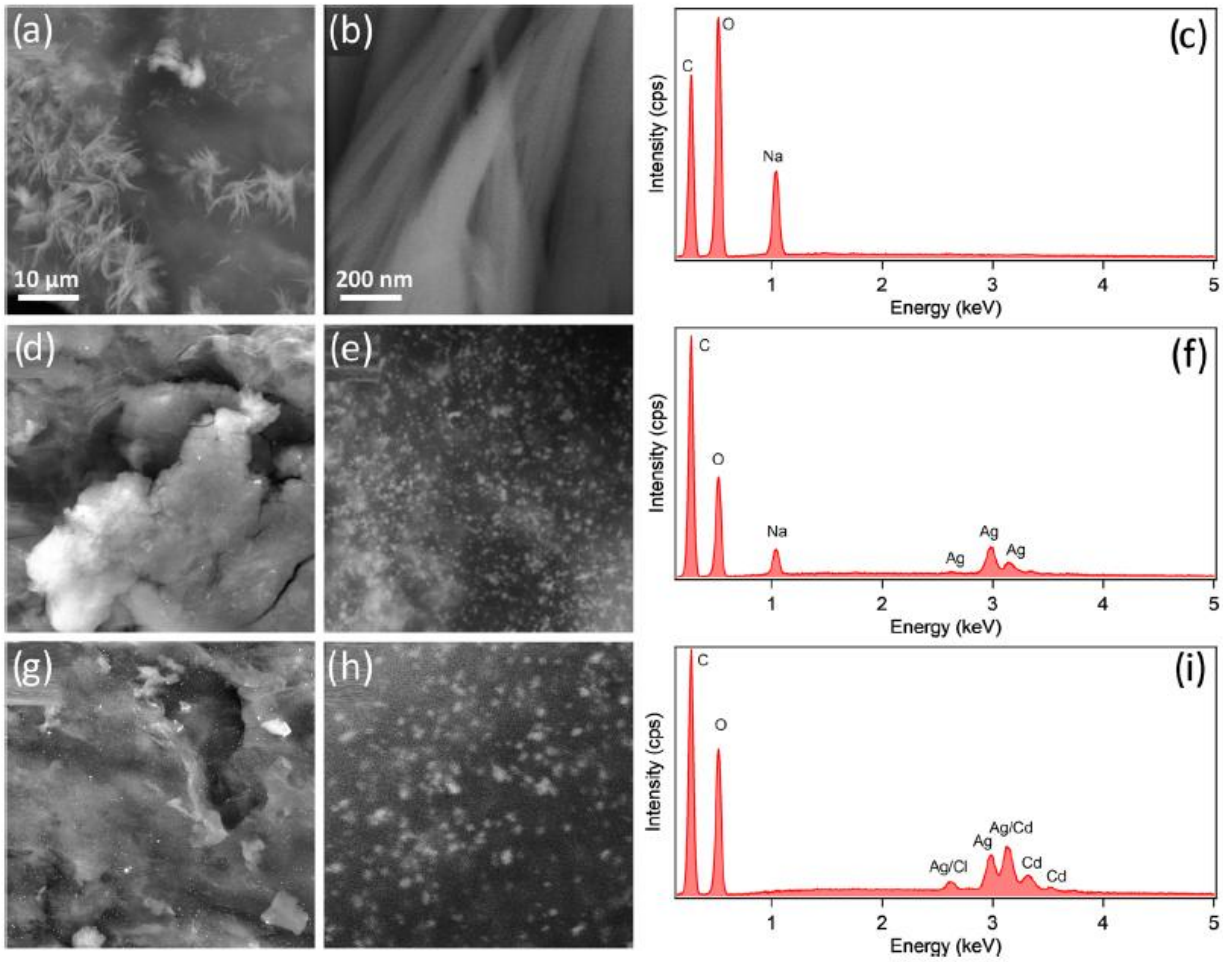

Figure 31: FE-SEM images and EDX profiles acquired on TOCNF (a–c), TOCNF-Ag (d–f), and TOCNF-Ag + Cd (g–i). (Riva et al., 2024)

When we performed Cd^{2+} sorption tests, we synthesized a clear comparison of performance: the AgNP-decorated nanofibers reached a sorption capacity of 116.5 mg/g, a significant increase over the 78 mg/g achieved by TOCNF alone (Figure 32). We prepared alkaline-conditioned versions of these materials and found that deprotonating the carboxylic groups boosted the performance of TOCNF to levels comparable to the silver-decorated version, which provided a vital clue regarding the interaction mechanism.

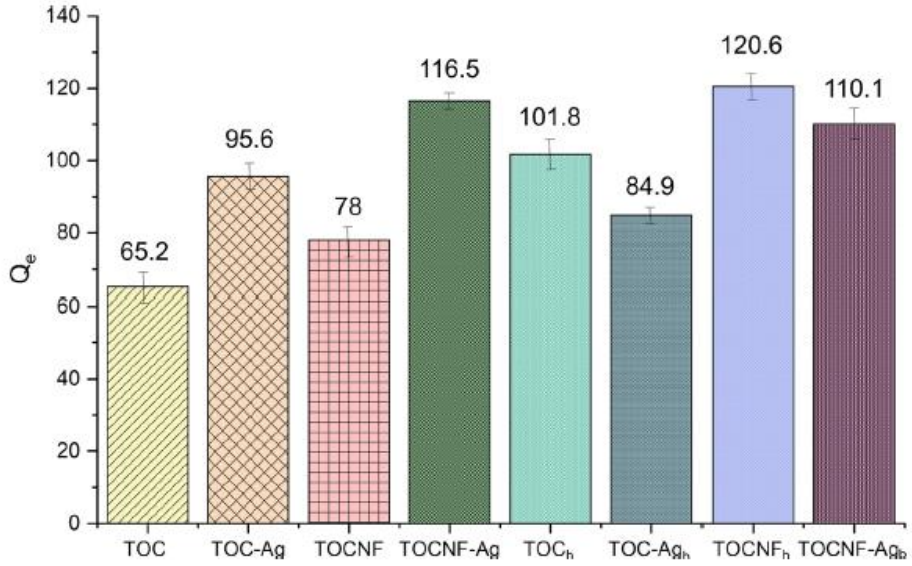

Figure 32: Scheme of adsorption tests conducted with neutral and alkaline materials in 150 mg L^{-1} of Cd^{2+} solutions. (Riva et al., 2024)

To explain why the AgNPs improved adsorption, we conducted a multi-physics investigation. While EDX showed Cd^{2+} localized in the neighborhood of silver, our XPS analysis (Figure 33) revealed that the AgNPs actually increase the surface exposure of carboxylic groups compared to pristine TOCNF. Crucially, we used XAS to study the local coordination environment and confirmed that there is no direct interaction between the metallic silver (Ag^0) and the cadmium ions. Instead, we found that Cd^{2+} coordinates directly with the carboxylate groups, substituting for Na^+ ions. Consequently, we concluded that cellulose support remains the active sorbent, while the AgNPs act as structural facilitators that enhance functional group accessibility.

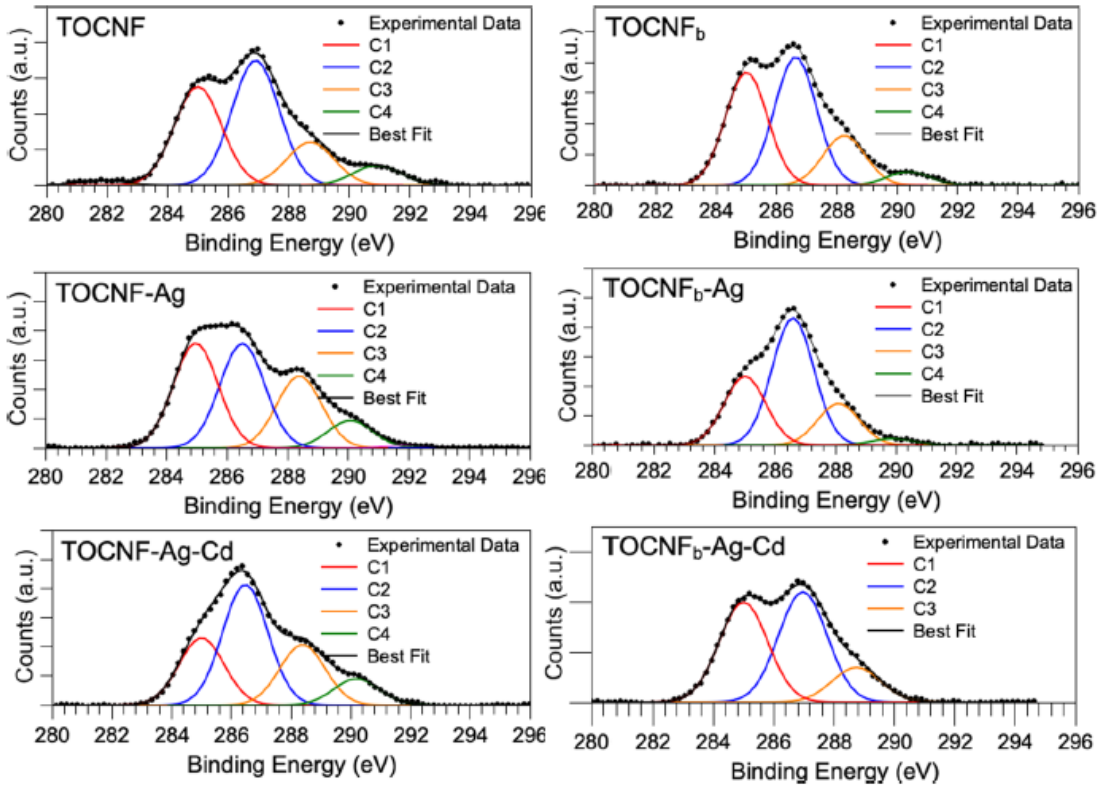

Figure 33: XPS C 1s spectra of TOCNF, TOCNF-Ag, and TOCNF-Ag + Cd (on the left) and $TOCNF_b$, $TOCNF_b$-Ag, and $TOCNF_b$-Ag + Cd (on the right). (Riva et al., 2024)

Finally, we tested the material's selectivity against competitive ions (Figure 34). We found that Na^+ and Ca^{2+} hinder Cd^{2+} capture through a shielding effect, which confirms that the primary interaction is electrostatic. However, we observed that the system remains highly selective toward the heavy metal at realistic environmental concentrations.

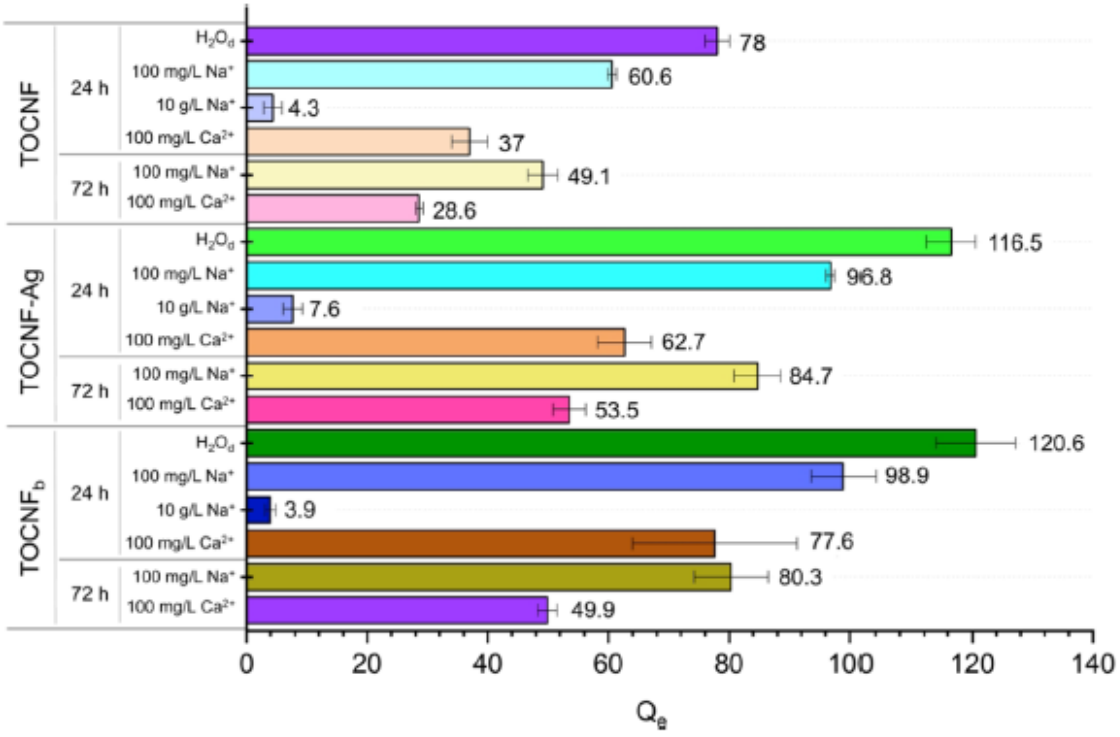

Figure 34: Results of the adsorption experiments conducted in the presence of interfering cations (comparison between 24 and 72 h). (Riva et al., 2024)

4.2.1.4 Conclusions

We synthesized a sustainable nanocomposite by depositing AgNPs in situ onto TOCNF. We prepared this material to address water decontamination, specifically targeting Cd^{2+} removal. Our results showed that the AgNP-decorated composite significantly outperforms the bare TOCNF, reaching a sorption capacity of ~116 mg/g.

Through our multi-physics investigation, we unveiled a synergistic mechanism that explains this enhancement. Crucially, our XPS and XAS analyses proved that metallic silver does not interact directly with Cd^{2+} ions. Instead, we discovered that the AgNPs increase the surface exposure of the carboxylic groups on the cellulose nanofibers. Therefore, the cellulose support remains the active sorbent, utilizing its carboxylic moieties to capture the heavy metal via electrostatic and coordination interactions.

We also demonstrated that the synthesized system maintains high selectivity at realistic environmental concentrations. By anchoring AgNPs to a biobased support, we followed eco-design principles to limit nanoparticle mobility and ecotoxicity while maximizing decontamination efficiency. This study emphasizes the power of combining advanced characterization techniques to understand and improve complex nanostructured materials for environmental remediation.

4.2.2 Cellulose Nanosponges for Phosphorus Recovery and Leachate Decontamination

4.2.2.1 Introduction

The recovery of phosphorus from secondary resources has become increasingly important due to the growing demand for fertilizers and the progressive depletion of high-quality phosphate rock (Desmidt et al., 2015). In this context, sewage sludge ash has been identified as a promising alternative phosphorus source. We applied wet chemical extraction to leach phosphorus; however, this process also co-dissolved hazardous heavy metals, making the recovered product unsuitable for direct agricultural use (Boniardi et al., 2021). To address this limitation, we synthesized sustainable cellulose nanosponges (CNS) as innovative bio-based adsorbents for the decontamination of these leachates. The nanostructured materials were prepared through thermal cross-linking between regioselectively oxidized cellulose nanofibers and branched polyethylenimine (Fiorati et al., 2020; Melone et al., 2015; Riva et al., 2020).

We designed laboratory-scale adsorption experiments to evaluate the removal of metals and metalloids, including iron, aluminum, copper and zinc, across a wide pH range. Citric acid was incorporated to stabilize the system, allowing us to explore broader operating conditions without premature precipitation. We observed that CNS effectively adsorbed significant amounts of metallic ions, particularly iron and aluminum, even under strongly acidic conditions. Following the decontamination step, phosphorus was precipitated as calcium phosphate through the addition of calcium hydroxide.

Through this approach, we obtained a solid precipitate at pH 8 that complied with EU Regulation 2019/1009 for inorganic fertilizers. While the effectiveness and eco-safety of these materials had previously been demonstrated for water remediation, this work represented their first application to phosphorus recovery. Overall, we established a circular strategy that converted waste-derived leachates into high-purity fertilizers while minimizing environmental impact.

4.2.2.2 Materials and Methods

Cotton linters and high-purity reagents were used to prepare all chemical solutions. The primary phosphorus source was obtained by subjecting sewage sludge ash (SSA) to acid leaching with 0.2 M sulfuric acid at a liquid-to-solid ratio of 20 for two hours. The resulting suspension was subsequently treated by centrifugation and vacuum filtration (0.45 µm) to obtain a stable leachate solution.

CNS were synthesized starting from TOCNF, produced from cotton linters via regioselective oxidation. A stable hydrogel was prepared by mixing the nanofibers with branched polyethylenimine (bPEI) and citric acid. The material was then freeze-dried and thermally cross-linked at 98°C to promote the formation of covalent amidic bonds. The resulting solid was ground into a fine powder to obtain the final adsorbent.

Laboratory-scale adsorption tests were carried out by dispersing CNS in both synthetic phosphate solutions and real SSA leachate. Different sorbent dosages (1, 3, and 10 g/L) were evaluated over a pH range of 1.8 to 10. Citric acid was added as a stabilizing agent to prevent premature precipitation of metals and phosphorus at higher pH values.

Phosphorus was subsequently precipitated from the decontaminated leachate by the addition of calcium hydroxide until target pH values of 3.5, 5, and 8 were reached. Recovery efficiency and elemental composition of the resulting solids were determined using ICP-MS for metal content and UV-Vis spectroscopy for phosphate concentration. Surface characterization of CNS after adsorption was performed by SEM-EDS analysis to assess the distribution of retained metals.

4.2.2.3 Results

In our investigation, we characterized the initial sulfuric acid leachate, which contained 3100 mg/L of phosphorus alongside high concentrations of aluminum (2120 mg/L) and iron (689 mg/L). We evaluated the interaction between phosphate ions and our CNS, finding that while synthetic solutions showed high phosphorus adsorption at low pH, real SSA leachate exhibited much lower phosphorus adsorption (9–22%). We attribute this decrease to the presence of heavy metals, which synthesize a competitive environment for the CNS active sites (Figure 35).

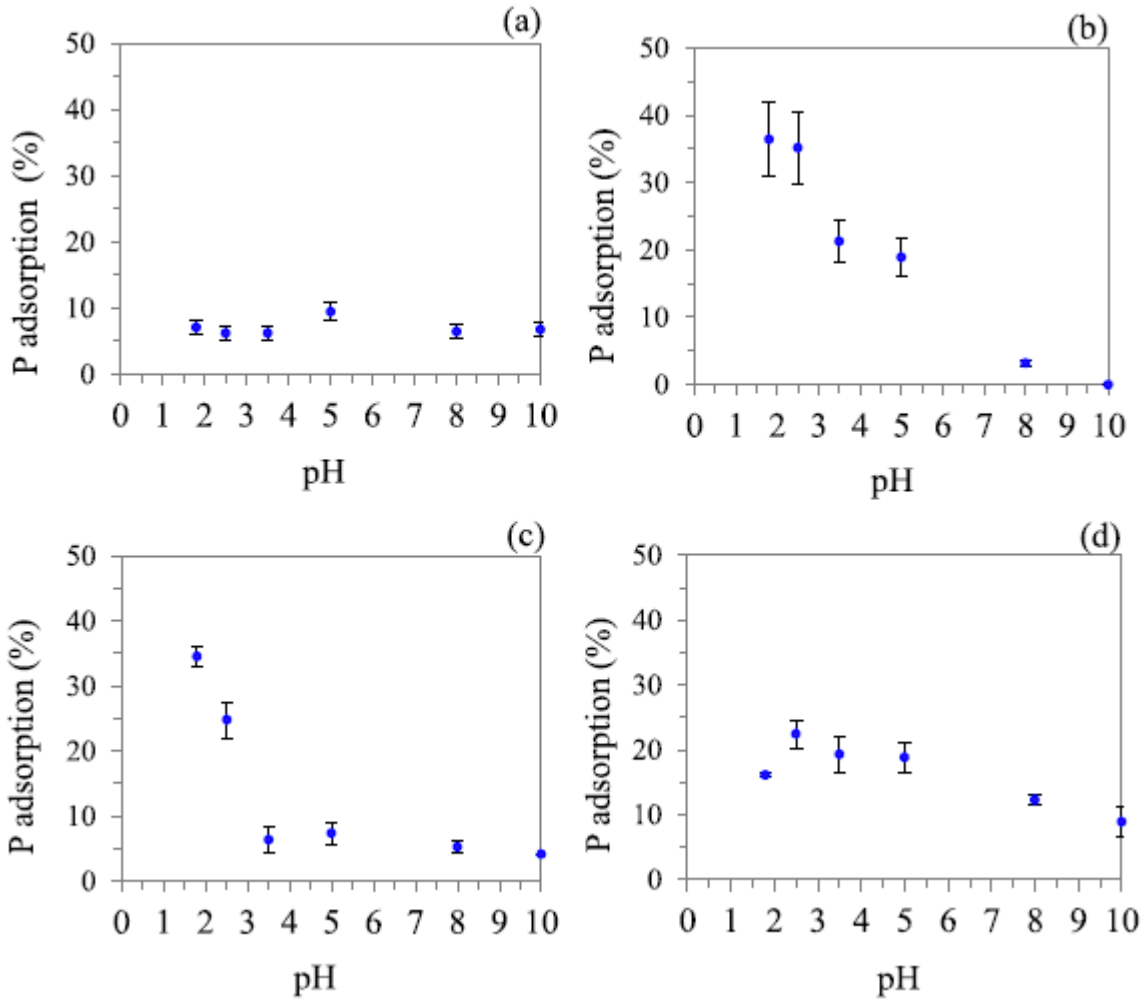

Figure 35: Average phosphate ions ($P\text{-}PO_4^{3-}$) adsorption efficiency (expressed as %) by CNS as a function of pH: (a) 0.1 M H_3PO_4 solution, 1 $g_{CNS}/L_{solution}$, absence of citric acid, (b) 0.1 M H_3PO_4 solution, 10 $g_{CNS}/L_{solution}$, absence of citric acid, (c) 0.1 M H_3PO_4 solution, 10 $g_{CNS}/L_{solution}$, presence of citric acid (10 $g/L_{solution}$), (d) SSA leachate solution, 10 $g_{CNS}/L_{solution}$, presence of citric acid (10 $g/L_{leachate}$). (Boniardi et al., 2024)

We conducted metal adsorption tests and observed that at a dosage of 10 g/L, the CNS effectively removed copper and nickel, reaching efficiencies of 78% and 96%, respectively. Most importantly, we attained significant removal of iron (38%) and aluminium (28%) under strong acidic conditions. This step is vital because these metals otherwise cause phosphorus to precipitate prematurely in undesired forms, such as iron or aluminium phosphates (Figure 36). To facilitate testing across a wider pH range, we incorporated citric acid as a stabilizing agent to prevent spontaneous precipitation. We noted that in the absence of citric acid at pH 1.8, the adsorption of iron, chromium, and arsenic was slightly higher, suggesting that citric acid forms large metal-chelates that may hinder diffusion into the CNS pores.

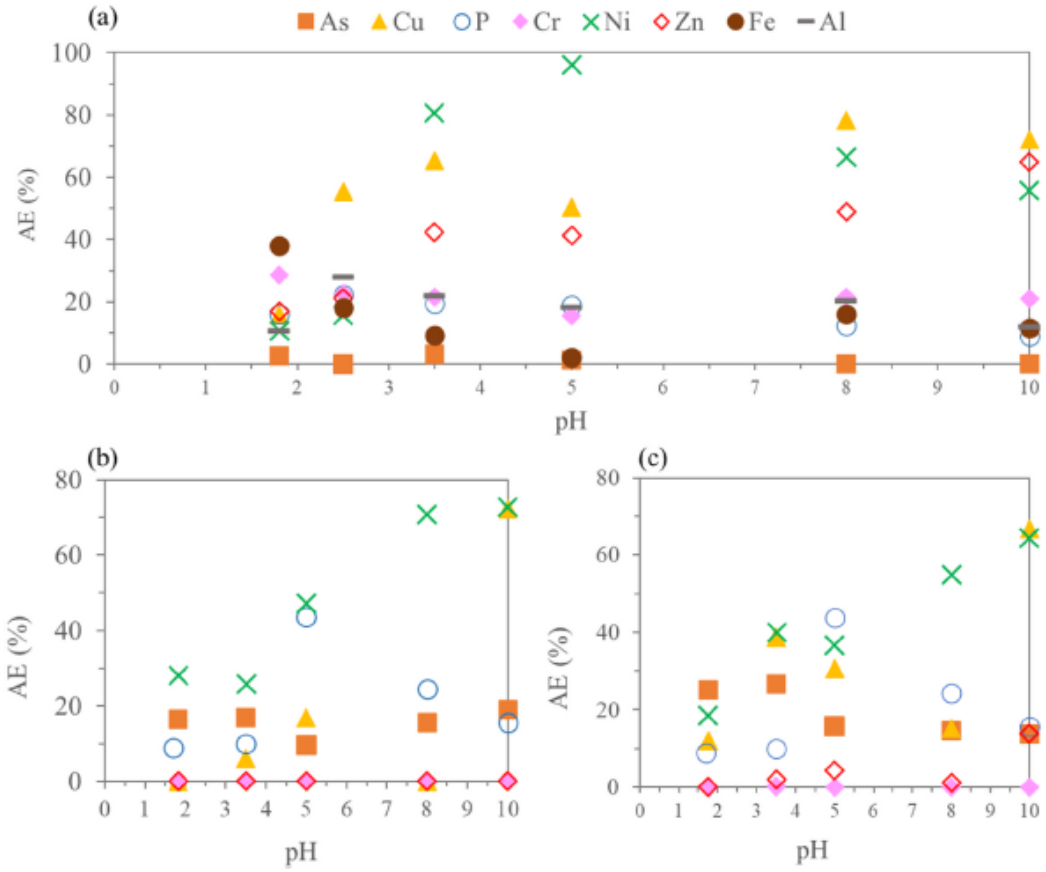

Figure 36: Average phosphate ($P\text{-}PO_4^{3-}$) and metal Adsorption Efficiency (AE, expressed as %) by CNS in the SSA leachate solution as a function of pH in presence of 10 g/L (a), 3 g/L (b), and 1 g/L (c). Uncertainty given by the measurements ±10%. (Boniardi et al., 2024)

To recover the phosphorus, we precipitated decontaminated leachate using calcium hydroxide. We found that precipitates from untreated leachate or those prepared without citric acid failed to meet EU Regulation 2019/1009 due to excessive iron and aluminum content. However, by synthesizing a process that utilized 10 g/L of CNS and 10 g/L of citric acid, we attained a solid product at pH 8 that was fully compliant with European standards. This final precipitate contained 27% P_2O_5 and satisfied the criteria for Component Material Category 12 for inorganic fertilizers (Table 11).

Table 11: Phosphorus and metals concentration in the P-rich precipitate compared to the EU Regulation 2019/1009. Values in bold exceeded the limits for fertilizer use. Legend: solid precipitate (PR), not available data (n.a.). [-] refer to the absence of precipitation at selected pH. (Boniardi et al., 2024)

	Element	P_2O_5	Al	As	Cd	Cr	Fe	Hg	Ni	Pb	Cu	Zn	Fe + Al	PR
Tests	pH	%	%	mg/kg	mg/kg	mg/kg	%	mg/kg	mg/kg	mg/kg	mg/kg	mg/kg	mg/kg (%)	g
P0_CA0	3.5	33.5	10.4	<20.0	<2	105.0	4.2	<0.5	49.0	<50.0	85.9	98.6	146000.0 (**14.6**)	0.42
	5	35.7	10.5	20.7	<2	112.0	4.0	<0.6	<40	<50.0	**812.0**	1350.0	145000.0 (**14.5**)	0.43
	8	28.0	8.4	22.1	<2	92.3	3.3	<0.7	99.1	<50.0	**739.0**	**2422.0**	117000.0 (**11.7**)	0.62
P0_CA10	3.5	[-]	[-]	[-]	[-]	[-]	[-]	[-]	[-]	[-]	[-]	[-]	[-]	0.00
	5	[-]	[-]	[-]	[-]	[-]	[-]	[-]	[-]	[-]	[-]	[-]	[-]	0.00
	8	[-]	[-]	[-]	[-]	[-]	[-]	[-]	[-]	[-]	[-]	[-]	[-]	0.00
P10_CA10	3.5	[-]	[-]	[-]	[-]	[-]	[-]	[-]	[-]	[-]	[-]	[-]	[-]	0.00
	5	[-]	[-]	[-]	[-]	[-]	[-]	[-]	[-]	[-]	[-]	[-]	[-]	0.00
	8	27.1	6.0	<20.0	<2	56.4	1.3	<0.5	58.3	<50.0	377.0	1330.0	73000.0 (7.3)	0.46
P10_CA0	3.5	39.4	11.9	<20.0	<3	82.7	1.8	<0.6	<40	<50.0	273.0	194.0	137000.0 (**13.7**)	0.34
	5	41.2	11.6	22.3	<4	91.7	1.9	<0.7	<41	<50.0	502.0	**2430.0**	135000.0 (**13.5**)	0.30
	8	31.9	9.1	24.0	<5	78.8	1.4	<0.8	75.5	<50.0	346.0	**1990**	105000.0 (**10.5**)	0.44
EU limits	n.a.	>12	n.a.	40.0	60.0	n.a.	n.a.	n.a.	100.0	120.0	600.0	1500.0	100000.0 (10.0)	n.a.

Finally, we evaluated our results against existing literature and found that we achieved these decontamination levels using significantly lower adsorbent-to-leachate ratios (1–10 g/L) compared to the higher dosages required for Zr-based adsorbents or ion-exchange resins. Through this work, we synthesize an innovative, circular strategy that transforms hazardous waste into a high-purity raw material for the fertilizer industry.

4.2.2.4 Conclusions

In conclusion of our study, it is possible to state that sewage sludge ash is a vital phosphorus source, though its metal content necessitates decontamination. We synthesized sustainable cellulose nanosponges to prepare a decontaminated leachate, achieving significant adsorption of iron and aluminum. Through our optimized process, we attained a phosphorus-rich precipitate at pH 8 with 27% P_2O_5 that fully complies with EU Regulation 2019/1009 for fertilizers. We synthesized a circular strategy that transforms waste into high-quality raw materials. Future research will evaluate continuous up-scaling and the regeneration potential of these bio-based materials to further enhance sustainability

4.2.3 Scientific products and dissemination

Peer Reviewed Journals

Boniardi, G., Volonterio, A., Canziani, R., Punta, C., Riva, L., & Turolla, A. (2024). Cellulose-based nanostructured aerogels for leachate decontamination: Towards sustainable phosphorus recovery from sewage sludge ash. Journal of Cleaner Production, 475. https://doi.org/10.1016/j.jclepro.2024.143638.

Riva, L., Dotti, A., Iucci, G., Venditti, I., Meneghini, C., Corsi, I., Khalakhan, I., Nicastro, G., Punta, C., & Battocchio, C. (2024). Silver Nanoparticles Supported onto TEMPO-Oxidized Cellulose Nanofibers for Promoting Cd^{2+} Cation Adsorption. ACS Applied Nano Materials, 7(2), 2401–2413. https://doi.org/10.1021/acsanm.3c06052.

4.3 Remediation of polluted soils and wastewater using bioelectrochemical systems and the removal of microplastics with electrochemical and photoelectrochemical techniques (UNICA)

(Contributors: Annalisa Vacca, Michele Mascia)

4.3.1 Introduction

The research for innovative methods able to remove pollutants from waters and soils has grown along with the detection of new contaminants in the environment, the so-called emerging pollutants, that can affect both flora and fauna and human health: they include products used daily in households, industry, pharmaceuticals and personal care products, gasoline additives, pesticides, plasticizers and microplastics. Two main issues of emerging contaminants are the difficulty of removal by conventional treatment technologies and their threat, even at a trace level, because their real impact on human health is unknown. During recent years, techniques based on electrochemistry, such as photoelectrochemical or bio-electrochemical processes have demonstrated their capacity to efficiently remove many of these compounds. Starting from the early 1980s, research on electrochemical methods for treating wastewater has grown significantly, and thousands of papers now appear in the literature. Moreover, thanks to the possible exploitation of renewable energies, the use of electricity is no longer the weakest point of the electrochemical processes, and therefore their applications are regaining the deserved attention. Recently, combined techniques such as photoelectrochemical processes in which electrochemical and photochemical processes are combined have attracted increasing interest, thanks to the synergy of the two processes. In a similar way, the combination of biological and electrochemical processes may offer solutions to current environmental problems. This is why, in the last two decades, the number of articles on these topics have quickly increased, and the publication of these articles in specific journals indicates that technology is moving from the fundamentals to real applications.

In this context, the research activities were focused on two main topics:

1. assess the effectiveness of bio-electrochemical systems for the remediation of soil and wastewater (research line 1).

2. assess the effectiveness of electrochemical and photoelectrochemical techniques for the removal of microplastics from waters (research line 2).

4.3.2 Materials and methodologies

Research line 1: Carbon felt was used as anode while the cathode was carbon cloth coupled with a mixture of activated carbon and carbon black (AC/CB) for all the bio-electrochemical experiments. Soil microbial fuel cells were prepared using a real soil collected near Cagliari, which was characterized both for ionic content and organic content. After 3 weeks of stabilization, the growth of anodic and cathodic biofilm was observed, and the cells were characterized by measuring the power curves and electrochemical impedance spectroscopies. The soil was polluted with different amounts of 2,4-D herbicide. At prefixed time intervals, samples of soil were withdrawn and analyzed to measure the residual concentration of the pollutant, by extracting the herbicide with Soxhlet extraction and performing HPLC analyses.

Single chamber air-cathode MFC with a tubular ceramic membrane were used for the treatment of wastewaters. The external cylinder served as the anode, where biofilm was grown, while the internal cylinder was the

cathode, which was in direct contact with air. Polarization and power density curves were measured to characterize the systems. The degradation ability of the microbial cell was assessed by monitoring the total organic carbon during the time. Also, the gas phase was analyzed to check the formation of hydrogen or other valuable by-products generated during the degradation.

Research line 2: Different experimental set-ups were designed and realized. The electrochemical system was un undivided cell equipped commercial electrodes: Boron Doped Diamond or dimensionally stable anodes (DSA) coated with Iridium and Ruthenium oxide. In the case of photo-electrochemical system, the photoanode was constituted by titania nanotubes, prepared by anodization of titanium foils in our laboratory. A 300 W xenon lamp equipped with air mass (AM) 0 and 1.5 D filters was used to simulate the solar radiation. The degradation of MPs was assessed by analysing the weight loss of MPs and the concentration of oxidants produced by the process. In addition, TOC and HPLC analyses have been performed to evaluate the presence of by-products, as well as Fourier-transform infrared spectroscopy (FTIR) and scanning electron microscopy (SEM) analysis were used to characterize the MPs during the degradation.

4.3.2 Results and Discussion

Research line 1: Soil and wastewater treatment have been studied using both microbial fuel cells (MFC) and microbial electrochemical cells (MEC). Different set-ups for soil remediation have been developed in lab-scale, and their characterization have been performed by measuring the potential generated by the system and the power density (Figure 37).

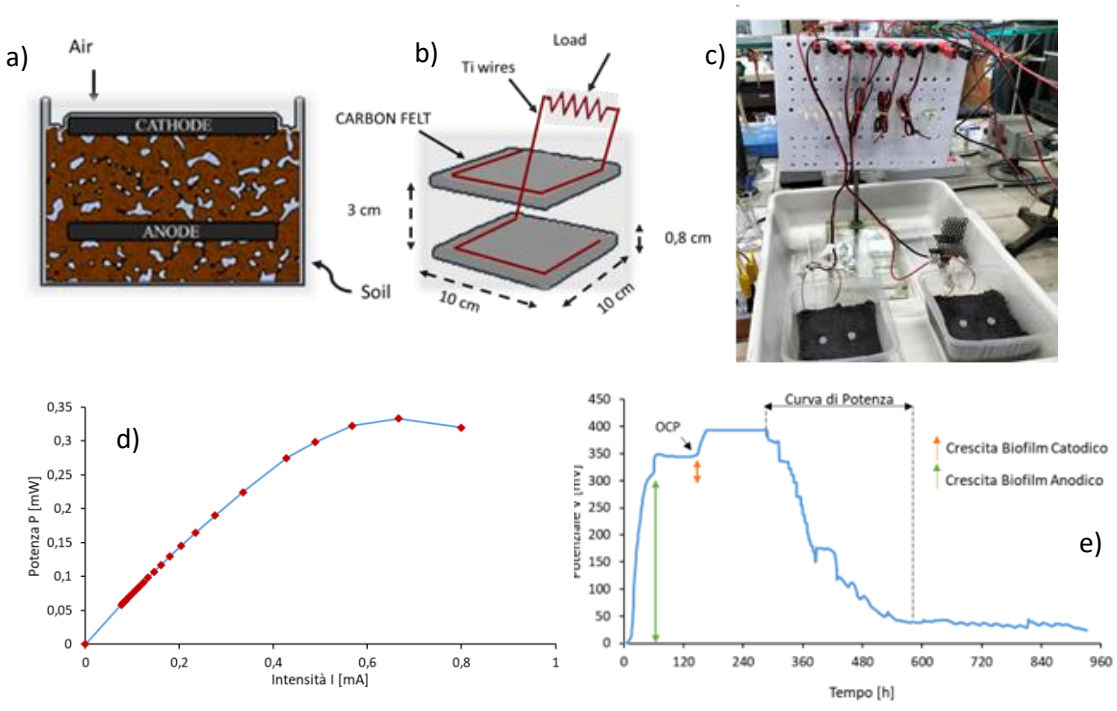

Figure 37: Standard experimental set-up of soil microbial fuel cell (a-c), power curve (d) and potential generated during the bacteria growth at the anode and cathode (e).

Test on the removal of herbicide (2, 4 D) from polluted soils have been done obtaining concentration distribution inside the solid matrix: a complete removal of the herbicide was obtained in the anodic zone

(Figure 38a). A mathematical model of the system using CFD techniques has been developed with the aim to describe the diffusion and the degradation of organic pollutant generated by the electrochemical and bio-electrochemical reactions involved in the MFC, which can be used to scale-up the technology or to predict the removal of a specific contaminant using different configuration (Figure 38b). Figure 39 reports the results of the CFD model for a different configuration.

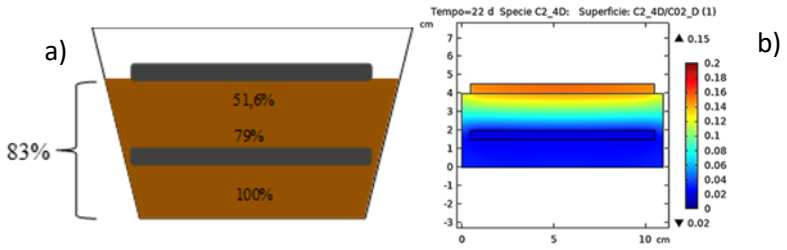

Figure 38: Experimental results of the removal of 2,4 -D herbicide in different zones of the polluted soil (a) and mathematical model of the experimental system (b).

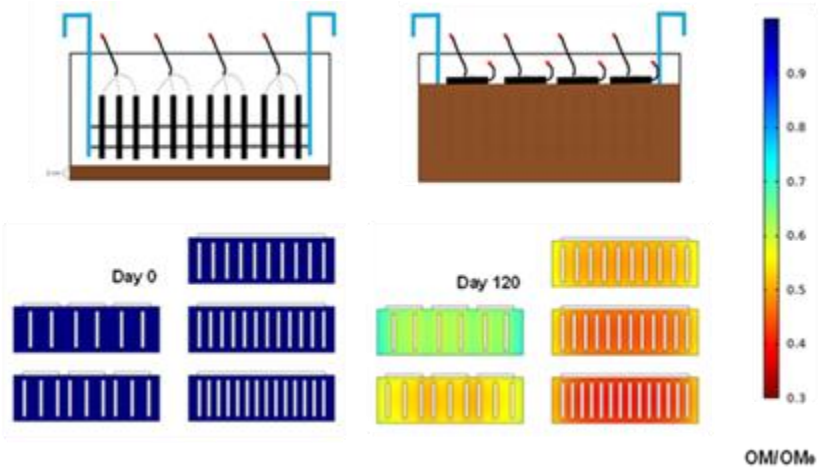

Figure 39: Experimental set-up (a) and results of the model at different time of treatment (b).

Regarding the wastewater treatment, both MFC and MEC configuration have been tested to remove pollutants form water deriving from agro-industries. A first set of tests have been performed using synthetic solutions containing sodium acetate as carbon sources. Sample of real wastewater collected from local olive oil mill industries, which are characterised by high organic load and recalcitrant pollutants as phenols and polyphenols, have been tested in MEC configuration with the aim to remove the pollutants and simultaneously obtain hydrogen and other valuable fuels. Figure 40 shows the experimental set-up of microbial electrochemical system with ceramic membranes, the trend with time of the degradation of pollutants, the production of gaseous products and the mathematical model of the system.

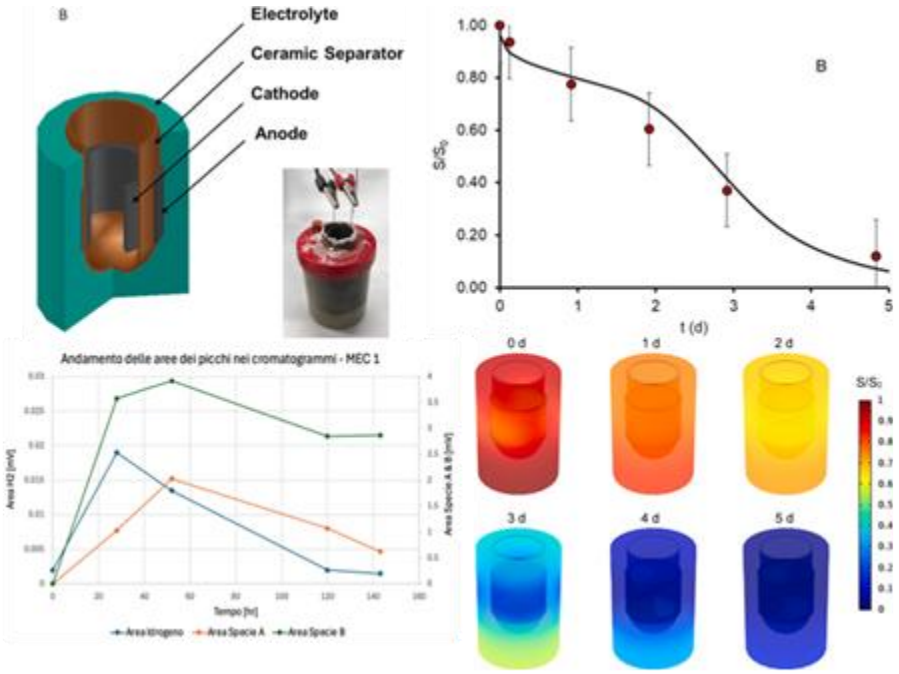

Figure 40: Experimental set-up of microbial electrochemical system with ceramic membranes (a), the trend with time of the degradation of pollutants (b), the production of gaseous products (c) and the mathematical model of the process (d).

Research line 2: The removal of microplastics with electrochemical and photoelectrochemical techniques have been studied. The set-up of the electrochemical and the photo-electrochemical reactors assisted by solar light and their characterization have been performed considering that waters polluted with microplastic are suspension of organic particles rather than homogenous solutions. Test of the removal of polyethylene (PE) and polyethylene terephthalate (PET) microplastics from water have been performed under different operative conditions. With the electrochemical reactor, removal up to 70% of MPs has been measured depending on the conditions, with very low values of by-product concentrations indicating that the processes are able to mineralise the MPs (Figure 41). FT-IR analyses of the electrochemically treated PE and PET have been carried out in order to understand the oxidation process. No changes in PET surface were detected during the electrochemical treatment suggesting a fragmentation of PET during the process. At PE the formation of hydroxyl functionalities (signal at ca. 3300 cm^{-1}) and the reduction in intensities of the characteristic peaks of PE indicate structural changes in the molecular skeleton. The low TOC accumulation during the degradation of PET indicates its degradation intermediates are more easily oxidable.

In the case of photo-electrochemical reactor, the result indicates that PEC exhibits a synergistic effect in degradation, resulting in a weight loss of MPs comparable to that achieved with the electrochemical process. From FIT-IR analyses it can be observed a greater amount of hydroxyl groups in PET surface. This behaviour indicates the formation of shorter polymer chains through a hydrolysis-like mechanism, leading to the generation of carboxyl groups. This consideration is further supported by the analysis of carbonyl index (CI). The trend with time of TOC measured during the photo-electrochemical process indicates that the byproducts formed by the MPs degradation are not effectively mineralised: oxalic acid was identified as the main by-product by HPLC analyses, which can be formed as oxidation by-product of the ethylene glycol moiety of PET structure (Figure 42).

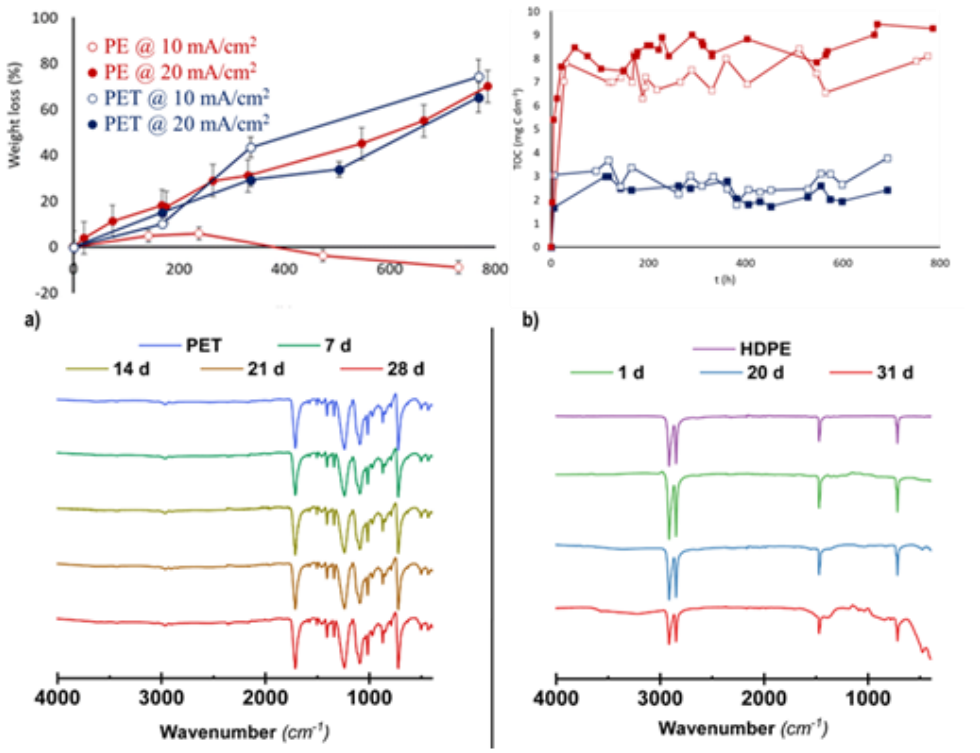

Figure 41: Weight removal obtained during the degradation tests for PET ad PE (a). Trend with time of TOC measured in solution during the degradation tests (b). FIT-IR measured at different treatment times (c).

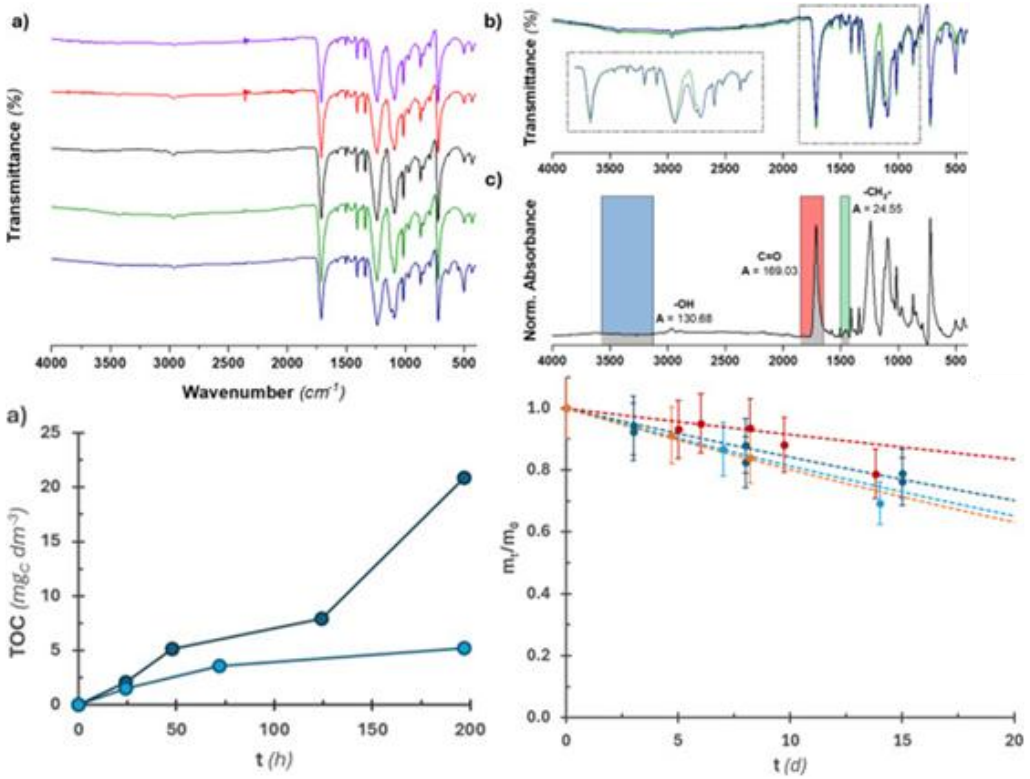

Figure 42: FT-IR measurement of pristine PET (black), and PET after 8 days of electrochemical (red and purple) and photoelectrochemical treatment (green and blue) (a, b and c). Trend with time of TOC measured in solution during the degradation tests (d) and weight loss obtained during the degradation tests for PET: red and orange (1000 and 100 mg/L) with PEC; dark and light blue (1000 and 100 mg/L) with electrochemical process (e).

4.3.3 Main conclusions of the activity

In conclusion, this research demonstrates the significant potential of bio-electrochemical, electrochemical, and photoelectrochemical systems as innovative and sustainable solutions for the remediation of polluted soils and wastewater, as well as for the removal of microplastics from aquatic environments. Bio-electrochemical systems proved effective in degrading organic pollutants such as 2,4-D herbicide and high-strength agro-industrial wastewaters, while simultaneously enabling energy or valuable by-product recovery. Electrochemical and photoelectrochemical approaches showed promising results in the degradation and mineralization of polyethylene and PET microplastics, with evidence of synergistic effects under solar-assisted conditions. The integration of experimental investigations with mathematical modeling further supports the scalability and practical implementation of these technologies, highlighting their potential role in advancing environmentally friendly and energy-efficient treatment strategies.

4.3.4 Scientific products and dissemination

Research papers

Mascia, M., Melis, N., Piro, V.M.I., Rubanu, M.G., Vacca, A., Mais, M. (2026). Mapping hydrogen research frontiers: a multi-query bibliometric analysis of electrochemical and biotechnological pathways. Energies, 19(1), 166. https://doi.org/10.3390/en19010166

Melis, N., Rubanu, M.G., Mais, L., Mascia, M., Vacca, A. (2025). Removal of polyethylene terephthalate microplastics from water with reactive oxygen species generated by electrochemical and photoelectrochemical processes. Electrochimica Acta, 537, 146905. https://doi.org/10.1016/j.electacta.2025.146905

Mais, M., Rodriguez, J., Campana, R., Melis, N., Vacca, A., Mascia, M. (2025). Modelling and EIS characterization of a tubular microbial fuel cell with slip-casted ceramic membrane. Journal of Power Sources, 630, 236143. https://doi.org/10.1016/j.jpowsour.2024.236143

Mais, L., Rodriguez, J., Melis, N., Vacca, A., Mascia, M. (2024). Computational modelling as a design tool for bioelectrochemical systems. Current Opinion in Electrochemistry, 44, 101460. https://doi.org/10.1016/j.coelec.2024.101460

Mais, L., Mascia, M., Vacca, A. (2024). Assessing the Performance of Continuous-Flow Microbial Fuel Cells and Membrane Electrode Assembly with Electrodeposited Mn Oxide Catalyst. Energies, 17(4), 943. https://doi.org/10.3390/en17040943

Mais, M., Melis, N., Vacca, A., Mascia, M. (2023). Electrochemical removal of PET and PE microplastics for wastewater treatment. Environmental Science: Water Research and Technology, 10(2), 399–407. https://doi.org/ 10.1039/d3ew00582h

Conference Proceedings

Melis N., Mais L., Mascia M., Vacca A. (2024) Electrochemical and photoelectrochemical degradation of PET. 5th E3 Mediterranean Symposium Electrochemistry for Environment and Energy. Bilbao (Spain) July 2024.

Melis N., Mais L., Mascia M., Vacca A. (2024) Alkaline Electrolysis for the treatment of Tar-containing wastewater and hydrogen production. 5th E3 Mediterranean Symposium Electrochemistry for Environment and Energy. Bilbao (Spain) July 2024.

Mascia M., Mais M., Melis N., Piro V.M.I., Vacca, A. (2025) Microbial Electrolysis Cells for fish industry wastewater treatment and Hydrogen production: a modelistic approach. 15th European Congress of Chemical Engineering (ECCE) & 8th European Congress of Applied Biotechnology (ECAB) & 3rd Iberoamerican Congress on Chemical Engineering (CIBIQ). 8-10 September 2025, Lisbon/Portugal.

Melis N., Mais M., Piro V.M.I., Rubanu M.G., Vacca A., Mascia M. (2025) Modelling Microbial Electrolysis Cells for Hydrogen Generation and Wastewater Treatment in the fish industry. 76th Annual Meeting of the Internation Society of Electrochemistry. Mainz (Germany) 7-12 September 2025.

4.4 Supramolecular materials, non-canonic aminoacids and natural biopolymers for sensing and remediation in environmental samples (UNICA)

(Contributors: Claudia Caltagirone and Giacomo Picci (supramolecular gels), Andrea Porcheddu (green chemistry) and Angelo Frongia (non-conventional aminoacids)).

4.4.1 Introduction

The development of innovative functional materials and efficient synthetic methodologies plays a central role in advancing modern organic and materials chemistry, particularly in response to growing environmental and technological challenges. The design of structurally complex non-conventional amino acids expands the toolbox for the synthesis of bioactive molecules and advanced building blocks, while supramolecular systems based on low molecular weight gelators (LMWGs) offer versatile platforms for environmental remediation through tunable non-covalent interactions. In parallel, the valorization of natural biopolymers within green chemistry approaches represents a sustainable strategy for catalytic and industrial applications. In this context, the present work explores: (i) the development of new synthetic routes toward structurally relevant cyclobutan-β-amino acid derivatives; (ii) the design, characterization, and environmental application of supramolecular gels for pollutant removal from water matrices; and (iii) the implementation of eco-friendly keratin-based systems as aqueous emulsifying media for catalytic hydroformylation processes. Together, these studies highlight an integrated approach combining synthetic innovation, supramolecular chemistry, and sustainable materials for advanced functional and environmental applications.

4.4.2 Methodologies and main Results

Non-conventional aminoacids. Development of an efficient synthetic procedure to synthesise a variety of structurally relevant 2-oxabycyclo [3.2.0] eptan-3-ones bearing a benzo[d]oxaazol-2(3H) -one pendant group in the quaternary center of the junction, with moderate yields in a single synthetic step. Further reactions on the reactivity of this new system demonstrate the synthetic relevance of these products in the synthesis of novel cyclobutan-β-aminoacidic derivatives (Figure 43).

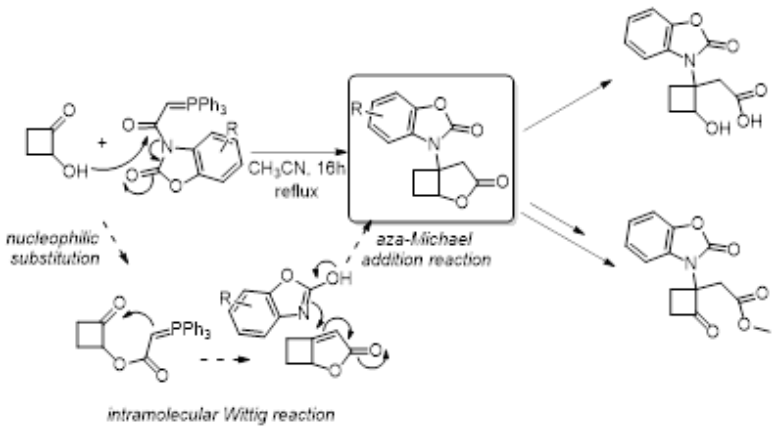

Figure 43: Chemical structure of the synthesized non-conventional amino acids.

Supramolecular Gels. New Low Molecular Weight Gelators (LMWGs) have been synthesized and characterized by means different techniques (Figure 44). The new gelators presented urea and squaramide scaffolds and fluorophore and acidic moieties as substituents. The design of these molecules has been developed taking into account the presence of functional groups as -NH or -COOH groups or aromatic substituents able to establish non-covalent interactions, such as hydrogen-bond or □-□ interactions. The possible abilities of the novel gelators to form supramolecular gels has been investigated, highlighting that almost all LMWGs synthetised were able to form gels, in particular hydrogels. Three different triggers were exploited to promote the gel formation: pH, temperature and solvent. All materials obtained were characterised by means different techniques: rheology (to study the viscoelastic behaviour and the mechanical properties of the gel obtained), TEM (to investigate the inner structure of the xerogels and the formation of fibers, typical of this type of materials), SAXS (to probe and examine the primary fibers in terms of size and shape). In some cases, fluorescence studies were performed to study the changes in emission during the gelation process. The most stable gels were tested as adsorbent materials to remove pollutants from water matrix. These tests were performed by using different experimental setups, in particular contact test, flow test and dispersion test were carried out, in this way has been possible to evaluate the best experimental setup for each gel, depending on the characteristics of the materials. The removal of four different classes of pollutants has been investigated, dyes, heavy metals, PFAS and NSAIDs were studied. The studies performed highlighted the removal abilities of the materials obtained.

It has been possible to observe the complete removal of dyes such as rose bengal or nile blue A, while in the case of heavy metals the highest removal efficiency has been observed in presence of mercury. Concerning PFAS and NSAIDs impressive results has been obtained, highlighting the possible use of the supramolecular gels studied as adsorbent materials also for emerging pollutants.

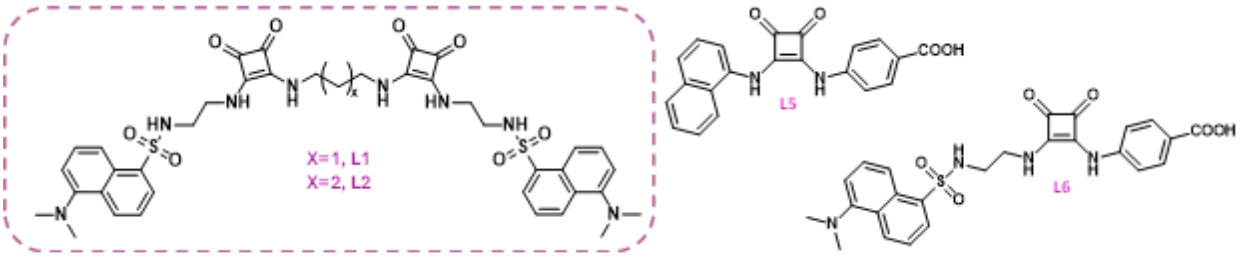

Figure 44: Chemical structure of the synthesized gelators.

- L1 and L2 gels obtained in DMSO/H_2O at various ratio are able to adsorb in a good removal efficiency (RE%) organic dyes by contact test , particularly Rose Bengal.
- The most stable gels were studied as possible filters (Flow Test) to remove dyes from water, in particular Rose Bengal and Nile Blue A.
- The possible reuse of gels was investigated, highlighting that all gels studied could be used at least 3 cycles with both dyes.
- The possible release of gelators and DMSO was investigated. To avoid the presence of DMSO in the treated water all gels were washed before using them as filters. Washed gels showed a better RE%, increasing the number of reusing cycles.
- The two gelators were tested as potential material to remove emerging pollutants from water matrices, in particular PFAS (PFOA e PFOS) and NSAIDs (Na-Ibuprofen).
- All gels tested showed a higher removal ability towards PFOS and Na-Ibuprofen, with an average RE% of 90%.

- Gels obtained with L5 and L6 were used dispersed in water containing different pollutants. After only 1 hour of stirring the gels were able to remove completely Rose Bengal.
- The test in presence of dyes was performed also by using a dialysis membrane, confirming the same trend.
- The same test was performed in presence of heavy metals, in particular gel obtained with L5 at 1 mg/mL + 8 mg of GdL was able to remove mercury from water with a RE% of 98%.
- All gels were tested as potential material to remove emerging pollutants from water matrices, in particular PFAS (PFOA e PFOS) and NSAIDs (Na-Ibuprofen), showing a higher removal ability towards PFOS and Na-Ibuprofen around 95%-99%.
- The most promising gels (L5 gel in DMSO:H_2O (3:7 v/v) at 0.5% w/v and L6 gel, 0.2% w/v + 11 mg of GdL) were selected to assess their ability to remove higher pollutant concentrations from a water matrix (2.5 mg/mL, 5 mg/mL, 7.5 mg/mL and 10 mg/mL).

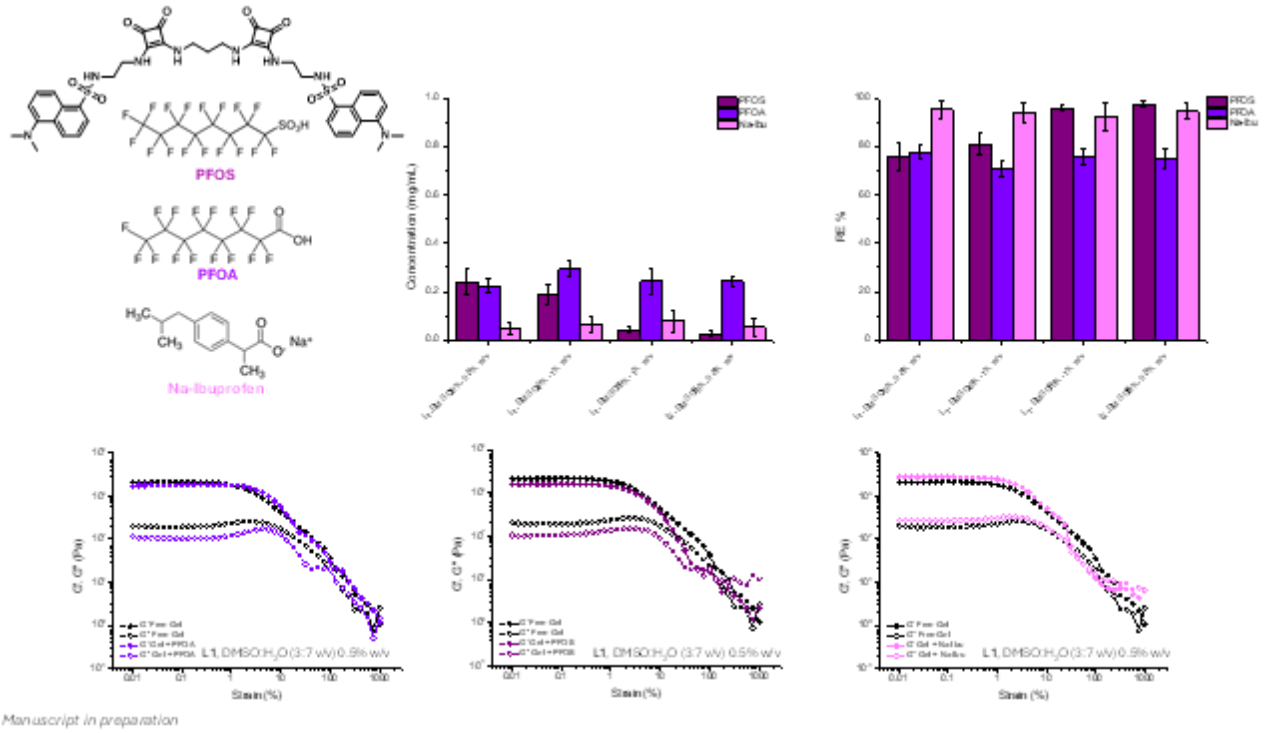

Figure 45: Main adsorption results achieved with the supramolecular gels.

Natural biopolymers. The research group led by Prof. Andrea Porcheddu has devised a green strategy to generate wool-derived keratin powder that is free of lanolin and other surface contaminants. This eco-friendly powder now serves as an aqueous emulsifying agent in hydroformylation processes. Under microwave irradiation, well-defined micelles form in water, positioning the metal at the micellar periphery and thereby promoting the conversion of olefins into linear aldehydes. Purification is accomplished with Bertagnini salts in water.

4.4.3 Main Conclusions of the study

In conclusion, this work demonstrates the successful integration of synthetic innovation, supramolecular design, and sustainable materials for advanced chemical and environmental applications. An efficient single-step synthetic strategy enabled the preparation of structurally relevant 2-oxabicyclo[3.2.0]heptan-3-ones as valuable precursors to novel cyclobutan-β-amino acid derivatives, highlighting their synthetic versatility. The newly developed low molecular weight gelators proved highly effective in forming stable supramolecular hydrogels and exhibited remarkable adsorption performance toward a wide range of pollutants, including dyes, heavy metals (notably mercury), PFAS, and NSAIDs, with high removal efficiencies and good reusability. Finally, the development of a lanolin-free, wool-derived keratin powder as a green aqueous emulsifying system demonstrated an environmentally friendly approach to catalytic hydroformylation, enabling efficient conversion of olefins under mild conditions. Overall, the results underline the potential of combining advanced organic synthesis, supramolecular chemistry, and bio-based materials to address both synthetic and environmental challenges.

4.4.4 Scientific products and dissemination

S. Barranco, M. Uras, V. Frau, P. Caboni, R. Guillot, D. J. Aitken, A. Frongia, Eur. J. Org. Chem. 2025, 00, e202500332

M. Uras, S. Barranco, F. Zedda, A. Frongia, Eur. J. Org. Chem. 2025, 28, e202500171

J. Milia et al., Squaramide-based supramolecular gels for the removal of organic dyes from water matrices. Soft Matter, 2025, 21, 6047. https://doi.org/10.1039/d4sm01538j

Coccia et al. Wool-supported Pd and Rh nanoparticles for selective hydrogenation of maleic acid to succinic acid in batch and flow systems. RSC Adv., 2025, 15, 36760. https://doi.org/10.1039/D5RA05365J

4.5 Development of novel adsorbent media based on Extracellular Polymeric Substances (EPS) extracted from wastewater treatment sludge for the removal of heavy metals (UNIFI)

(Contributors: C. Lubello, B. Pagliaccia, T. Lotti)

4.5.1 Introduction

The growing environmental concern related to water pollution – including that generated by heavy metals, organic micropollutants, etc. – is driving scientific community and water treatment stakeholders to design highly performing and low-impact remediation technologies (Morin-Crini et al., 2022). Adsorption is recognized as a viable strategy for water purification purposes thanks to its advantages in terms of easy operation, cost-effectiveness and efficiency (Touihri et al., 2021). These benefits are emphasized when bio-based waste-derived adsorbent media are used. Value-added biomaterials suitable for adsorption applications can be recovered by re-thinking wastewater treatment trains according to circular economy logics. The potential for resource recovery could be further increased in the case of advanced technologies for biological wastewater treatment such as aerobic granular sludge (AGS) processes (Kehrein et al., 2020). Aerobic granules are dense pseudospherical microbial aggregates, consisting of self-aggregating biofilms, which provide major advantages for wastewater treatment such as better settling properties, potential for simultaneous carbon, nitrogen and phosphorous removal, less energy input, more compact treatment facilities, etc. (Pronk et al., 2015). Moreover, with respect to conventional activated sludge (CAS), waste AGS can be concentrated by simply draining up to about 11 wt% thanks to its dense granular structure, providing a concentrated feedstock for downstream recovery processes (Pagliaccia et al., 2024). In AGS, microorganisms produce large quantities of extracellular polymeric substances (EPS) to form a hydrogel matrix in which they are self-immobilized (Felz et al., 2016; Flemming & Wingender, 2010; Seviour et al., 2019). The fraction of EPS able to form hydrogels, exerting the main contribution to the structural integrity of bioaggregates, are usually defined within the scientific community as structural EPS (sEPS) (Felz et al., 2016). The recovery of EPS from excess sludge and their conversion into valuable products is expected to play a crucial role in the transition towards a circular economy-based wastewater sector (Kehrein et al., 2020). This would allow not only to yield high-value resources for material development, but also to decrease the mass of residues to be handled, with environmental and economic benefits for wastewater treatment.

In this perspective, this research aims to evaluate the feasibility of exploiting AGS-derived sEPS for the treatment of heavy metal-contaminated wastewater. The metal removal performance of sEPS – in the form alkaline aqueous dispersions – and freeze-dried sEPS hydrogel beads were compared in equilibrium adsorption studies to treat both synthetic single- and multi-metal solutions containing increasing concentrations of M^{2+} (M^{2+}=Pb^{2+}, Cu^{2+} and Ni^{2+}) as well as real wastewater. The residual metal concentrations at equilibrium were determined through ICP-AES, while the adsorption mechanisms were investigated through a complete set of spectroscopic and microscopic techniques. Guidelines for future process implementation were suggested.

4.5.2 Methodologies

The extraction of sEPS from AGS was carried out by adapting the physical-chemical method developed by Felz et al. (2016) which first involves the thermo-alkaline solubilization of the EPS matrix (80 °C, Na2CO3, pH=11.3) followed by the acidic precipitation of the gel-forming sEPS (HCl, pH=2.2). The sEPS acidic pellets

recovered after centrifugation was re-suspended by adding NaOH until pH=8.5–9. The extraction yield was calculated on a volatile solids (VS) basis as mass ratio of extracted sEPS to initial AGS. The hydrogel-formation was carried out via ionic cross-linking by applying an extrusion method: the sEPS aqueous suspension at 5 wt% concentration was added dropwise into a 2.5 % (w/w) $CaCl_2$ solution and then left overnight to stabilize. The sEPS hydrogel beads were cut into smaller fragments and freeze-dried to use them in biosorption tests. The adsorbent media preparation is summarized in Figure 46.

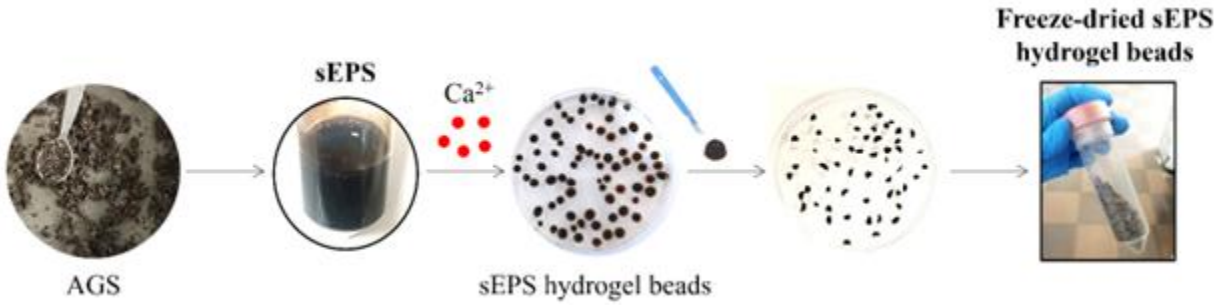

Figure 46: Schematization of the EPS-based adsorbent media preparation.

The equilibrium adsorption studies were carried out at a controlled temperature of 20 ± 0.5 °C to treat multi-metal aqueous solutions containing increasing concentrations of $Pb(NO3)_2$, CuCl2·2H2O and $NiCl_2·6H_2O$ (C0 = 4 – 470 mg M^{2+}/L for each target metal). Similarly, single-metal adsorption experiments were also conducted in the C0 ranges from 7 to 666 mg M^{2+}/L for sEPS and from 8 to 759 mg M2+/L for sEPS hydrogel beads. Additionally, urban wastewater (to which 150 mg M2+/L was added for each target metal) was tested to assess the treatment stability in the case of real matrices. sEPS – in the form of aqueous suspensions at 2 wt% concentration – and freeze-dried hydrogel beads were kept in contact under stirred conditions with the targeted metal solutions / wastewater overnight at pH=5. After centrifugation/settling, the supernatants were 0.45 µm-filtered and analysed by ICP-AES to measure the residual metal concentrations at equilibrium (Ce, mg/L). In both cases, an adsorbent dose (i.e. sEPS or hydrogel beads) of about 6.5 g TS/L was used. The adsorption capacity (Qe, mg/g TS) and removal efficiency (%Removal, %) were determined through Eqs. 1 and 2, respectively, where m (g TS) is the adsorbent mass and V (L) is the solution volume.

$$Q_e = \frac{(C_0 - C_e) \cdot V}{m} \quad (1)$$

$$\%Removal = \frac{(C_0 - C_e)}{C_0} \cdot 100\% \quad (2)$$

The experimental Qe vs. Ce profiles were fitted by Langmuir and Freundlich models using Eqs. 3 and 4, respectively, where Q_m (mg/g) is the maximum adsorption capacity, b (L/mg) is the Langmuir constant, K_F (mg1-(1/n)·L1/n/g) and n (-) are the Freundlich constants related to adsorption capacity and intensity, respectively (Touihri et al., 2021).

$$Q_e = \frac{b \cdot Q_m \cdot C_e}{1 + b \cdot C_e} \quad (3)$$

$$Q_e = K_F \cdot {C_e}^{1/n} \quad (4)$$

Referring to the Langmuir model fitting, the separation factor RL was determined according to Eq. 5, where $C_{0,max}$ (mg/L) is the maximum initial metal concentration tested: RL indicates either the adsorption is unfavourable (RL > 1), linear (RL = 1), favourable (0 < RL < 1) or irreversible (RL = 0) (Touihri et al., 2021).

$$R_L = \frac{1}{1 + b \cdot C_{0,max}} \quad (5)$$

The adsorption mechanisms were investigated by combining multiple advanced techniques such as ICP-AES, scanning electron microscopy (SEM) coupled with energy dispersive X-ray spectroscopy (EDX) and three-dimensional excitation-emission matrix (3D-EEM) fluorescence spectroscopy.

4.5.3 Results

The applied extraction method yielded an average amount of sEPS of 234 ± 32 g VSsEPS/g VSAGS (898 mg VSsEPS/g TSsEPS). As shown in Figure 47, the extrusion method enabled the formation of sEPS hydrogel beads with homogeneous shape and size distributions (equivalent diameter = 5.2 ± 0.7 mm), thus suggesting promising opportunities for large-scale development. The ICP-AES results confirmed the inclusion of large quantities of Ca^{2+} ions into the polymeric matrix during the cross-linking reaction (calcium concentrations = 0.6 vs. 48.0 mg Ca/g TS in sEPS and hydrogel beads, respectively). Ca^{2+} ions reasonably act as reversible cross-linkers binding to multiple sites on different polymer chains, thus contributing to the establishment of a 3D network that traps water.

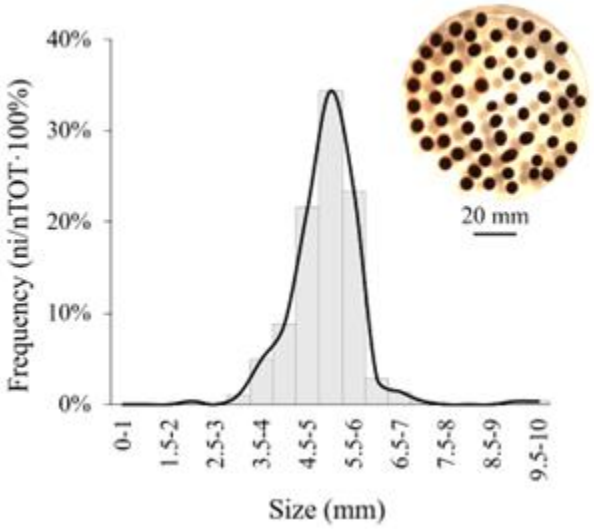

Figure 47: Size distribution of sEPS hydrogel beads.

For both sEPS and hydrogel beads a decrease in removal efficiency and an increase in Qe was observed with increasing C_0 (Figure 48). The progressively higher driving force provided by raising C0 reasonably made available an increasing number of binding sites for further M^{2+} adsorption. Metal-binding capacities comparable or even higher than those reported for conventional adsorbent media were observed (e.g. eucalyptus bark-derived activated carbon: Qe = 29 mg Cu^{2+}/g at C0 = 635 mg Cu^{2+}/L; Kongsuwan et al., 2009). The treatment performance decreased in the following order among the tested M^{2+}: Pb^{2+} > Cu^{2+} > Ni^{2+}. The

same trend was observed for EPS of different origin (Pagliaccia et al., 2022), thus suggesting a selective affinity towards the targeted metals.

sEPS displayed higher metal uptake, especially for the highest C_0. In the case of sEPS hydrogel beads, a certain number of binding sites were expected to be unavailable due to the cross-link with Ca^{2+}, thus potentially leading to lower adsorption performance. However, a significant heavy metal uptake was still enabled by the 3D hydrogel structure that likely promoted diffusion of M^{2+} into the polymeric network upon swelling and their subsequent adsorption. It is worth noting that the structural integrity of sEPS hydrogel beads was preserved along the entire experiments: indeed, M^{2+} adsorption likely increased the cross-linking density of the polymeric network and hence its chemical and mechanical stability over the treatment.

In the presence of initial metal concentration C_0 higher than approximately 130 mg M^{2+}/L, sEPS dispersions underwent flocculation and co-precipitation with metals. Multiple-bridging complexation phenomena could be reasonably promoted by increasing C_0, and therefore the amount of heavy metal ions adsorbed on the sEPS binding sites. In line with this hypothesis, divalent cations M_{2+} ions could act as bridges for different polymer chains: this would result in a strong increase in particle size, and in a reduction in the repulsive force among sEPS units, thus leading to aggregation and finally to precipitation (Pagliaccia et al., 2022).

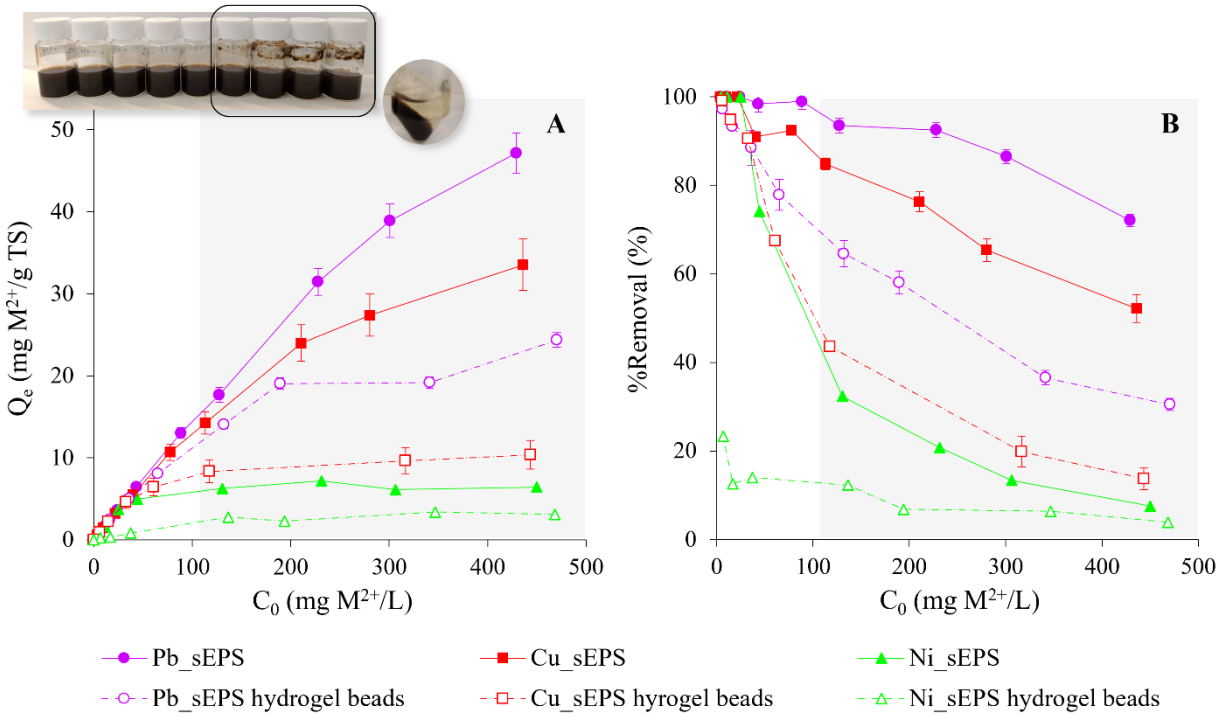

Figure 48: Trends of adsorption capacity (A) and removal efficiency (B) at increasing C0 in the case of synthetic multi-metal solutions. The grey rectangles highlight the C0 range in which sEPS flocculation and subsequent precipitation with metals were observed.

For both sEPS and hydrogel beads, large releases of X^{n+} ions (such as Ca^{2+}, Na^{+}, Mg^{2+} and K^{+}) in the liquid bulk were observed during M^{2+} adsorption (Figure 49), thus suggesting the occurrence of ion exchange mechanisms in the heavy metal uptake. However, the M^{2+}/X^{n+} ratios were always lower than 1 mEq/mEq, especially for sEPS hydrogel beads: this would indicate that ion release was also driven by other mechanisms, mainly related to ion concentration gradient between the polymeric network and the surrounding medium. In the case of sEPS hydrogels beads, Ca^{2+} accounted for more than 95 % of the total ion release detected upon M^{2+} adsorption: it should be noted that not all Ca^{2+} ions diffused into the sEPS matrix during gelation

participated to the effective cross-linking: most of them dissolved in the free water filling the voids within the 3D polymeric network (Pagliaccia et al., 2024), thus being more prone to release.

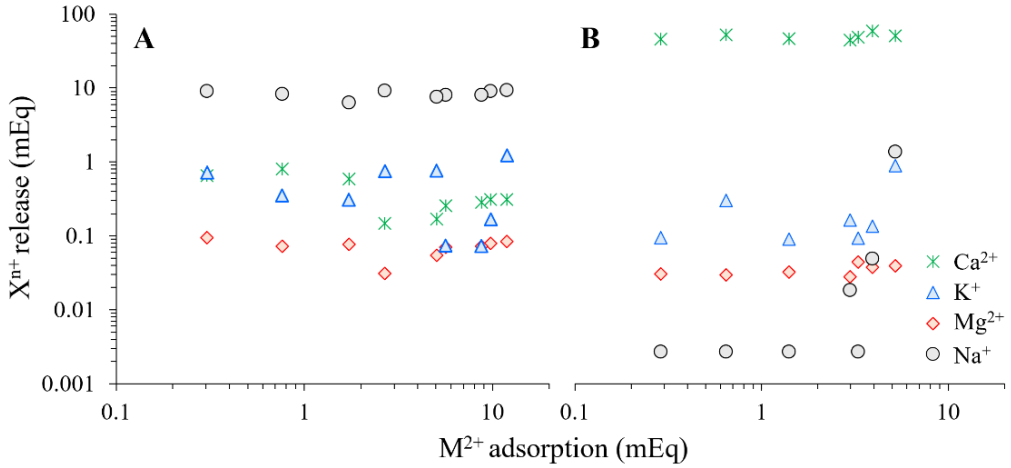

Figure 49: Release of Xn+ ions (i.e. Ca2+, K+, Mg2+ and Na+) during heavy metal adsorption for both sEPS (A) and sEPS hydrogel beads (B). For clearer visualization, both X- and Y-axes are in log-scale. Data refer to the same adsorption tests shown in Figure 46.

SEM-EDX measurements confirmed that M2+ were homogeneously adsorbed on the available binding sites on polymer chains, including those located in the inner porosity of sEPS hydrogel beads. Additionally, regular crystalline structures ascribable to metal micro-precipitates were revealed on the surface of the polymer composite aggregates/hydrogels (Figure 50). This evidence was confirmed by literature data reporting that the EPS-heavy metal interactions are largely governed by ion exchange, complexation and surface precipitation phenomena (Li & Yu, 2014). Bearing in mind the above, it can be stated that heavy metal adsorption reasonably took place through a multifaceted mechanism, involving ion exchange, complexation and precipitation.

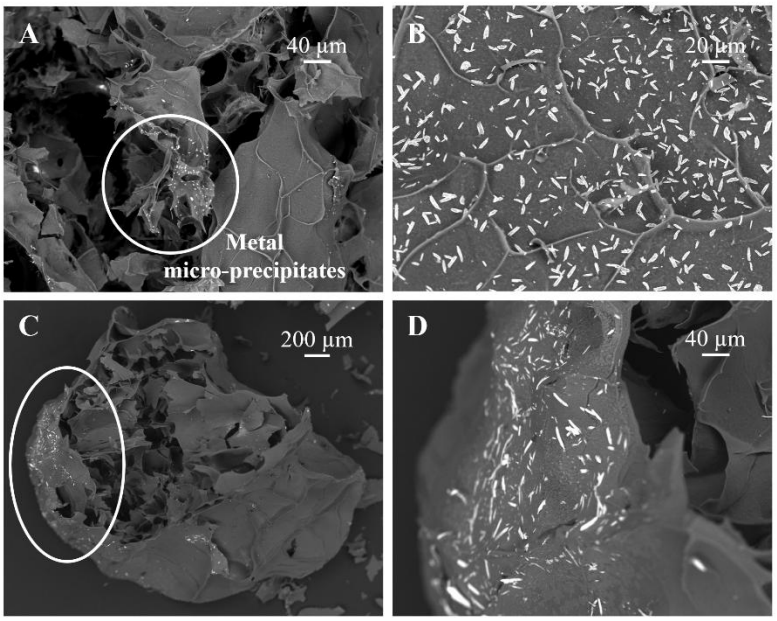

Figure 50: Microphotographs obtained through a scanning electron microscope (SEM Zeiss Evo MA15) of both sEPS (A, B) and sEPS hydrogel beads (C, D) after heavy metal adsorption. The images refer to the adsorption experiments carried out with multi-metal solutions at the highest tested C_0.

In the 3D-EMM fluorescence spectra of sEPS (Figure 51A), two main peaks were identified at excitation/emission (Ex/Em) wavelengths of 285/338 nm and 340/449 nm, which were assigned to protein (PN)- and humic-like substances, respectively, as similarly reported by Wei et al. (2016). The intensity of the fluorescence peaks progressively decreased after the addition of increasing dosages of M^{2+} – which are readily adsorbed by sEPS – (Figure 51B), thus implying the interaction of M^{2+} ions with both PN and humic substances during the adsorption processes (Wei et al., 2016).

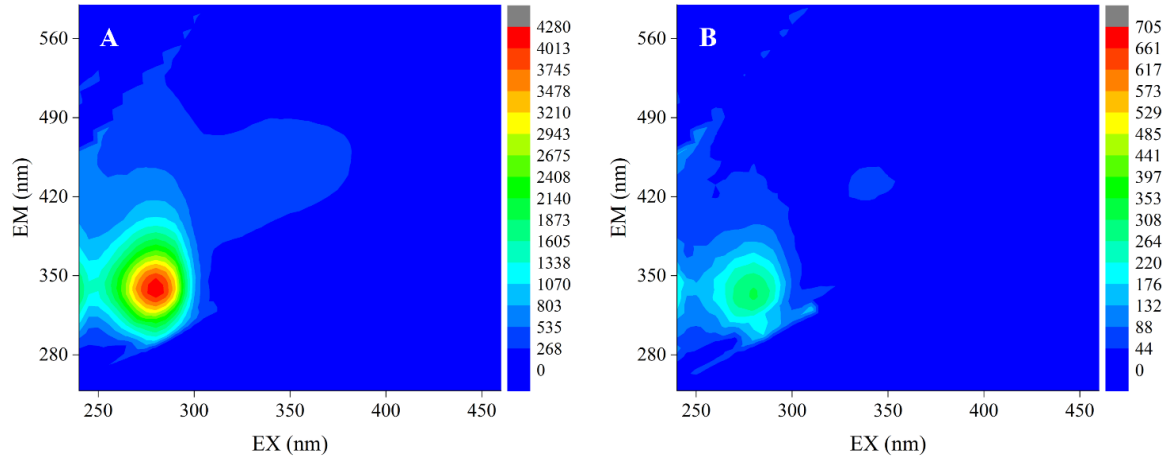

Figure 51: 3D-EEM of sEPS aqueous dispersions (at a concentration of 0.02 wt%) before M2+ dosage (A) and after the addition of 10 µg M2+/L of each target metal, i.e. Pb2+, Cu2+ and Ni2+ (B). The 3D-EEM fluorescence spectra were collected through an Aqualog® spectrofluorometer system (HORIBA Scientific) with subsequent scanning emission (Em) spectra from 248 to 826 nm by varying the excitation (Ex) wavelength from 240 to 820 nm at 5 nm increments.

The experimental C_e vs. Qe profiles were well-simulated by Langmuir or Freundlich adsorption isotherm models (Figure 52, Table 12). The values of the separation factor RL between 0 and 1 would indicate a favorable adsorption (Touihri et al., 2021) towards all target heavy metals for both sEPS and hydrogel beads.

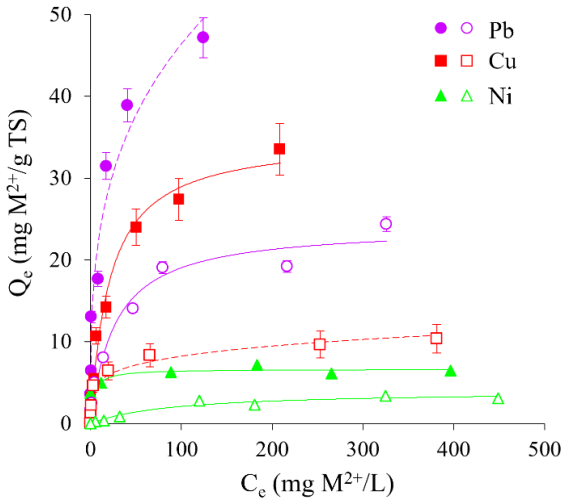

Figure 52: Experimental adsorption isotherms of both sEPS and sEPS hydrogel beads, in full and empty markers, respectively, and their fitting through Langmuir (continuous lines) and Freundlich (dotted lines) models. For clearer visualization, only the best model fittings are reported. Data refer to experiments carried out with multi-metal aqueous solutions.

It is worth noting that the competition among the different M^{2+} ions for the available binding sites reasonably decreased the Qe values compared to those achievable in the case of single-metal aqueous system: this evidence is visible in Figure 53 for Cu^{2+} selected as reference M^{2+} for these kinds of investigations.

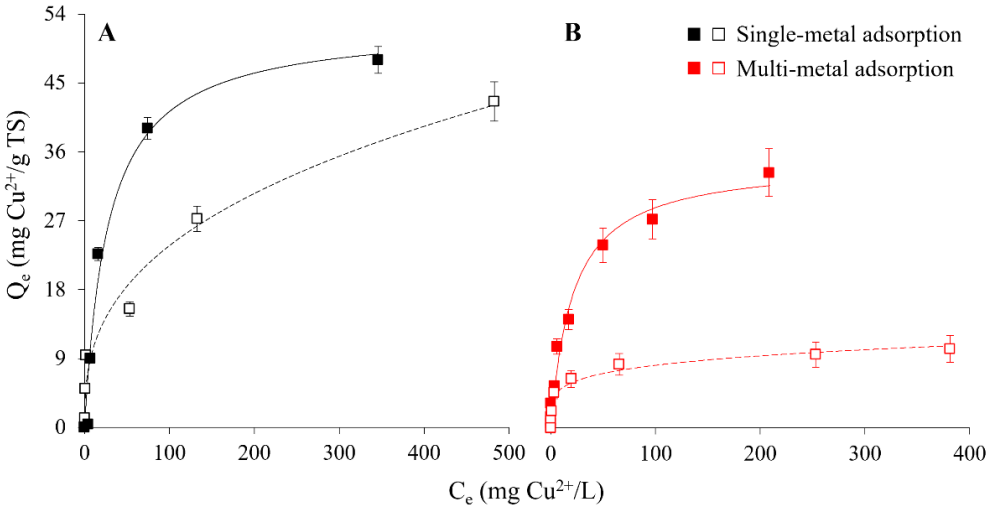

Figure 53: Cu^{2+} experimental adsorption isotherms of both sEPS and sEPS hydrogel beads, in full and empty markers, respectively, and their fitting through Langmuir model (continuous lines) and Freundlich model (dotted lines) in the cases of single-metal (A) and multi-metal (B) aqueous systems. For clearer visualization, only the best model fittings are reported. Model fitting parameters related to the single-metal adsorption are listed in Table A2 in Appendix.

The heavy metal uptake was maintained and even improved in the case of real wastewater, as evidenced in Figure 54 for sEPS hydrogels beads. This evidence would indicate that the presence of organic matter (both in solubilized and particulate forms) could positively influence the M^{2+} adsorption: such a synergic effect could be promoted by multiple mechanisms including adsorbent surface modification, formation of metal-organic complexes, etc. The stability of treatment performance in the presence of complex wastewater matrices is a crucial factor for process development, since real effluents often contain competing ions, organics, etc. Demonstrating this stability is particularly significant for sEPS hydrogel beads, as their Ca^{2+} cross-linked structure could limit the number of available binding sites for M2+ adsorption.

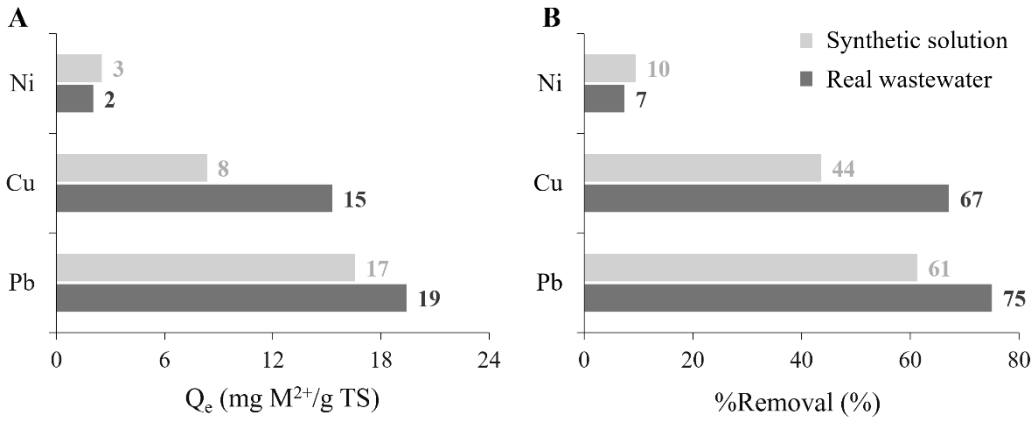

Figure 54: Comparison of the adsorption capacities (A) and removal efficiencies (B) of sEPS hydrogels beads in the treatment of synthetic multi-metal aqueous systems and real wastewater. Data refer to experiments carried out at C0 ≈ 150 mg M^{2+}/L for each target metal.

Guidelines for the large-scale process implementation were suggested by the findings described above. From a technological standpoint, the use of sEPS hydrogel beads would have advantages in terms of adsorbent storage / transport (powder vs. liquid forms) and post-treatment separation (gravity vs. filtration). In the presence of relatively low C_0, the beneficial effect due to the 3D polymer chain arrangement would make hydrogels the eligible option: although not cross-linked sEPS enabled higher M^{2+} uptake, their nature – i.e. stable colloidal dispersions – would hinder the effluent clarification process. In the case of highly concentrated heavy metal-contaminated wastewater – including a wide range of industrial discharges, such as those originated from electroplating, metal finishing, etc. – a multi-stage treatment approach could be implemented (Figure 55A). sEPS could be used in the form of aqueous dispersions in a pre-treatment phase, where the high C0 would allow the formation of composite aggregates that can be easily separated from the clarified effluent by gravity. Hydrogel beads could be then applied on the pretreated effluents to achieve higher heavy metal removals. This multi-stage treatment was tested on multi-metal aqueous systems showing an increase in the removal performance for all target metals (Figure 55B).

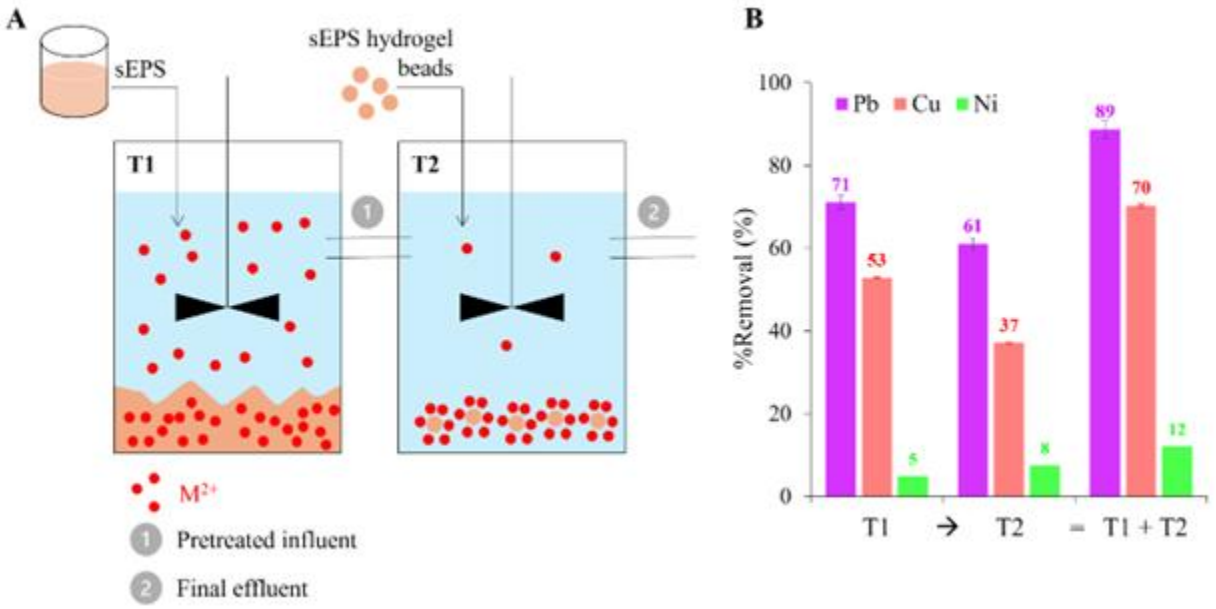

Figure 55: Schematization of the multi-stage process proposed for the treatment of highly concentrated heavy metal-contaminated wastewater (A) and its removal performance in the treatment of multi-metal aqueous solutions containing about 457 mg M^{2+}/L of each target metal (B).

4.5.4 Main conclusions of the activity

The present study proved the high potential of AGS-derived sEPS in the development of effective biomaterials for the treatment of heavy metal-contaminated wastewater, suggesting guidelines for future process implementations. Particularly, a multi-step treatment approach was recommended in the case of high levels of heavy metal contamination, combining a sEPS-based pretreatment with a refining stage using hydrogel beads. As a more general outcome, the work proposes an effective waste-to-value strategy based on sewage sludge-derived EPS that could potentially contribute to enhance the environmental and economic sustainability of wastewater treatment in the broader context of circular economy and resource recovery, while offering an effective strategy for heavy metal removal.

4.5.5 Appendix

Table 12: Langmuir and Freundlich fitting parameters related to the adsorption isotherms curves of both sEPS and sEPS hydrogel beads in the case of synthetic multi-metal solutions.

		sEPS			sEPS hydrogel beads		
Model	**Model parameter**	**Pb**	**Cu**	**Ni**	**Pb**	**Cu**	**Ni**
Langmuir	b (L/mg)	0.20	0.05	0.26	0.04	0.26	0.01
	Q_m (mg/g)	49.05	35.05	6.64	24.12	9.41	4.00
	R_L at C_{max} (-)	0.011	0.046	0.008	0.054	0.009	0.165
	R^2	0.955	0.985	0.853	0.976	0.962	0.957
Freudlich	n (-)	3.35	2.90	11.50	3.05	4.95	2.21
	K_f ($mg^{1-1/n} \cdot L^{1/n}/g$)	11.73	5.52	4.07	3.68	3.24	0.23
	R^2	0.970	0.979	0.853	0.965	0.975	0.911

Table 13: Langmuir and Freundlich fitting parameters related to the Cu^{2+} adsorption isotherms curves of both sEPS and sEPS hydrogel beads in the case of synthetic single-metal solutions.

	Langmuir model				**Freundlich model**		
	b (L/mg)	Q_m (mg/g)	R^2 (-)	R_L (-)	K_F ($mg^{1-1/n} \cdot L^{1/n}/g$)	n (-)	R^2 (-)
sEPS	0.04	52.69	0.973	0.04	6.59	2.84	0.924
sEPS hydrogel beads	0.01	53.43	0.965	0.14	4.44	2.75	0.984

4.5.6 Scientific products and dissemination

Pagliaccia, B., Severi, M., Lubello, C., Lotti, T., Biopolymers recovered from wastewater treatment sludge: a valuable resource for circular bioeconomy and green chemistry, ECOMONDO, 3–6/11/2025, Rimini (Italy). Oral presentation.

Pagliaccia, B., Severi, M., Lubello, C., Lotti, T., Development of novel adsorbent biomaterials based on structural extracellular polymeric substances (sEPS) recovered from aerobic granular sludge for the treatment of heavy metal-contaminated wastewater, IWA Resource Recovery Conference 2025 (IWA RR 2025), 19–23/05/2025, Leeuwarden (Netherlands). Poster pitch presentation.

4.6 Removal of rare earth elements and organophosphorus pesticides from aqueous phases by adsorption onto natural and synthetic phases (UNINA)

(Contributors: Fulvio De Paola, Armando Zarrelli, Gabriella Pinto, Marco Trifuoggi, Mauro Iuliano, Giancarlo Germano, Gaetano De Tommaso)

4.6.1 Description of the activities

The archaeological area of Cumae, situated along the Tyrrhenian coast of Campania, is characterized by a geological and hydrogeological context of considerable complexity. The volcano-sedimentary successions present on the site include sands, silts and clays of a marine-lagoonal environment, partly interbedded with pyroclastic levels and banks of yellow tuff. From a hydrogeological perspective, the domain is distinguished by the presence of a shallow phreatic aquifer and a deeper semi-confined aquifer, which are separated by a tuffaceous aquitard. In the proximity of the coastline, the aquitard is absent, and the water system functions as a single phreatic aquifer, subject to brackish intrusions during the recession phase.

In the present study, 14 groundwater samples were analyzed to characterize the distribution of natural radionuclides ((^{40}K, ^{222}Rn, ^{226}Th, ^{228}Ra, total alpha and beta activities) and rare earths (Sc, Y and lanthanides). The analysis was also used to assess any correlations between the radionuclides and rare earths. The radionuclides were quantified by standard radiometric techniques, while the determination of trace elements was performed by plasma source-coupled mass spectrometry (ICP-MS).

The entire dataset was processed in the MATLAB environment, with the application of multivariate statistical techniques, in particular Principal Component Analysis (PCA), in order to highlight common patterns and significant differences between the two hydrogeological domains. The PCA incorporates variables pertaining to both radionuclide and rare earth element concentrations. The data underwent a process of normalization, and the correlations between the parameters were represented by means of bi-plotting maps and graphs. This facilitated the identification of geochemical affinities and the potential presence of distinctive signatures associated with borehole depth.

Preliminary results indicate significant disparities between the two groups of samples with regard to their elemental composition and geochemical behaviors. It has been demonstrated that certain elements (e.g. Ce, Nd, ^{226}Th) exhibit preferential relationships as a function of aquifer level. This observation suggests the influence of selective fractionation processes, adsorption on a solid matrix, and mobilization under different redox conditions. The association with rare earths, a well-documented phenomenon in scientific literature due to their utility as natural tracers, has facilitated the refinement of the hydrogeochemical interpretation of the system.

In light of the ongoing seismic events in the Phlaegrean region, it is anticipated that a new sampling campaign will be initiated in order to assess potential variations in water composition and tracer distribution. The integration of this multivariate approach with spatial and temporal analyses has the potential to establish a methodological framework for the surveillance and sustainable management of groundwater resources in contexts characterized by high environmental and anthropic vulnerability.

4.6.2 Scientific products and dissemination

De Tommaso G., Iuliano, M. , Zarrelli, A., Piccialli,V., Montagnaro, F., Balsamo, M., Pinto, G., Tarallo, O., Vitale, L., Maglione, G., De Paola, F. 2025. Proceedings of MedLife 2025, 09-11- December 2025, Naples.

De Paola, F., Iuliano, M., Zarrelli, A., Piccialli,V., Montagnaro, F., Balsamo, M., Pinto, G., Tarallo, O., De Tommaso G. 2025. Proceedings of MedLife 2025, 09-11- December 2025, Naples.

4.7 Electro-Kinetic Remediation Technology for Soil contaminated by Heavy Metals (Eni Rewind)

(Contributors: S. A. Frisario (Eni Rewind), F. Villani (Eni Rewind), A. Conte (Eni), A. De Folly D'Auris (Eni), S. Ferro (INSTM), M. Vocciante (INSTM)).

4.7.1 Introduction

The application of electric fields through porous media, such as soils, generates transport phenomena that mobilize the impregnating solution (electro-osmosis) and the individual ionic species dissolved in it (electro-migration). Electro-osmotic flow is influenced by the external electric field (E), the electrokinetic potential (ζ), which depends on the properties of the soil particles, and the composition of the impregnating solution. In soils with a dominant clayey character, low salinity in the impregnating solution, and neutral or weakly alkaline pH, electro-osmosis is favored. This effect has important applications in soil dewatering and stabilization treatments, and the technology is also of great interest for removing pollutants from contaminated areas, including both heavy metals and organic substances. Electro-migration can significantly aid in the removal of ionic species. Both electro-osmosis and electro-migration require the soil to have a water content close to saturation.

Depending on the contaminant to be removed, the EKRT (electrokinetic remediation treatment) can be carried out either in situ, by installing electrode structures in the soil, or ex situ on site, by removing the contaminated material and transferring it to treatment tanks. After decontamination, the soil can be returned to its original site. The choice between these two approaches should depend on the specific characteristics of the site. In cases where it is necessary to introduce electrolytes or other components to facilitate contaminant removal (such as for mercury), maintaining a near-saturation condition in the soil is required, as this is a key part of the electrokinetic technique. This condition can be guaranteed in an ex situ on-site treatment but may be difficult to achieve with an in-situ approach. In such cases, the treatment's efficiency could be severely compromised, and there is a significant risk of worsening the site's conditions due to the uncontrolled release of electrolyte solution (and potentially mobilized pollutants) into deeper soil layers, which could have serious environmental and economic consequences. While these site-specific aspects do not invalidate the use of in situ treatment, they must be carefully considered when selecting the appropriate EKRT approach.

4.7.2 Techniques for Monitoring the Decontamination Process

Monitoring the progress of soil decontamination is inherently complex, due to the heterogeneity of contaminant distribution and the possible presence of the contaminant in various forms with different chemical stability. This results in varying degradation times and mechanisms. This is especially true for mercury contamination, where the monitoring process is influenced both by the solubilization and mobilization of different contaminant fractions, and by the need for a precise chemical speciation approach to identify the truly mobile fractions from those that are too stable to be attacked. These more stable fractions remain in the soil and are not released into the impregnating solution, and ultimately, the environment.

It is also important to note that mercury's toxicity is highly dependent on its chemical forms. Therefore, the goal of remediation should account for the actual capabilities of the available technologies, including the realistic expectation of mobilizing the various fractions present in the soil. To avoid incorrect assessments, it is essential to monitor the decontamination process by analyzing the process waters (i.e., the solution that

impregnates the soil after treatment with reagents designed to help remove the target contaminant). Well-conducted soil sample analysis is also crucial for completing the overall picture of the process.

Data produced from environmental monitoring are always the result of analyzing a limited number of samples. While analytical uncertainty can be minimized during laboratory analysis, sampling-related uncertainty is typically not addressed due to the high costs per sample. As demonstrated by several field studies, the overall uncertainty of environmental data is largely governed by sampling-related uncertainty (Jenkins et al., 1997). Moreover, analytical methods can be influenced by interference from the physical or chemical constituents of the sample. The more complex the sample matrix, the more likely these interferences are to cause significant analytical problems.

Therefore, data from any characterization campaign always contains some degree of error, a fact that is often overlooked by decision-making authorities. The rigorous chemometric approach proposed by the US EPA, known as the Data Quality Objectives (DQO) Process, involves an iterative process that uses analytical data and their variability to reconstruct the contamination scenario (US EPA, 2006). However, if the area of interest exhibits high variability, a statistically reliable approach requires many samples to produce results representative of the average contamination.

Due to the costs of sampling and analysis, initial contamination (or "pre-intervention baseline") is usually assessed as an average of a relatively small number of data points (discrete sampling). Estimating the corrected average value is important, as it influences decisions regarding the need for remediation and plays a crucial role in evaluating its effectiveness. A low average contamination value might initially seem beneficial for the remediation process (indicating minimal contamination), but the poor reliability of the data could lead to problems during post-treatment evaluation. If the remediation method fails to fully remove the contamination, post-treatment sampling could reveal a contamination value higher than the preliminary one, depending on local contamination levels. An additional concern is the potential presence of contaminants in different forms, each with varying abilities to interact with the matrix they are contained in. This is particularly significant in environmental contamination, as these different forms have distinct environmental mobility and bioavailability characteristics.

Sequential analysis procedures for speciation of metallic species in sediments (or soils) vary, both nationally and internationally, depending on the forms (compounds) being considered (Tessier et al., 1979; Schultz et al., 1996; Schultz et al., 1998; Craba et al., 2004; Outola et al., 2009). In the case of mercury, rather than focusing on detailed information about its various species, it is common practice to classify mercury compounds based on their behavior. These categories include: (a) water-soluble, (b) acid-soluble, (c) mercury bound to organic substances, (d) elemental mercury, and (e) insoluble mercury (such as mercury sulfide). The aim is to establish detection limits low enough to apply the proposed protocol effectively in environmental investigations.

In practice, when addressing mercury from an environmental perspective (since it is considered an undesirable pollutant), most regulations refer only to total mercury. This approach overlooks the fact that numerous studies have shown that mercury's toxicity depends heavily on its chemical forms. For example, mercury amalgams and sulfides are relatively low in toxicity, while organomercury and halogenated compounds (particularly through the action of methylmercury ion, CH_3Hg^+) can have irreversible, harmful effects on the central nervous system.

In 2010, as part of the Eni "New Environmental Technologies" project, in collaboration with the Ferrara Research Consortium – Electrochemistry Group of the University, the Eni Donegani Institute in Novara, and TPS Labs in Occhiobello (RO), an analytical approach was developed based on the method proposed by Boszke et al. (2008). This method includes five stages:

1. Organic mercury compounds (soluble in CH_3Cl)

2. Water-soluble mercury compounds

3. Mercury compounds soluble in acid (0.5M HCl)

4. Mercury bound to humic acids (soluble in 0.2M NaOH)

5. Insoluble mercury, further subdivided into metallic mercury, mercury sulfide, and calomel.

Additionally, Eni Donegani and TPS Labs introduced a specialized method for preparing "dry" samples for analysis. During the drying phase, temperature plays a key role in ensuring accurate data. To avoid the potential loss of metallic mercury, which may be present, the samples were equilibrated with ambient humidity instead of being conventionally heated at 105°C. For this purpose, the soil samples were placed in wide, low containers that allowed the sample to be spread over a large surface (such as Petri dishes or filter paper). These containers were left open to the air under a fume hood, with the sliding sash lowered so that the airflow gently touched the surface of the containers. This setup allowed the sample to reach a constant weight within 2-4 days.

Using the speciation approach proposed by Boszke et al., which involves thermal treatment at 150°C, it is possible to determine the presence of metallic mercury through calculation, as outlined in Equation 1.

$$\text{Metallic Hg} = \text{Residual Hg before thermal treatment} - \text{Residual Hg after thermal treatment} \quad (1)$$

After carefully analyzing the sequential extraction procedure described in Boszke et al. (2008) (and in Tessier et al., 1979, and Okoro et al., 2012), some uncertainty remains regarding whether the "residual" mercury is exclusively due to the presence of sulfides, or if it also includes other contributions, such as mercury(I) chloride (Hg2Cl2). To address this uncertainty, the following modified protocol was applied.

After analyzing the first five mercury species according to the Boszke et al. protocol, the fifth fraction is treated with a few drops of concentrated ammonia solution (approximately 30%) until the solid is fully wetted. The sample is then subjected to a second, complete selective extraction procedure following Boszke et al.'s protocol to detect any potential formation of elemental mercury from the treatment with ammonia, in accordance with the disproportionation reaction (2):

$$Hg_2Cl_2 \rightarrow Hg + HgCl_2 \quad (2)$$

Assuming that the reaction is quantitative, the amount of calomel (Hg2Cl2) initially present in the soil sample can be estimated based on the metallic mercury measured after treatment with ammonia. Similarly, the actual amount of mercury sulfide present in the sample will correspond exactly to the residual mercury determined after the basic treatment.

The analytical approach described above allows for the quantification of the following mercury species:

- Organic mercury compounds (e.g., methylmercury chloride, ethyl mercury chloride, phenylmercury)
- Water-soluble mercury compounds (e.g., $HgCl_2$)
- Acid-soluble mercury compounds
- Mercury associated with humic acids
- Elemental mercury
- Insoluble mercury ($HgS+Hg_2Cl_2$)
- Calomel (Hg_2Cl_2)

- Mercury sulfide (HgS)
- Total mercury

The most critical aspect of the work carried out is the introduction of the disproportionation reaction, which allows for a deeper chemical characterization of the insoluble residue. This step is not included in the Boszke et al.'s protocol. To assess the effectiveness of the ammonia treatment in promoting disproportionation and ensure the reaction is quantitative, tests were conducted by the LabAnalysis Environmental Sciences laboratory. Known quantities of HgS, Hg_2Cl_2, and $HgCl_2$ were added to a soil sample, with tests performed in duplicate. Each test treated approximately 5 g of soil, and the final volume of the solutions for the various fractions to be analyzed by ICP-MS was adjusted to 50 mL. The application of the protocol to these two replicates yielded the results reported in Table 14. In table 14, the theoretical concentrations are based on the data obtained from the original sample (before spiking).

By comparing the theoretical and experimental data, the percentage recovery for each mercury species was calculated. In the first replicate, recoveries ranged from 93.5% to 101.6%, while in the second replicate, they ranged from 87.8% to 99.4%. Overall, recoveries varied between 87.8% and 101.6%, indicating that the method is quantitative for the mercury species analyzed.

Based on these results, the laboratory has internally adopted this protocol under code P-AM-101338 rev0 2024.

Table 14: Calculation of percentage recoveries

	Parameter	Theoretical concentration (mg/kg)	Measured concentration (mg/kg)	Recovery (%)
Test 1	Organic mercury	N.A.	N.A.	N.A.
	Water-soluble mercury	N.A.	78.6	N.A.
	Acid-soluble mercury	883.8	810.2	100.6
	Mercury associated with humic acids	N.A.	N.A.	N.A.
	Elemental mercury	N.A.	N.A.	N.A.
	Insoluble mercury ($HgS+Hg_2Cl_2$)	1,654.4	1,592.4	96.2
	Calomel (Hg_2Cl_2)	851.5	796.0	93.5
	Mercury sulfide (HgS)	802.9	815.3	101.6
	Total mercury	2,538.2	2,486.8	98.0
Test 2	Organic mercury	N.A.	N.A.	N.A.
	Water-soluble mercury	N.A.	98.5	N.A.
	Acid-soluble mercury	720.3	617.6	99.4
	Mercury associated with humic acids	N.A.	N.A.	N.A.
	Elemental mercury	N.A.	N.A.	N.A.
	Insoluble mercury ($HgS+Hg_2Cl_2$)	1,826.04	1,604.1	87.8
	Calomel (Hg_2Cl_2)	828.3	798.3	96.4
	Mercury sulfide (HgS)	997.7	985.2	98.7
	Total mercury	2,546.3	2,377.8	93.4

N.A. = NOT APPLICABLE, as the species was not added.

4.7.3 The Various Applications and Implementations of EKRT Technology

Electrokinetic technology has been in practical use since the mid-20th century, primarily for stabilizing soft clay soils in geotechnical engineering. More recently, it has found applications in the remediation of

contaminated soils. Literature now includes reports on field tests targeting the removal of contaminants such as chromium and cadmium (Gent et al., 2004), total petroleum hydrocarbons (TPH) and BTEX compounds (Kim et al., 2011), and chlorinated solvents (Lageman et al., 2007).

In Italy, EKRT technology has been tested by Eni Rewind at industrial sites, evaluating systems proposed by ElectroChemical Processes LLC, Holland Environment, and Lynntech Inc. As will be explained in the following sections, it is important to clarify that past experiences have sometimes led to misconceptions and unrealistic expectations surrounding EKRT. For instance, the technology has frequently been associated with the version developed and patented in Germany by ElectroChemical Processes LLC. However, it's essential to note that simply applying electric potentials on the order of V/cm to a soil does not automatically generate the electrokinetic effects necessary for effective remediation.

The following sub-sections outline the different EKRT approaches, focusing on the key challenges observed over the last decade. These issues have been addressed through further studies and revisions, ultimately leading to the development of a proprietary patent by Eni.

4.7.3.1 EKRT according to ElectroChemical Processes LLC

ElectroChemical Processes LLC, based in Stuttgart, Germany, has been a key player in the development of electrokinetic remediation technologies. Their approach to the EKRT is centered around the application of low-voltage electric fields to contaminated soil or groundwater to facilitate the movement of contaminants towards collection or neutralization points.

The often-referenced technology is known as ElectroChemical Geo-Oxidation, ECGO (Wittle et al., 2009), developed by Falk and Niels Döring in the early 2000s as an evolution of the Induced Polarization (IP) concept. According to the IP principle (Ward and Fraser, 1967), when a high-voltage direct current is applied to porous, conductive surface materials – such as soil or rock – via in-situ electrodes, polarization sites on the mineral grain surfaces become polarized. This results in each polarization site acting as an electric dipole, opposing the applied electric field.

ECGO introduces five key distinctions from traditional IP:

1. ECGO is specifically designed for use in soils, which contain a diverse range of minerals.

2. While IP studies the decay of voltage once the electric field is switched off, ECGO continuously applies direct current over an extended period.

3. ECGO distinguishes between two types of electrodes in soil: a) Working electrodes, which introduce electricity into the ground, and (b) Soil particles, which function as micro-electrodes, including the solid/electrolyte interface.

4. Unlike IP, which requires high-voltage applications, ECGO operates at low voltages (generally under 100 V), producing electric fields ranging from 0.25 to 25 V/m.

5. ECGO incorporates alternating current (AC) alongside direct current (DC), with the AC ripple exceeding 10% of the DC input.

The technology developed by Falk and Niels Döring was patented in Europe in 1998 (EP 0578925 B1) and again in 2005 (EP 1123755 B1).

Between July 25, 2002, and November 11, 2003, ECGO technology was tested on PAH-contaminated sediments at the port of Duluth, Minnesota, USA. The contaminated material, stored at the Erie Pier Confined Disposal Facility (CDF), was chosen for the test due to its assumed homogeneity after prior mixing. This provided better control, avoiding further contamination during the test. The test cell, measuring 382 m3, was constructed from the stored sediments. After treatment, the average PAH concentration decreased by 17.3%, lower than the expected 50% reduction (Wittle et al., 2009).

A similar test was conducted by ECP at an industrial site owned by Eni Rewind (formerly Syndial) in 2008. Initially, six anodes and one cathode were placed in a hexagonal configuration, but ECP adjusted the setup, using three anodes and three cathodes based on contaminant distribution. The electrodes were installed to a depth of 6 meters. ECP used low-cost, carbon steel electrodes in direct contact with the soil, without creating housing pits. Water extraction from the saturated aquifer was needed to balance the electroosmotic flow, but the inevitable ohmic drop along the electrodes led to uneven polarization. The goal was to dissolve mercury (Hg0) through external and local electric fields, with the solubility of mercury linked to other chemical species in the soil. Both electromigration and electroosmosis were expected to assist in extracting the metal, with electro-deposition occurring at the cathodes and mercury oxide precipitation at the anodes.

Post-test, several limitations were identified:

- Difficulty tracking remediation progress via a mass balance.
- No control over solution composition near the electrodes.
- Challenges in controlling soil saturation levels.

Advantages of ECP technology included low invasiveness and installation costs. However, the approach is rather empirical, with positive results potentially due to the heterogeneous nature of soil contamination. The assumption that any soil particle can act as an electric dipole and trigger electrochemical reactions is highly questionable. Additionally, the claim that 5% residual soil moisture is sufficient for the process is unsupported, as transport mechanisms require a solvent capable of dissolving ionic species and enabling the movement of non-ionic ones.

4.7.3.2 EKRT according to Holland Environment

Holland Environment's EKRT technology is an electrochemically assisted soil washing process. It involves applying an electric field through a matrix of electrodes in vertical wells, circulating chemically conditioned electrolytic solutions through anodic and cathodic wells. These solutions disperse into the soil, maintaining moisture levels. The approach works for both saturated and unsaturated soils with interstitial fluids.

Eni Rewind tested this technology at an industrial site in 2008, aiming to decontaminate mercury from 50 m2 of soil. Electrodes (3 anode rows and 4 cathode rows) were placed in bentonite-lined wells, with potassium iodide solutions used to mobilize mercury. The process included mercury removal via an electrochemical cell (EnViroCell®). The results over nine months confirmed the effectiveness of the chemical and electrokinetic processes.

However, the following limitations were highlighted:

- The setup required 49 electrode wells for a small area.
- Reducing mercury in the electrochemical cell was difficult.

- The process solution spread horizontally and vertically, contaminating surrounding areas.

In conclusion, while ECP's experiment failed, Holland Environment's method showed promising results. The main challenge was solution dispersion, which can be mitigated with suitable site characteristics. Without those, ex-situ remediation offers advantages like equipment reuse and reduced treatment time.

4.7.3.3 EKRT according to Lynntech Inc.

Lynntech Inc.'s technology is also an electrochemically assisted soil washing treatment, similar to the Holland Environment's approach. It involves applying an electric field through electrodes placed in vertical wells within the contaminated material. Electrolysis of water near the electrodes produces H+ at the anode and OH– at the cathode, causing pH changes that affect the soil's zeta potential, solubility, ionic charge, and contaminant adsorption. Monitoring pH near the electrodes is crucial to prevent an acidic front from reducing electro-osmotic flow and halting the process. Lynntech Inc. suggests using compounds like citric acid or EDTA to modify the soil's zeta potential, enhancing electro-osmotic flow (US 6,193,867 B1).

Like Holland Environment, the wells are hydraulically connected to the soil, dispersing solutions and maintaining necessary moisture levels. Eni Rewind tested the technology at its site, using 3 + 3 anode wells and 2 cathode wells arranged in rows covering 200 m2, with a simpler and less invasive setup than Holland Environment's. Field results showed that mercury primarily moved from the cathode to the anode, indicating anionic species migration. The movement was mostly due to electro-migration, not enhanced electro-osmotic flow. Due to the high ionic strength of the solutions, mercury transport was slow, and remediation was inefficient.

4.7.3.4 4 EKRT according to Eni

In November 2012, following research conducted by the Electrochemistry Group of the University of Ferrara in collaboration with Eni R&D, Eni filed a patent application for a Process for Purifying a Soil Matrix Contaminated by Heavy Metals, which was granted by the Italian Patent Office in March 2015 (patent number 0001414308).

This patent describes a technology for the remediation of soil contaminated by heavy metals, particularly mercury, using an electrochemically assisted process. The method involves the use of cathode and anode wells inserted into the soil, where a potential difference is applied to displace the contaminating metals in the form of ionic complexes. Effective application requires a soil saturation level of at least 80%, underscoring the reliance on near-saturation conditions. It also requires continuous recirculation of process waters (anode, cathode, and impregnation solutions), with metal removal activated once contaminant concentrations reach a predefined threshold.

While these requirements can be met in ex-situ applications, they present challenges for in-situ use, particularly in porous or arid soils. Furthermore, in-situ recirculation of contaminated water may conflict with Italian regulations, requiring coordination with the relevant authorities to set a safe treatment threshold. Unlike other methods, Eni's technology uses auxiliary wells to extract contaminants, which accelerates the remediation process compared to approaches that rely solely on electrode wells.

More details on Eni's technology are described in the following section.

4.7.4 Further Details on Eni's Technology

Eni's patented soil remediation technology, designed primarily for treating soil contaminated with heavy metals, involves a series of steps aimed at improving contaminant removal efficiency. The main process uses a combination of electrokinetic techniques and chemical mobilizers to accelerate the migration of contaminants, particularly mercury, from the soil matrix.

Well configuration and electrochemical setup. The technology uses both anodic and cathodic wells positioned in the contaminated soil. These wells are filled with electrolyte solutions, which allow generating an electric field when a potential difference is applied to the electrodes. The electric field drives the migration of contaminants in the form of ionic complexes, moving them from the soil to the respective wells. The system is designed to effectively treat larger soil areas by promoting widespread electrokinetic migration.

Introduction of complexing agents. A key feature of the technology is the introduction of complexing agents into the soil matrix. These agents help solubilize metal contaminants, forming soluble metal-complex ions that can then migrate more easily through the soil. This process significantly improves remediation efficiency, especially for contaminants that would otherwise be highly bound to the soil matrix.

Continuous recirculation of process waters. Process waters, including anodic, cathodic, and impregnation solutions, is continuously recirculated in the system. After being extracted from the soil, these solutions are mixed and reintroduced into the soil. This recirculation helps maintain optimal pH conditions, which can be further adjusted by adding acids as needed.

Soil saturation and conditioning. As described in the patent, the technology works most effectively when the soil is at least 80% saturated, with an ideal target of 90% saturation. This near-saturation condition ensures that electrokinetic forces can effectively penetrate the soil matrix and mobilize contaminants. The high saturation requirement limits the technology's application to specific soil conditions, such as those with high moisture retention (e.g., high clay content) or soils that can be artificially conditioned to achieve the required saturation (e.g., in ex-situ applications).

Contaminants removal and threshold monitoring. Contaminant removal begins when the contaminant concentration in process water reaches a predefined threshold. This threshold is critical for process control, ensuring that contaminants are efficiently extracted without excessive energy or resources consumption. Constant monitoring of contaminant concentrations in recirculating water is required, and for in-situ applications, coordination with regulatory bodies may be necessary to ensure compliance with environmental standards.

Auxiliary wells for improved contaminant removal. Unlike traditional electrokinetic methods that rely exclusively on electrode wells for contaminant extraction, ENI's technology also uses strategically placed auxiliary wells to enhance the removal process. This approach accelerates remediation because the contaminants do not necessarily need to reach the electrode wells to be extracted. The integration of auxiliary wells allows for faster contaminant recovery, improving the overall efficiency of the technology.

4.7.5 Pilot Plant for testing Eni's EKRT Technology

Constructing a pilot plant for ex-situ, on-site, electrokinetic soil remediation requires replicating the typical system configuration used in laboratory studies (Figure 56), with appropriately scaled-up dimensions.

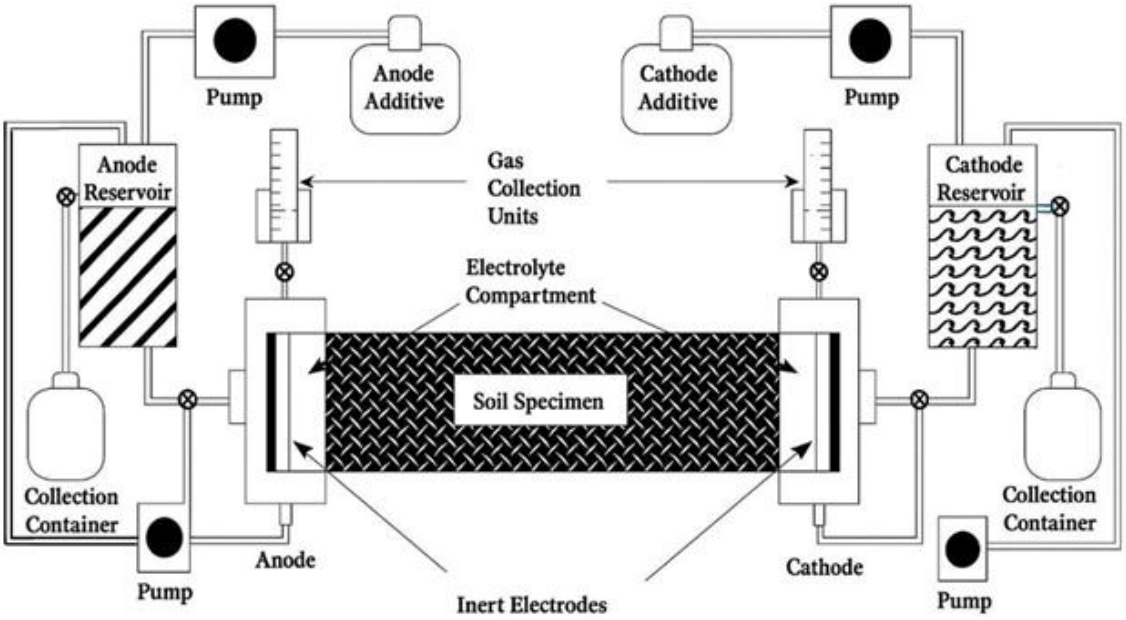

Figure 56: Layout of benchtop device for experiments on electro-osmotic extraction of pollutants from soil samples (Pictures Source: Unknown)

The pilot plant for testing Eni's electrokinetic soil remediation technology was set up in a prefabricated, reinforced concrete tank with certified water tightness, located within an existing warehouse owned by Eni Rewind (Figure 57). The tank was filled with mercury-contaminated soil, saturated with an electrolyte solution consisting of potassium iodide and nitric acid to facilitate mercury mobilization.

The electrodes were inserted into the contaminated soil via plastic piezometers (electrode wells). The system included three positive electrodes arranged in a row at one end of the tank, and three opposing electrodes positioned at the other end, approximately 3.65 meters apart. Two rows of monitoring wells were positioned between the electrode wells. The application of a potential difference between the electrodes generated an electric field, mobilizing the electrolyte solution and directing the contaminants toward the electrodes based on their charge.

After initial saturation of the soil, the electrolyte solution was recirculated via two pumps, which managed its extraction, homogenization, and reinjection into the electrode wells. The system ensured proper operation, preventing partial emptying or overflowing of the wells thanks to level sensors installed in the wells themselves. The hydraulic system also facilitated the extraction of the electrolyte solution for periodic quality controls. The extracted solution was analyzed to monitor the concentration and type of dissolved contaminants.

Recirculating the solution from different parts of the system ensured the neutralization of any pH fluctuations caused by electrochemical processes, improving the efficiency of contaminant removal. In the case of mercury-contaminated soil, this process can also enhance reduction reactions at the cathode, further contributing to mercury removal. pH adjustments were made automatically by adding nitric acid to the system.

Dewatering occurred every four weeks to remove about 50% of saturated electrolyte solution and replace it with a fresh one. Once dewatering was activated, the "used" electrolyte solution was aspirated from all wells, including the monitoring wells (referred to as dewatering wells), and properly disposed of.

To prevent the potential release of airborne contaminants due to volatilization or electrochemical reactions, the system was placed under negative pressure. The air extracted from the system was routed through an activated carbon filtration system to ensure environmental safety and regulatory compliance.

Figure 57: Pictures of EKRT Pilot Plant

4.7.6 Field test results on Eni's EKRT technology

The system used for the tests is shown in Figure 58. Due to issues encountered during the start up phase, management constraints and limited time availability, the test was able to run continuously for a total duration of approximately two months. System performance was monitored by periodically sampling the process solutions and continuously recording operating parameters at one-minute intervals.

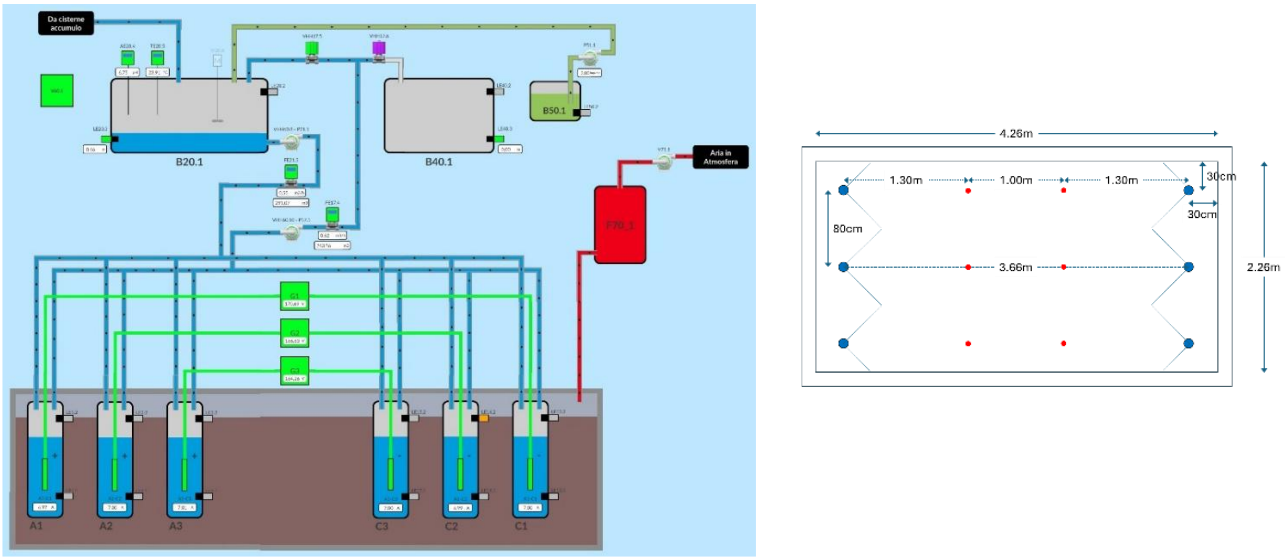

Figure 58: Representation of the pilot plant used (screenshot extracted from the control panel HMI) and dimensions of the watertight tank containing the mercury-contaminated soil.

Figure 59 presents the recorded current and potential trends, highlighting the different operating conditions adopted during the test.

During the first month, a constant current of 3.39A was imposed to each pair of electrodes (corresponding to 3A/m^2 of treated soil section). When the current was increased to 5A (4.42 A/m^2), operational instability

emerged. These issues were mainly related to deposit formation in the hydraulic lines, which caused oscillations in pH and fluctuations in solution levels within the electrode wells.

Periodic process water analysis showed a progressive increase in mercury concentration in solution, reaching a maximum value of 3.54 mg/L. However, beginning at the end of January (immediately before the current was increased from 3.39 to 5A), a decrease in dissolved mercury concentration was observed. This decline is plausibly attributable to reduction and/or precipitation phenomena occurring at the cathodes. The reduction in concentration also suggests that no additional mercury was being mobilized from the soil matrix.

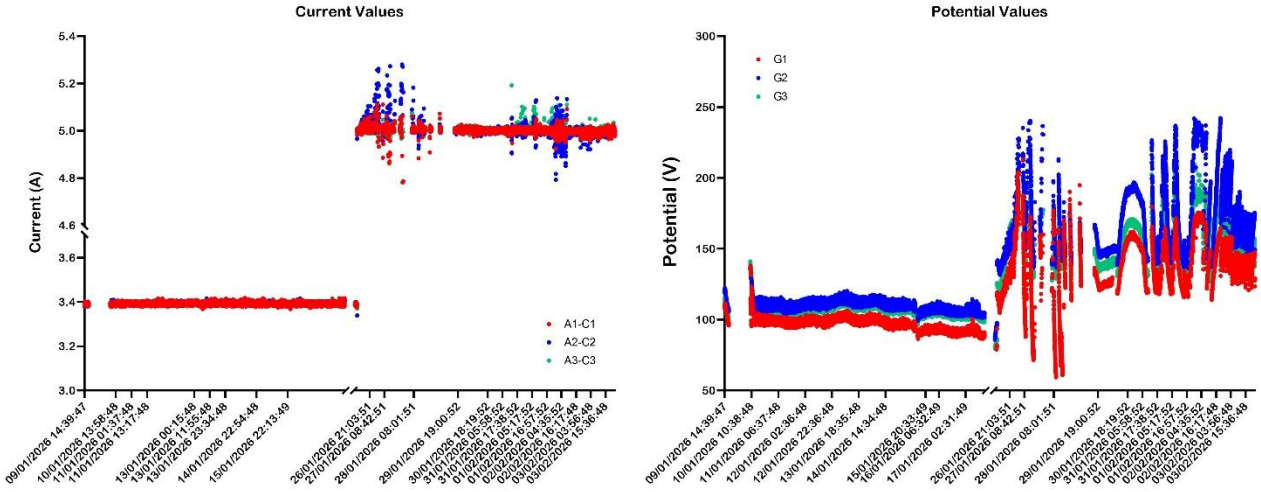

Figure 59: Current and potential values recorded during the electrokinetic decontamination test.

The maximum measured concentration (3.54 mg/L), multiplied by the volume of electrolyte solution saturating the soil (3.3 m^3), corresponds to an estimated 11.7 g of mercury removed from the soil. This value can be compared with the theoretically removable mercury species determined through soil speciation analysis. The soil volume in the tank was approximately 10.8 m^3 (14.1 m^3 total soil and electrolyte solution minus 3.3 m^3 electrolyte solution). The concentration of theoretically removable mercury species (water- and acid-soluble Hg, metallic Hg, and Hg_2Cl_2) was approximately 0.5 mg/kg. Using an estimated bulk density of 1.51 g/cm3 and assuming 95% dry residue at 105°C, the total soil mass is estimated at approximately 16,310 kg, corresponding to 15,495 kg of "dry" soil. Based on these values, the total extractable mercury is estimated at 7.75 g.

The total extractable mercury in the soil (7.75 g) is therefore significantly lower than the amount estimated to have been removed (11.7 g). This discrepancy may be related to the well-known heterogeneity of contamination in real soils, which can result in local concentration variability and sampling bias. Alternatively, it may indicate the partial removal of mercury species that were theoretically classified as non-removable based on the speciation analysis.

Following the observed decline in mercury concentration in the process water, an inspection of the cathodes was conducted on February 10. Whitish deposits were identified on the cathode surfaces and subsequently removed by acid washing during system dewatering. Analysis of a sample collected prior to acid dissolution indicated a total mercury concentration of 165 ± 4.03 mg/kg (dry matter). However, because the total mass of material removed from the cathodes was not measured, it was not possible to quantify the amount of mercury removed during the cleaning operations.

4.7.7 Physics-Based Digital Twin of the EKRT Pilot

In parallel with the field deployment of the EKRT pilot, a physics-based digital twin was developed to (i) mitigate operational risks associated with delays and unforeseen events, and (ii) complement pilot-scale monitoring through scenario analyses (e.g., alternative electrode configurations, voltage setpoints, and hydraulic operating regimes).

The digital twin (Figure 60) reproduces the key transport phenomena governing EKRT performance in saturated porous media, namely ion electromigration, electro-osmotic pore fluid flow, and coupled mass transfer processes, in accordance with the fundamental electrokinetic principles underlying the technology.

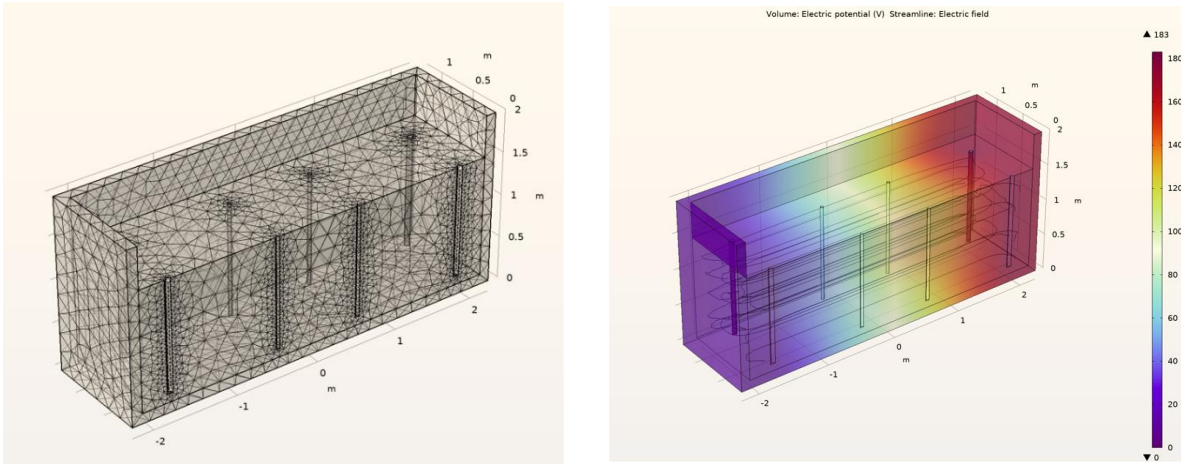

Figure 60: Sketch of digital twin showing the computational grid and the map of electrical potential in the system

The model solves the steady-state current continuity equation to determine the electric potential distribution within the soil domain. Fluid flow is described by combining Darcy flow with electro-osmotic contributions. Species transport is modeled using a Nernst-Planck framework, accounting for diffusion, electromigration, and advective fluxes. Mercury release from the solid phase is represented by a first-order desorption term calibrated against available laboratory data, thereby enabling simulation of mass transfer from the solid matrix to the pore solution.

Model input properties (e.g., porosity, electrical resistivity, and target moisture/saturation conditions) were derived from site-specific soil characterization and bench-scale testing. In particular, the electrical resistivity of the saturated-soil was estimated at approximately 9 Ω·m based on controlled cell measurements.

The digital twin replicates the pilot's containerized on-site configuration, featuring opposing banks of Ti-MMO electrodes installed in perforated wells to promote a broadly homogeneous electric field within the treated volume. Safety and operability constraints were explicitly incorporated into the model, including a step-voltage criterion (< 50 V m^{-1}) to limit the applied potential gradient.

In the baseline scenario, an imposed potential difference of approximately 180 V produces simulated currents on the order of ~5 A, consistent with the measured soil resistivity. Using an electric field threshold of $E \geq 30$ V·m-1 to define effective treatment conditions, the model estimates an effective treatment volume of approximately 86%.

Model outputs include electric-field distribution maps and effective-volume estimates, quantification of the relative contributions of hydraulic and electro-osmotic components to the total convective flux, ion-specific

electromigration velocities, and indicative mercury removal trajectories under different operating regimes. These simulations support pilot-scale decision-making (such as optimization of applied voltage, electrode spacing, and electrolyte management) and provide a contingency analytical layer to complement field measurements.

Current model predictions are preliminary and are conditional upon (i) calibration of desorption kinetics using pilot-specific chemistry data, and (ii) consolidation and quality control of field monitoring data for validation. Accordingly, time-to-target estimates are presented only as indicative trends pending full integration of pilot data. Future work will incorporate monitored currents, applied voltages, electrolyte chemistry, and concentration profiles to refine kinetic parameters and update performance projections.

4.7.8 Main conclusions of the activity

The pilot-scale electrokinetic remediation system successfully replicated laboratory configurations under real-scale conditions to treat mercury-contaminated soil. The setup enabled effective mobilization and removal of mercury through controlled electric fields, electrolyte recirculation, and pH management. Although operational challenges such as hydraulic line deposits and system instability emerged at higher current intensities, the process achieved measurable mercury removal. Notably, the estimated amount of mercury extracted exceeded the theoretically removable fraction determined by soil speciation analysis, likely due to soil heterogeneity or partial mobilization of previously classified non-removable species. Overall, the results demonstrate the technical feasibility of the pilot system while highlighting operational factors that influence process efficiency and performance.

In parallel with the pilot deployment, a physics-based digital twin was developed to enhance operational resilience and support decision-making through scenario analysis. The model reproduces the key electrokinetic transport mechanisms governing EKRT performance—electric potential distribution, coupled hydraulic and electro-osmotic flow, multi-species transport, and mercury desorption—using site-specific parameters and safety constraints consistent with the pilot configuration. Baseline simulations indicate technically feasible operating conditions, with effective treatment volumes reaching approximately 86% under defined electric field thresholds. While current predictions remain preliminary pending full calibration and validation with pilot data, the digital twin provides a robust analytical framework to optimize operating conditions, interpret field results, and refine performance projections as additional monitoring data become available.

5. Conclusions

In light of the results presented in Chapter 4, "Assessment of Remediation Methodologies Performance", the activities carried out within Task 4.51 enabled the development of a comprehensive, multidisciplinary, and experimentally validated framework for evaluating the potential, limitations, and optimal operational conditions of advanced physical-chemical, electrochemical, and bio-electrochemical remediation technologies. The systematic assessment of performance across different case studies has clearly demonstrated that the effectiveness of a remediation strategy cannot be measured solely in terms of contaminant removal efficiency. Instead, it must incorporate a broader set of criteria, including environmental sustainability, potential secondary impacts (such as residual phytotoxicity or unintended mobilization of contaminants), compatibility with the intended post-remediation land or water use, operational robustness, and scalability from laboratory to pilot and full scale. This integrated perspective has been a guiding principle throughout the activities described in this Deliverable and constitutes a key outcome of the work performed.

With specific reference to hydrocarbon-contaminated soils and marine sediments, the experimental investigations have confirmed that surfactant-enhanced soil flushing significantly improves the removal of total petroleum hydrocarbons (TPHs) compared to water flushing alone. Both anionic and non-ionic surfactants demonstrated the ability to increase contaminant solubilization and mobilization, although with markedly different behaviors depending on concentration, flow rate, and contact time. The conclusions drawn from the individual studies highlighted the existence of optimal operational windows: increasing surfactant concentration does not necessarily lead to proportional improvements in removal efficiency, and in some cases may even reduce performance due to micellar competition phenomena or changes in interfacial interactions. Furthermore, the interaction between hydraulic conditions and surfactant chemistry proved to be critical, with certain systems benefiting from higher leaching effects, while others showed stronger dependence on extended contact time.

Equally important were the findings related to residual phytotoxicity. Germination index tests and pot-scale cultivation of Vicia faba clearly demonstrated that remediation efficiency must be evaluated in conjunction with ecotoxicological compatibility. While significant reductions in TPH concentrations were achieved, the persistence of certain surfactants—particularly anionic formulations—was associated with adverse effects on seed germination and plant growth. Conversely, non-ionic surfactants showed lower phytotoxic impact and, in some cases, even enhanced germination performance. These results underline the necessity of integrating ecotoxicological indicators into the assessment of remediation performance, especially in scenarios where treated soils are intended for agricultural reuse. Future activities should therefore focus on the development and testing of low-impact or bio-based surfactants, as well as on combined remediation approaches capable of mitigating residual toxicity while maintaining high contaminant removal efficiency.

The experimental campaigns devoted to chemical oxidation processes, particularly those employing potassium ferrate as an innovative oxidizing agent, demonstrated promising degradation efficiencies for petroleum hydrocarbons in both soils and sediments. Comparative analyses with conventional oxidants confirmed the potential of ferrate-based treatments, while also emphasizing the importance of dosage optimization, reaction sequencing (especially when combined with surfactants), and matrix-specific characteristics. The conclusions indicate that the performance of advanced oxidation processes is strongly influenced by soil composition, organic matter content, and contaminant distribution. Consequently, future developments should include in-depth mechanistic investigations, kinetic modelling, and validation at pilot and pre-industrial scale to assess long-term stability, by-product formation, and operational feasibility under real field conditions.

Significant advances were also achieved in the field of heavy metal removal and resource recovery through the development and testing of nanostructured cellulose-based materials, including silver-decorated nanofibers

and cellulose nanosponges. These materials exhibited high adsorption capacities, favorable kinetics, and, in some cases, enhanced selectivity toward specific metal ions. The experimental findings underscored the relevance of surface functionalization, pH control, and competitive ion effects in determining adsorption performance. In parallel, the development of adsorbent media based on extracellular polymeric substances (EPS) extracted from wastewater treatment sludge represented a notable example of circular economy application, transforming a waste-derived material into a value-added remediation product. The conclusions of these studies emphasize the need for further research on material regeneration, structural stability over multiple adsorption–desorption cycles, and long-term behavior in real wastewater matrices. Life cycle assessment (LCA) and techno-economic analysis will be essential to quantify the environmental and economic advantages of these innovative materials compared to conventional adsorbents.

In relation to phosphorus recovery and the removal of rare earth elements and organophosphorus pesticides from aqueous systems, the adsorption-based processes investigated demonstrated both contaminant reduction and potential resource valorization. The ability to recover phosphorus in forms potentially suitable for agricultural reuse aligns with European regulatory frameworks and sustainability goals. However, the results also indicate that adsorption performance is highly sensitive to pH, competing ions, and matrix complexity. Therefore, future activities should address process integration within existing wastewater treatment infrastructures, evaluation under continuous-flow conditions, and assessment of regulatory compliance for recovered products.

Electrochemical and bioelectrochemical systems applied to contaminated soils and wastewaters provided additional innovative perspectives. The experimental results confirmed the potential of microbial electrochemical technologies for the degradation of organic contaminants and the removal of microplastics, as well as the applicability of electrokinetic remediation for soils contaminated with heavy metals. In particular, electrokinetic treatments demonstrated that the spatial distribution of electric potential, ionic transport phenomena, and operational control of current density are key parameters governing contaminant migration and extraction efficiency. The integration of mathematical modeling and digital twin approaches allowed for improved interpretation of system behavior and offered valuable predictive capabilities. Future developments should therefore prioritize energy optimization, scaling-up validation, and the implementation of real-time monitoring and control systems to enhance operational reliability and cost-effectiveness.

Another innovative contribution of the activities described in this Deliverable concerns the development of supramolecular materials, non-canonical amino acids, and natural biopolymers for combined sensing and remediation applications. The studies demonstrated that such materials can act both as selective adsorbents and as responsive sensing platforms, opening new possibilities for integrated monitoring–remediation systems. The conclusions suggest that further research should focus on device miniaturization, stability in complex environmental matrices, long-term performance evaluation, and integration into distributed environmental monitoring networks.

Overall, the activities conducted within this Deliverable have validated, under laboratory and pilot-scale conditions, a broad portfolio of innovative remediation technologies targeting both organic and inorganic contaminants in soils, sediments, and water systems. A key overarching conclusion is that no single technology can be considered universally optimal. Instead, effective remediation requires site-specific, integrated strategies supported by thorough preliminary characterization, performance testing, and environmental impact assessment. The knowledge generated through these activities contributes directly to the objectives of enhancing environmental resilience and supporting climate adaptation strategies.

In view of the project's final phase and future post-project developments, several priority actions can be identified. First, the consolidation and standardization of the operational protocols developed during the experimental campaigns should be pursued, leading to the preparation of technical guidelines for practitioners

and stakeholders. Second, validation under real-case scenarios, in collaboration with industrial partners and environmental authorities, will be essential to demonstrate transferability and operational robustness. Third, comprehensive techno-economic and environmental comparative analyses should be carried out to support decision-making processes and facilitate technology selection based on sustainability criteria. Fourth, the continued development of modeling tools, digital twin platforms, and advanced monitoring systems will strengthen predictive capacity and optimize remediation performance. Finally, targeted dissemination and technology transfer activities should be promoted to ensure that the scientific advances achieved translate into practical, scalable solutions capable of addressing current and emerging contamination challenges.

Through this integrated approach, the results achieved within Work Package 4.5 provide not only scientific advancement but also a concrete foundation for the implementation of innovative, sustainable, and resilient remediation strategies, contributing meaningfully to the broader objectives of environmental protection and climate-responsive risk management.

6. References

Abdel-Mawgoud, A.M., Aboulwafa, M.M., Hassouna, N.A.H., 2009. Characterization of Rhamnolipid produced by pseudomonas aeruginosa isolate Bs20. Appl. Biochem. Biotechnol. 157, 329–345. doi:10.1007/s12010-008-8285-1.

Acosta-Rangel, A., Sánchez-Polo, M., Rozalen, M., Rivera-Utrilla, J., Polo, A.M.S., Berber-Mendoza, M. S., Lopez-Ramon, M.V., 2020. Oxidation of sulfonamides by ferrate (VI): Reaction kinetics, transformation byproducts and toxicity assessment, J. Environ Manage. 255, 109927, https://doi.org/10.1016/j.jenvman.2019.109927.

Ailijiang, N., Zhong, N., Zhou, X., Mamat, A., Chang, J., Cao, S., Hua, Z., Li, N. 2022. Levels, sources, and risk assessment of PAHs residues in soil and plants in urban parks of Northwest China. Nature. 12-21448. https://doi.org/10.1038/s41598-022-25879-8

Ali, A., Mannan, A., Hussain, I., Hussain, I., & Zia, M. (2018). Effective removal of metal ions from aquous solution by silver and zinc nanoparticles functionalized cellulose: Isotherm, kinetics and statistical supposition of process. Environmental Nanotechnology, Monitoring and Management, 9(November 2017), 1–11. https://doi.org/10.1016/j.enmm.2017.11.003

Ambaye, T., Vaccari, M., Prasad, S., Rtimi, S., 2021. Preparation, characterization and application of biosurfactant in various industries: A critical review on progress, challenges and perspectives. Environ. Technol. Innov. 24, 102090.

Ambaye, T.G., Formicola, F., Sbaffoni, S., Lima, A.T.M., Franzetti, A., Vaccari, M., 2024. Environmental and economic performance of chemical and biological processes for treating petroleum hydrocarbon-contaminated soil: An experimental study. J. Environ. Chem. Eng. 12, 113672. doi:10.1016/j.jece.2024.113672.APAT, 2004. Guida tecnica su metodi di analisi per il suolo e i siti contaminati – Utilizzo di indicatori biologici ed ecotossicologici. 72–81.

Ambaye, T.G., Formicola, F., Sbaffoni, S., Lima, A.T.M., Franzetti, A., Vaccari, M., 2024. Environmental and economic performance of chemical and biological processes for treating petroleum hydrocarbon-contaminated soil: An experimental study. J. Environ. Chem. Eng. 12, 113672. doi:10.1016/j.jece.2024.113672.

APAT, 2004. Guida tecnica su metodi di analisi per il suolo e i siti contaminati - Utilizzo di indicatori biologici ed ecotossicologici 72–81.

Avona, A., Capodici, M., Di Trapani, D., Giustra, M.G., Greco Lucchina, P., Lumia, L., Di Bella, G., Rossetti, S., Tonanzi, B., Viviani, G., 2022. Hydrocarbons removal from real marine sediments: Analysis of degradation pathways and microbial community development during bioslurry treatment. Sci. Total Environ. 838, 156458. https://doi.org/10.1016/j.scitotenv.2022.156458

Azevedo, M.A., Teixeira, J.A., Pastrana, L., Cerqueira, M.A., 2024. Rhamnolipids: A biosurfactant for the development of lipid-based nanosystems for food applications. Compr. Rev. Food Sci. Food Saf. 23, 1–21. doi:10.1111/1541-4337.13252.

Babaei, M., Copty, N.K., 2019. Numerical modelling of the impact of surfactant partitioning on surfactant-enhanced aquifer remediation. J. Contam. Hydrol. 221, 69–81. https://doi.org/10.1016/j.jconhyd.2019.01.004.

Barışçı, S., 2017. The disinfection and natural organic matter removal performance of electro-synthesized ferrate (VI). J. Water Process Eng. 20, 84–89. https://doi.org/10.1016/j.jwpe.2017.10.005.

Barışçı, S., 2017. The disinfection and natural organic matter removal performance of electro-synthesized ferrate (VI). J. Water Process Eng. 20, 84–89. https://doi.org/10.1016/j.jwpe.2017.10.005.

Befkadu, A.A., Chen, Q., 2018. Surfactant-Enhanced Soil Washing for Removal of Petroleum Hydrocarbons from Contaminated Soils: A Review. Pedosphere 28(3): 383–410. DOI:10.1016/S1002-0160(18)60027-X

Besha, A. T., Bekele, D. N., Naidu, R., Chadalavada, S., 2018. Recent advances in surfactant-enhanced in-situ chemical oxidation for the remediation of non-aqueous phase liquid contaminated soils and aquifers. Environ. Technol. Innov. 9, 303–322. https://doi.org/10.1016/j.eti.2017.08.004.
Besha, A. T., Bekele, D. N., Naidu, R., Chadalavada, S., 2018. Recent advances in surfactant-enhanced in-situ chemical oxidation for the remediation of non-aqueous phase liquid contaminated soils and aquifers. Environ. Technol. Innov. 9, 303–322. https://doi.org/10.1016/j.eti.2017.08.004.
Bolan, S., Padhye, L.P., Mulligan, C.N., Alonso, E.R., Saint-Fort, R., Jasemizad, T., Wang, C., Zhang, T., Rinklebe, J., Wang, H., 2023. Surfactant-enhanced mobilization of persistent organic pollutants: potential for soil and sediment remediation and unintended consequences. J. Hazard Mater. 443, 130189.

Boniardi, G., Turolla, A., Fiameni, L., Gelmi, E., Malpei, F., Bontempi, E., & Canziani, R. (2021). Assessment of a simple and replicable procedure for selective phosphorus recovery from sewage sludge ashes by wet chemical extraction and precipitation. Chemosphere, 285(November 2020), 131476. https://doi.org/10.1016/j.chemosphere.2021.131476

Boniardi, G., Volonterio, A., Canziani, R., Punta, C., Riva, L., & Turolla, A. (2024). Cellulose-based nanostructured aerogels for leachate decontamination: Towards sustainable phosphorus recovery from sewage sludge ash. Journal of Cleaner Production, 475. https://doi.org/10.1016/j.jclepro.2024.143638

Caetano, G., Machado, R. de M., Correia, M.J.N., Marrucho, I.M., 2024. Remediation of soils contaminated with total petroleum hydrocarbons through soil washing with surfactant solutions. Environ. Technol. (United Kingdom) 45, 2969–2982. doi:10.1080/09593330.2023.2198733.

Chen, G., Strevett, K.A., Vanegas, A., 2001. Napthalene, phenanthrene and surfactant biodegradation. Biodegradation 12, 433–442.

Chen, J., Fan, B., Li, J., Wang, X., Li, W., Cui, L., Liu, Z., 2020. Development of human health ambient water quality criteria of 12 polycyclic aromatic hydrocarbons (PAH) and risk assessment in China. Chemosphere 252, 126590. https://doi.org/10.1016/j.chemosphere.2020.126590

Chen, K., Li, F., Huang, H., 2017. Desorption of petroleum pollutants from soil in presence of surfactants. Environ. Protect. Chem. Indust. 37, 497–502. Chen, J., Fan, B., Li, J., Wang, X., Li, W., Cui, L., Liu, Z., 2020. Development of human health ambient water quality criteria of 12 polycyclic aromatic hydrocarbons (PAH) and risk assessment in China. Chemosphere 252, 126590. https://doi.org/10.1016/j.chemosphere.2020.126590.

Cheng, M., Zeng, G., Huang, D., Yang, C., Lai, C., Zhang, C., Liu, Y., 2017. Advantages and challenges of Tween 80 surfactant-enhanced technologies for the remediation of soils contaminated with hydrophobic organic compounds. Chem. Eng. J. 314, 98–113. https://doi.org/10.1016/j.cej.2016.12.13.

Corsi, I., Winther-Nielsen, M., Sethi, R., Punta, C., Della Torre, C., Libralato, G., Lofrano, G., Sabatini, L., Aiello, M., Fiordi, L., Cinuzzi, F., Caneschi, A., Pellegrini, D., & Buttino, I. (2018). Ecofriendly nanotechnologies and nanomaterials for environmental applications: Key issue and consensus recommendations for sustainable and ecosafe nanoremediation. Ecotoxicology and Environmental Safety, 154, 237–244. https://doi.org/10.1016/j.ecoenv.2018.02.037

Cui, J., Tang, Z., Lin, Q., Yang, L., Deng, Y., 2024. Interactions of ferrate(VI) and aquatic humic substances in water treatment. Science of the Total Environment 919, 170919. https://doi.org/10.1016/j.scitotenv.2024.170919

De Marines, F., Di Bella, G., Laudicina, V.A., Paliaga, S., Di Trapani, D., 2025. Remediation of a diesel contaminated soil by means of anionic and non-ionic surfactants: Effect on soil phosphorus availability and Vicia Faba L. growth. Sci. Total Environ. 958, 177999. https://doi.org/10.1016/j.scitotenv.2024.177999

Deng, Y., Jung, C., Liang, Y., Goodey, N., Waite, T.D., 2018. Ferrate(VI) decomposition in water in the absence and presence of natural organic matter (NOM). Chem. Eng. J. 334, 2335–2342. https://doi.org/10.1016/j.cej.2017.12.006.

Desmidt, E., Ghyselbrecht, K., Zhang, Y., Pinoy, L., Van Der Bruggen, B., Verstraete, W., Rabaey, K., & Meesschaert, B. (2015). Global phosphorus scarcity and full-scale P-recovery techniques: A review. Critical Reviews in Environmental Science and Technology, 45(4), 336–384. https://doi.org/10.1080/10643389.2013.866531

Di Trapani, D., De Marines, F., Greco Lucchina, P., Viviani, G., 2023. Surfactant-enhanced mobilization of hydrocarbons from soil: Comparison between anionic and nonionic surfactants in terms of remediation efficiency and residual phytotoxicity. Process Saf. Environ. Prot. 180, 1–9. https://doi.org/10.1016/j.psep.2023.09.071.

Eras-Muñoz, E., Farré, A., Sánchez, A., Font, X., Gea, T. (2022). Microbial biosurfactants: a review of recent environmental applications. Bioengineered, 13(5), 12365–12391. https://doi.org/10.1080/21655979.2022.2074621.

Esposito, M. C., Corsi, I., Russo, G. L., Punta, C., Tosti, E., & Gallo, A. (2021). The era of nanomaterials: A safe solution or a risk for marine environmental pollution? Biomolecules, 11(3), 1–25. https://doi.org/10.3390/biom11030441

Fang, G.D., Dionysiou, D.D., Zhou, D.M., Wang, Y., Zhu, X.D., Fan, J.X. Cang, L., Wang, Y.J., 2013. Transformation of polychlorinated biphenyls by persulfate at ambient temperature, Chemosphere 90, 1573–1580.

Felz, S., Al-Zuhairy, S., Aarstad, O. A., van Loosdrecht, M. C. M., & Lin, Y. (2016). Extraction of structural extracellular polymeric substances from aerobic granular sludge. Journal of Visualized Experiments, 115, e54534. https://doi.org/10.3791/54534

Feng, M., Cizmas, L., Wang, Z., Sharma, V.K., 2017. Synergistic effect of aqueous removal of fluoroquinolones by a combined use of peroxymonosulfate and ferrate(VI), Chemosphere 177, 144–148.

Feng, X., Liu, Y., Li, X., Liu, H., 2022. RSM, ANN-GA and ANN-PSO modeling of SDBS removal from greywater in rural areas via Fe2O3- coated volcanic rocks. RSC Adv. 12, 6265–6278. doi:10.1039/d1ra09147f.

Fiol, N., Vásquez, M. G., Pereira, M., Tarrés, Q., Mutjé, P., & Delgado-Aguilar, M. (2019). TEMPO-oxidized cellulose nanofibers as potential Cu(II) adsorbent for wastewater treatment. Cellulose, 26(2), 903–916. https://doi.org/10.1007/s10570-018-2106-7

Fiorati, A., Grassi, G., Graziano, A., Liberatori, G., Pastori, N., Melone, L., Bonciani, L., Pontorno, L., Punta, C., & Corsi, I. (2020). Eco-design of nanostructured cellulose sponges for sea-water decontamination from heavy metal ions. Journal of Cleaner Production, 246, 119009. https://doi.org/10.1016/j.jclepro.2019.119009

Flemming, H. C., & Wingender, J. (2010). The biofilm matrix. Nature Reviews Microbiology, 8(9), 623–633. https://doi.org/10.1038/nrmicro2415

Garon, D., Krivobok,S., Wouessidjewe,D., Seigle-Murandi,F., 2002. Influence of surfactants on solubilization and fungal degradation of fluorene. Chemosphere, 47, pp. 303-309

Gautam, P., Bajagain, R., Jeong, S.W., 2020. Combined effects of soil particle size with washing time and soil-to-water ratio on removal of total petroleum hydrocarbon from fuel contaminated soil. Chemosphere 250, 126206.

Grasso, D., Subramaniam, K., Pignatello, J.J., Yang, Y., Ratté, D., 2001. Micellar desorption of polynuclear aromatic hydrocarbons from contaminated soil. Colloids Surfaces A Physicochem. Eng. Asp. 194, 65–74. https://doi.org/10.1016/S0927-7757(01)00800-7

Guigue, J. Lévêque, J., Mathieu, O., Schmitt-Kopplin, P., Lucio, M., Arrouays, D., Jolivet, C., Dequiedt, S., Chemidlin Prévost-Bouré, N., Ranjard, L., 2015. Water-extractable organic matter linked to soil physico-chemistry andmicrobiology at the regional scale. Soil Biol. Biochem., 84, pp. 158-167. https://doi.org/10.1016/j.soilbio.2015.02.016

Guo, H., Liu, Z., Yang, S., Sun, C., 2009. The feasibility of enhanced soil washing of pnitrochlorobenzene (pNCB) with SDBS/Tween 80 mixed surfactants, J. Hazard. Mater. 170, 1236–1241. https://doi:10.1016/j.jhazmat.2009.05.101

Han, Q., Wang, H., Dong, W., Liu, T., Yin, Y., Fan, H., 2015. Degradation of bisphenol A by ferrate(VI) oxidation: kinetics, products and toxicity assessment, Chem. Eng. J. 262, 34–40

Han, W., Tan, J., Peng, L., Liu, L., Zhou, X., Zhang, W., & Shi, B., 2019. Ecotoxicity and micellization behavior of anionic surfactant sodium dodecylbenzene sulfonate (SDBS) and its mixtures with nonionic surfactant fatty alcohol-polyoxyethylene ether (AEO). Aquatic toxicology, 216, 105313. https://doi.org/10.1016/j.aquatox.2019.105313

Herzog, B.M., Kleinknecht, S.M., Haslauer, C.P., Klaas, N., 2023. Experimental upscaling analyses for a surfactant-enhanced in-situ chemical oxidation (S-ISCO) remediation design. J. Contam. Hydrol. 258, 104230. https://doi.org/10.1016/j.jconhyd.2023.104230.

Huang, Z., Chen, Q., Yao, Y., Chen, Z., Zhou, J., 2021. Micro-bubbles enhanced removal of diesel oil from the contaminated soil in washing/flushing with surfactant and additives. Journal of Environmental Management 290, 112570. https://doi.org/10.1016/j.jenvman.2021.112570.

Huo, L., Liu, G., Yang, X., Ahmad, Z., Zhong, H., 2020. Surfactant-enhanced aquifer remediation: mechanisms, influences, limitations and the countermeasures. Chemosphere 252, 126620. https://doi.org/10.1016/j.chemosphere.2020.126620.

Islam, M.N.; Jung, S.K.; Jung, H.Y., Park, J.H., 2017. The feasibility of recovering oil from contaminatedsoil at petroleum oil spill site using a subcriticalwater extraction technology. Process Saf. Environ. Prot. 111, 52–59.

ISO 16703:2004. Soil quality — Determination of content of hydrocarbon in the range C10 to C40 by gas chromatography.

ISPRA, 2011. Procedura per l'analisi degli idrocarburi >C12 in suoli contaminati - Manuali e Linee Guida 75/11.

ITRC. Petroleum Vapor Intrusion: Fundamentals of Screening, Investigation, and Management; Interstate Technology and Regulatory Council, Vapor Intrusion Team: Washington, DC, USA, 2014.

Ji, W., Khalil, C.A., Parameswarappa Jayalakshmamma, M., Zhao, L., Boufadel, M.C., 2021. Behavior of surfactants and surfactant blends in soils during remediation: A review. Environ. Chall.,100007. https://doi.org/10.1016/j.envc.2020.100007.

Johansson, C., Bataillard, P., Biache, C., Lorgeoux, C., Colombano, S., Joubert, A., Pigot, T., Faure, P., 2020. Ferrate VI oxidation of polycyclic aromatic compounds (PAHs and polar PACs) on DNAPL-spiked sand: degradation efficiency and oxygenated by-products formation compared to conventional oxidants. Environ. Sci. Pollut. Res. 27(1):704-716.

Johansson, C., Bataillard, P., Biache, C., Lorgeoux, C., Colombano, S., Joubert, A., Pigot, T., Faure, P., 2020. Ferrate VI oxidation of polycyclic aromatic compounds (PAHs and polar PACs) on DNAPL-spiked sand: degradation efficiency and oxygenated by-products formation compared to conventional oxidants. Environ. Sci. Pollut. Res. 27(1):704-716.

Jones Jr., J.B. and Case, V.W. 1990. Sampling, Handling, and Analyzing Plant Tissue Samples. In: R. L. Westerman, Ed., Soil Testing and Plant Analysis, Book Series 3, Soil Science Society of America, Madison, 1990, pp. 389-427.

Kalev, S. D., Toor, G. S. 2018. The composition of soils and sediments. In Green Chemistry: Inclusive Approaches to Sustainable Development pp. 339–357. https://doi.org/10.1016/B978-0-12-809270-5.00014-5.

Karthick, A., Roy, B., Chattopadhyay, P., 2019. A review on the application of chemical surfactant and surfactant foam for remediation of petroleum oil contaminated soil. J. Environ. Manage. 243, 187–205. https://doi.org/10.1016/j.jenvman.2019.04.092.

Kehrein, P., Van Loosdrecht, M., Osseweijer, P., Garfí, M., Dewulf, J., & Posada, J. (2020). A critical review of resource recovery from municipal wastewater treatment plants-market supply potentials, technologies and bottlenecks. Environmental Science: Water Research and Technology, 6(4), 877–910. https://doi.org/10.1039/c9ew00905a

Kongsuwan, A., Patnukao, P., & Pavasant, P. (2009). Binary component sorption of Cu(II) and Pb(II) with activated carbon from Eucalyptus camaldulensis Dehn bark. Journal of Industrial and Engineering Chemistry, 15(4), 465–470. https://doi.org/10.1016/j.jiec.2009.02.002

Kopanichuk, I, Vedemchuk, E, Koneva, A, Vanin, A, (2018). Structural Properties of Span 80/Tween 80 Reverse Micelles by Molecular Dynamics Simulations. The Journal of Physical Chemistry B, 122 (33), 8047–8055.

Kumar, M., Bolan, N.S., Hoang, S.A., Sawarkar, A.D., Jasemizad, T., Gao, B., Keerthanan, S., Singh, L., Kumar, S., Vithanage, M., Li, Y., Zhang, M., Kirkham, M.B., Vinu, A., Rinklebe, J., 2021. Remediation of soils and sediments polluted with polycyclic aromatic hydrocarbons: To immobilize, mobilize, or degrade? J. Hazard. Mater. 420. https://doi.org/10.1016/j.jhazmat.2021.126534.

Kumar, M., Bolan, N.S., Jasemizad, T., Padhye, L.P., Sridharan, S., Singh, L., Bolan, S. O'Connor, J., Zhao, H., Shaheen, S.M., Song, H., Kadambot, H.M.S., Wang, H., Kirkham, M.B., Rinklebe, J., 2022. Mobilization of contaminants: Potential for soil remediation and unintended consequences. Sci. Total Environ. 839, 156373. http://dx.doi.org/10.1016/j.scitotenv.2022.156373.

Lai, C.C., Huang, Y.C., Wei, Y.H., Chang, J.S., 2009. Biosurfactant-enhanced removal of total petroleum hydrocarbons from contaminated soil. J. Hazard. Mater. 167, 609–614. doi:10.1016/j.jhazmat.2009.01.017.

Li, W. W., & Yu, H. Q. (2014). Insight into the roles of microbial extracellular polymer substances in metal biosorption. Bioresource Technology, 160, 15–23. https://doi.org/10.1016/j.biortech.2013.11.074

Li, Y., Liao, X., Huling, S. G., Xue, T., Liu, Q., Cao, H., & Lin, Q., 2019. The combined effects of surfactant solubilization and chemical oxidation on the removal of polycyclic aromatic hydrocarbon from soil. Science of the total environment, 647, 1106–1112. https://doi.org/10.1016/j.scitotenv.2018.07.420

Liu, J., Zhao, L., Liu, Q., Li, J., Qiao, Z., Sun, P., Yang, Y., 2021. A critical review on soil washing during soil remediation for heavy metals and organic pollutants. Int. J. Environ. Sci. Technol. 19, 601–624.

Liu, J.W., Wei, K.H., Xu, S.W., Cui, J., Ma, J., Xiao, X.L., Xi, B.D., He, X.S., 2021. Surfactant-enhanced remediation of oil-contaminated soil and groundwater: A review. Sci. Total Environ. 756

Liu, J.W., Wei, K.H., Xu, S.W., Cui, J., Ma, J., Xiao, X.L., Xi, B.D., He, X.S., 2021. Surfactant-enhanced remediation of oil-contaminated soil and groundwater: A review. Science of The Total Environment. 756, 144142. https://doi.org/10.1016/j.scitotenv.2020.144142.

Liu, M., Wu, N., Tian, B., Zhou, D., Yan, C., Huo, Z., Qu, R., 2022. Experimental and theoretical study on the degradation of Benzophenone-1 by Ferrate (VI): new insights into the oxidation mechanism. J. Hazard Mater. 425, 127877. https://doi.org/10.1016/j.jhazmat.2021.127877.

Luo, M., Zhou, H., Zhou, P., Lai, L., Liu, W., Ao, Z., Yao, G., Zhang, H., Lai, B., 2021. Insights into the role of in-situ and ex-situ hydrogen peroxide for enhanced ferrate (VI) towards oxidation of organic contaminants, Water Res. 203, 117548, https://doi.org/10.1016/j.watres.2021.117548.

Ma, M., Li, Junjian, Hu, J., Li, Jiamu, Dong, L., Ding, J., Jiang, H., 2024. Study on the differences in microscopic oil displacement effects and action mechanisms of different Rhamnolipid systems. Phys. fluids 36, 112029.

Mao, X., Jiang, R., Xiao, W., Yu, J., 2015. Use of surfactants for the remediation of contaminated soils: a review. J. Hazard Mater. 285, 419-435.

Masoudian Z, Salehi-Lisar SY, Norastehnia A., 2020. Phytoremediationpotential of Azolla filiculoides for sodium dodecyl benzene sulfonate(SDBS) surfactant considering some physiological responses, ef-fects of operational parameters and biodegradation of surfactant.Environ Sci Pollut Res 27:20358–20369. https://doi.org/10.1007/s11356-020-08286-2

Medjor, W.O., Akpoveta, V.O., Egharevba, F., 2018. Kinetics and physicochemical studies of surfactant enhanced remediation of hydrocarbons contaminated groundwater. Egypt. J. Pet. 27, 169–176. https://doi.org/10.1016/j.ejpe.2017.02.005.

Melone, L., Rossi, B., Pastori, N., Panzeri, W., Mele, A., & Punta, C. (2015). TEMPO-Oxidized Cellulose Cross-Linked with Branched Polyethyleneimine: Nanostructured Adsorbent Sponges for Water Remediation. ChemPlusChem, 80(9), 1408–1415. https://doi.org/10.1002/cplu.201500145

Meric, D., Barbuto, S.M., Alshawabkeh, A.N., Shine, J.P., Sheahan, T.C., 2012. Effect of reac-tive core mat application on bioavailability of hydrophobic organic compounds. Sci. Total Environ. https://doi.org/10.1016/j.scitotenv.2012.01.042.

Mirzaee, E., Sartaj, M., (2022). The application of surfactant-enhanced soil washing process combined with adsorption using a recoverable magnetic granular activated carbon for remediation of PAH-contaminated soil. Environmental Advances, Volume 9, 100274.

Mohinuzzaman, M., Yuan, J., Yang, X., Senesi, N., Li, S. L., Ellam, R. M., Mostofa, K. M. G., Liu, C. Q., 2020. Insights into solubility of soil humic substances and their fluorescence characterisation in three characteristic soils. The Science of the total environment, 720, 137395. https://doi.org/10.1016/j.scitotenv.2020.137395.

Morin-Crini, N., Lichtfouse, E., Fourmentin, M., Ribeiro, A. R. L., Noutsopoulos, C., Mapelli, F., Fenyvesi, É., Vieira, M. G. A., Picos-Corrales, L. A., Moreno-Piraján, J. C., Giraldo, L., Sohajda, T., Huq, M. M., Soltan, J., Torri, G., Magureanu, M., Bradu, C., & Crini, G. (2022). Removal of emerging contaminants from wastewater using advanced treatments. A review. Environmental Chemistry Letters, 20, 1333–1375. https://doi.org/10.1007/s10311-021-01379-5

Moscatelli, G, Barbati, B, Lorini, L, Caiazzo, L, Chiavarini, S, Pezza, M, Bellagamba, M, Petrangeli Papini, M, 2024. Preliminary study for polyciclic aromatic hydrocarbons mobilization from contaminated marine sediment using synthetic and natural surfactants. Chemical Engineering Science 298, 120317.

Naidu, R., Biswas, B., Willett, I.R., Cribb, J., Kumar Singh, B., Paul Nathanail, C., Coulon, F., Semple, K.T., Jones, K.C., Barclay, A., Aitken, R.J., 2021. Chemical pollution: A growing peril and potential catastrophic risk to humanity. Environ. Int. 156, 106616.

Ni, H., Zhou, W., Zhu, L., 2014. Enhancing plant-microbe associated bioremediation of phenanthrene and pyrene contaminated soil by SDBS-Tween 80 mixed surfactants. J. Environ. Sci. (China) 26, 1071–1079. https://doi.org/10.1016/S1001-0742(13)60535-5.

Niu, M., Yin, Z., Wang, Q., Li, G., Guo, S., Li, B., 2020. Selection of cleansing agents for petroleum-contaminated soil and assessment of their efficiency. Chinese J. Ecol. 39, 2302–2308

Pagliaccia, B., Campo, R., Carretti, E., Severi, M., Lubello, C., & Lotti, T. (2024). Towards resource recovery-oriented solutions in agriculture exploiting structural extracellular polymeric substances (sEPS) extracted from aerobic granular sludge (AGS). Chemical Engineering Journal, 485, 149819. https://doi.org/10.1016/j.cej.2024.149819

Pagliaccia, B., Carretti, E., Severi, M., Berti, D., Lubello, C., & Lotti, T. (2022). Heavy metal biosorption by Extracellular Polymeric Substances (EPS) recovered from anammox granular sludge. Journal of Hazardous Materials, 424, 126661. https://doi.org/10.1016/j.jhazmat.2021.126661

Parekh P, Varade D, Parikh J, Bahadur P. 2011. Anioniccationic mixed surfactant systems: Micellar interaction of sodium dodecyl trioxyethylene sulfate with cationic gemini surfactants. Colloid Surf A Physicochem Eng Asp. 385: 111–120. https://doi.org/10.1016/j.colsurfa.2011.05.057.

Paria S, Khilar K C. 2004. A review on experimental studies of surfactant adsorption at the hydrophilic solid–water interface. Adv Colloid Interface Sci. 110: 75–95.

Paria, S., 2008. Surfactant-enhanced remediation of organic contaminated soil and water. Adv. Colloid Interface Sci. 138, 24–58. https://doi.org/10.1016/j.cis.2007.11.001.

Pekdemir, T., Çopur M., Urum, K., 2005. Emulsification of crude oil-water system using biosurfactant, Process Safety Environ. Prot. 83, (38–46.)

Penn, C.J., Camberato, J.J., 2019. A Critical Review on Soil Chemical Processes that Control How Soil pH Affects Phosphorus Availability to Plants. Agriculture, 9, 120. https://doi.org/10.3390/agriculture9060120.

Perinelli, D. R., Cespi, M., Lorusso, N., Palmieri, G. F., Bonacucina, G., Blasi, P., 2020. Surfactant Self-Assembling and Critical Micelle Concentration: One Approach Fits All? Langmuir, 36, 5745−5753.

Picone, M., Distefano, G. G., Marchetto, D., Russo, M., Volpi Ghirardini A., Spiking organic Picone chemicals onto sediments for ecotoxicological analyses: an overview of methods and procedures. Environmental Science and Pollution Research. Volume 29, pages 31002–31024, (2022).

Proietto, F., D'Agostino, F., Bonsignore, M., Del Core, M., Sprovieri, M., Galia, A., Scialdone, O., 2024. Electrochemical remediation of synthetic and real marine sediments contaminated by PAHs, Hg and As under low electric field values. Chemosphere 350, 141009. https://doi.org/10.1016/j.chemosphere.2023.141009.

Pronk, M., de Kreuk, M. K., de Bruin, B., Kamminga, P., Kleerebezem, R., & van Loosdrecht, M. C. M. (2015). Full scale performance of the aerobic granular sludge process for sewage treatment. Water Research, 84, 207–217. https://doi.org/10.1016/j.watres.2015.07.011

Qiu, Y., Xu, M., Sun, Z., & Li, H., 2019. Remediation of PAH-Contaminated Soil by Combining Surfactant Enhanced Soil Washing and Iron-Activated Persulfate Oxidation Process. International Journal of Environmental Research and Public Health, 16(3), 441. https://doi.org/10.3390/ijerph16030441

Rai, P.K., Lee, J., Kailasa, S.K., Kwon, E.E., Tang, Y.F., Ok, Y.S., Kim, K.H., 2018. A critical review of ferrate(VI)-based remediation of soil and groundwater. Environ. Res. 160, 420-448. http://dx.doi.org/10.1016/j.envres.2017.10.016.

Rajabi, H., Sharifipour, M., 2018. Geotechnical properties of hydrocarbon-contaminated soils: a comprehensive review. Bulletin of Engineering Geology and the Environment 78(5). DOI:10.1007/s10064-018-1343-1

Rajabi, H., Sharifipour, M., 2018. Geotechnical properties of hydrocarbon-contaminated soils: a comprehensive review. Bulletin of Engineering Geology and the Environment 78(5). DOI:10.1007/s10064-018-1343-1

Rasheed, A., Hussain, S., Mushtaq, W., Zubair, M., Siddique, K., Attia, K., Khan, N., Fiaz, S., Azeem, F., & Chen, Y. (2023). Application of silver nanoparticles synthesized through varying biogenic and chemical methods for wastewater treatment and health aspects. Environmental Science and Pollution Research, (0123456789). https://doi.org/10.1007/s11356-022-24761-4

Ritoré, E., Coquelet, B., Arnaiz, C. et al., 2022. Guidelines for surfactant selection to treat petroleum hydrocarbon-contaminated soils. Environ Sci Pollut Res 29, 7639–7651. https://doi.org/10.1007/s11356-021-15876-1

Ritoré, E., Morillo, J., Arnaiz, C., Coquele, B., Usero, J., 2023. Chemical oxidation of hydrocarbon-contaminated soil: oxidant comparison study and soil influencing factors. Environ Eng Res. 28(6): 220610. http://dx.doi.org/10.4491/eer.2022.610.

Riva, L., Dotti, A., Iucci, G., Venditti, I., Meneghini, C., Corsi, I., Khalakhan, I., Nicastro, G., Punta, C., & Battocchio, C. (2024). Silver Nanoparticles Supported onto TEMPO-Oxidized Cellulose Nanofibers for Promoting Cd2+ Cation Adsorption. ACS Applied Nano Materials, 7(2), 2401–2413. https://doi.org/10.1021/acsanm.3c06052

Riva, L., Pastori, N., Panozzo, A., Antonelli, M., & Punta, C. (2020). Nanostructured Cellulose-Based Sorbent Materials for Water Decontamination from Organic Dyes. Nanomaterials, 10(8), 1570. https://doi.org/10.3390/nano10081570

Rogers, B., Logan, B.E., 2000. Bacterial transport in NAPL-contaminated porous media. J. Environ. Eng. 126, 657-666. https://doi.org/10.1061/(ASCE)0733-9372(2000)126:7(657).

Rosen, M, Kunjappu, J, 2012. Surfactants and Interfacial Phenomena. Publisher: John Wiley & Sons, Inc. ISBN: 9780470541944.

Russo Tiesi, M., Di Bella, G., Licitra, E., Oleszczuk, P., Vinti, G., Di Trapani, D. 2025. Role of mixed surfactants for hydrocarbons removal from real marine sediments: Removal efficiency and residual phytotoxicity after sediment washing treatment. Journal of Environmental Chemical Engineering, 13(6), 119873. https://doi.org/10.1016/j.jece.2025.119873.

Sakhaei, Z., Riazi, M., 2022. In-situ petroleum hydrocarbons contaminated soils remediation by polymer enhanced surfactant flushing: Mechanistic investigation. Process Saf. Environ. Prot. 161, 758–770. https://doi.org/10.1016/j.psep.2022.03.086.

Salehian, E., Khodadadi A., Hosseini, B., 2012. Remediation of Diesel Contaminated Soils Using Surfactants: Column Study. American Journal of Environmental Science, 8 (4), 352-359.

Saxena, N., Islam, M.M., Baliyan, S., Sharma, D., 2023. A comprehensive review on removal of environmental pollutants using a surfactant-based remediation process. RSC Sustain. 1, 2148–2161. doi:10.1039/d2su00069e.

Seviour, T., Derlon, N., Dueholm, M. S., Flemming, H. C., Girbal-Neuhauser, E., Horn, H., Kjelleberg, S., van Loosdrecht, M. C. M., Lotti, T., Malpei, M. F., Nerenberg, R., Neu, T. R., Paul, E., Yu, H., & Lin, Y. (2019). Extracellular polymeric substances of biofilms: Suffering from an identity crisis. Water Research, 151, 1–7. https://doi.org/10.1016/j.watres.2018.11.020

Sharma, V.K., 2013. Ferrate (VI) and ferrate(V) oxidation of organic compounds: kinetics and mechanism, Coord. Chem. Rev. 257, 495–510, https://doi.org/10.1016/j.ccr.2012.04.014.

Sharma, V.K., 2013. Ferrate (VI) and ferrate(V) oxidation of organic compounds: kinetics and mechanism, Coord. Chem. Rev. 257, 495–510, https://doi.org/10.1016/j.ccr.2012.04.014.

Sharma, V.K., Feng, M., Dionysiou, D.D., Zhou, H.C., Jinadatha, C., Manoli, K., Smith, M.F., Luque, R., Ma, X., Huang, C.H., 2022. Reactive high-valent iron intermediates in enhancing treatment of water by ferrate, Environ. Sci. Technol. 56 (2022) 30–47. https://doi.org/10.1021/acs.est.1c04616.

Shih, Y.J., Wu, P.C., Chen, C.W., Chen, C.F., Dong, C. Di, 2020. Nonionic and anionic surfactant-washing of polycyclic aromatic hydrocarbons in estuarine sediments around an industrial harbor in southern Taiwan. Chemosphere 256, 127044.

Si, R., Pu, J., Luo, H., Wu, C., & Duan, G. (2022). Nanocellulose-Based Adsorbents for Heavy Metal Ion. Polymers, 14(24), 1–23. https://doi.org/10.3390/polym14245479

Singh, S.K., John, S., 2013. Surfactant-enhanced remediation of soils contaminated with petroleum hydrocarbons. Int. J. Environ. Waste Manag. 11, 178–192. https://doi. org/10.1504/IJEWM.2013.051843

Sirguey, C., de Souza e Silva, P.T., Schwartz, C., Simonnot, M.O., 2008. Impact of chemical oxidation on soil quality. Chemosphere. 72(2): 282-289. https://doi.org/10.1016/j.chemosphere.2008.01.027.

Smith, M.J., Flowers, T.H., Duncan, H.J., Alder, J., 2006. Effects of polycyclic aromatic hydrocarbons on germination and subsequent growth of grasses and legumes in freshly contaminated soil and soil with aged PAHs residues. Environ. Pollut. 141, 519–525. https://doi.org/10.1016/j.envpol.2005.08.061

Smith, R., Pollard, S.J.T., Weeks, J.M., Nathanail, C.P., 2005. Assessing significant harm to terrestrial ecosystems from contaminated land. Soil Use Menage, 21, 527–540. https://doi.org/10.1079/sum2005345

Sun, S., Jiang, J., Qiu, L., Pang, S., Li, J., Liu, C., Wang, L., Xue, M., Ma, J., 2019. Activation of ferrate by carbon nanotube for enhanced degradation of bromophenols: Kinetics, products, and involvement of Fe(V)/Fe(IV). Water Res. 156, 1–8. https://doi.org/10.1016/j.watres.2019.02.057

Sun, Y., Xu, Y., Zhou, Q., Wang, L., Lin, D., Liang, X., 2013. The potential of gibberellic acid 3 (GA 3) and Tween-80 induced phytoremediation of co-contamination of Cd and Benzo [a] pyrene (B [a] P) using Tagetes patula, J. Environ. Manage. 114, 202–208.

Touihri, M., Guesmi, F., Hannachi, C., Hamrouni, B., Sellaoui, L., Badawi, M., Poch, J., & Fiol, N. (2021). Single and simultaneous adsorption of Cr(VI) and Cu (II) on a novel Fe3O4/pine cones gel beads nanocomposite: Experiments, characterization and isotherms modeling. Chemical Engineering Journal, 416, 129101. https://doi.org/10.1016/j.cej.2021.129101

U.S. EPA. Provisional Peer-Reviewed Toxicity Values for Complex Mixtures of Aliphatic and Aromatic Hydrocarbons (various CASRNs); EPA/690/R-22/003F U.S. Environmental Protection Agency, Office of Underground Storage Tanks: Washington, DC, USA, 2022. Available online: https://www.epa.gov/pprtv (accessed on 21 July 2025)

U.S. EPA. Technical Guide for Addressing Petroleum Vapor Intrusion at Leaking Underground Storage Tank Sites; EPA 510-R-15-001; U.S. Environmental Protection Agency, Office of Underground Storage Tanks: Washington, DC, USA, 2015. Available online: http://www.epa.gov/oust/cat/pvi/pvi-guide-final-6-10-15.pdf (accessed on 27 May 2025).

UNI EN ISO 9377-2:2002, 2002. Qualità dell'acqua. Determinazione dell'indice di idrocarburi. Metodo mediante estrazione con solvente e gascromatografia 9377.

Urum, K., Pekdemir, T., 2004. Evaluation of biosurfactants for crude oil contaminated soil washing. Chemosphere 57, 1139–1150. doi:10.1016/j.chemosphere.2004.07.048

USEPA, 1988. Protocols for short term toxicity screening of hazardous waste sites. Office of Research and Development, Corvallis, OR: EPA 600-3-88-029

Villarreal-Reyes, C., Díaz de León-Martínez, L., Flores-Ramírez, R., González-Lara, F., Villarreal-Lucio, S., Vargas-Berrones, K.X. (2022). Ecotoxicological impacts caused by high demand surfactants in Latin America and a technological and innovative perspective for their substitution, Sci. Tot. Environ., 816, 151661. https://doi.org/10.1016/j.scitotenv.2021.151661.

Wang, D., Zeng, Z., Zhang, H., Zhang, J., Bai, R., 2022. How does pH influence ferrate(VI) oxidation of fluoroquinolone antibiotics? Chem. Eng. J. 431, 133381. https://doi.org/10.1016/j.cej.2021.133381

Wang, J., Wang, S., 2020. Reactive species in advanced oxidation processes: Formation, identification and reaction mechanism, Chem. Eng. J. 401, 126158. https://doi. org/10.1016/j.cej.2020.126158.

Wei, D., Li, M., Wang, X., Han, F., Li, L., Guo, J., Ai, L., Fang, L., Liu, L., Du, B., & Wei, Q. (2016). Extracellular polymeric substances for Zn (II) binding during its sorption process onto aerobic granular sludge. Journal of Hazardous Materials, 301, 407–415. https://doi.org/10.1016/j.jhazmat.2015.09.018

Wei, K. H., Ma, J., Xi, B. D., Yu, M. D., Cui, J., Chen, B. L., Li, Y., Gu, Q. B., & He, X. S., 2022. Recent progress on in-situ chemical oxidation for the remediation of petroleum contaminated soil and groundwater. Journal of hazardous materials, 432, 128738. https://doi.org/10.1016/j.jhazmat.2022.128738

Wu, L., Liu, Y., Wang, X., Li, M., Li, J., Zhang, X., Gao, D., Li, H., 2024. Recognizing Functional Groups of MES/APG Mixed Surfactants for Enhanced Solubilization toward Benzo[a]pyrene. Environ. Sci. Technol. 58, 8565–8575. doi:10.1021/acs.est.3c10633.

Xu, J.C., Yang, L.H., Yuan, J.X., Li, S.Q., Peng, K.M., Lu, L.J., Huang, X.F., Liu, J.,2022. Coupling surfactants with ISCO for remediating of NAPLs: Recent progress and application challenges. Chemosphere. https://doi.org/10.1016/j.chemosphere.2022.135004.

Yan, G., Ma, W., Chen, C., Wang, Q., Guo, S., Ma, J., 2016. Combinations of Surfactant Flushing and Bioremediation for Removing Fuel Hydrocarbons from Contaminated Soils. Clean - Soil, Air, Water 44, 984–991. https://doi.org/10.1002/clen.201500571.

Yang K, Zhu L, Xing B. 2006. Enhanced soil washing of phenanthrene by mixed solutions of TX100 and SDBS. Environ Sci Technol. 40: 4274–4280.

Yen, C.H., Chen, K.F., Kao, C.M., Liang, S.H., Chen, T.Y., 2011. Application of persulfate to remediate petroleum hydrocarbon-contaminated soil: Feasibility and comparison with common oxidants. J. Hazard. Mater.186:2097–2102. https://doi.org/10.1016/j.jhazmat.2010.12.129

Yu, H., Zheng, L., Zhang, T., Ren, J., Cheng, W., Zhang, L., & Meng, P. (2021). Adsorption behavior of Cd (II) on TEMPO-oxidized cellulose in inorganic/ organic complex systems. Environmental Research, 195(October 2020). https://doi.org/10.1016/j.envres.2021.110848

Zhang, D., Jiang, J., Shi, H., Lu. L., Zhang, M., Lin, J., Lu, T., Huang, J., Zhong, Z., Zhao, H., 2024. Nonionic surfactant Tween 80-facilitated bacterial transport in porous media: A nonmonotonic

concentration-dependent performance, mechanism, and machine learning prediction. Environmental Research, Volume 251, Part 2,118670.
Zhang, M., Duan, T., Luo, Y., Zhang, H., Li, W., Wang, X., Han, J., 2024. Impact mechanisms of various surfactants on the biodegradation of phenanthrene in soil: bioavailability and microbial community responses. Sci. Total Environ. 950, 175225. https://doi.org/10.1016/j.scitotenv.2024.175225.
Zhang, Y., Labianca, C., Chen, L., De Gisi, S., Notarnicola, M., Guo, B., Sun, J., Ding, S., Wang, L., 2021. Sustainable ex-situ remediation of contaminated sediment: A review. Environ. Pollut. 287, 117333.
Zhang, Y., Labianca, C., Chen, L., De Gisi, S., Notarnicola, M., Guo, B., Sun, J., Ding, S., Wang, L., 2021. Sustainable ex-situ remediation of contaminated sediment: A review. Environ. Pollut. 287, 117333.
Zhao B W, Zhu L Z, Li W, Chen B L. 2005. Solubilization and biodegradation of phenanthrene in mixed anionic–nonionic surfactant solutions. Chemosphere. 58: 33–40.
Zhao, B., Che, H., Wang, H., Xu, J., 2016. Column Flushing of Phenanthrene and Copper (II) Co-Contaminants from Sandy Soil Using Tween 80 and Citric Acid. Soil Sediment Contam. 25, 50–63. https://doi.org/10.1080/15320383.2016.1088507
Zhao, Y.S., Li, L.L., Su, Y., Qin, C.Y., 2014. Laboratory evaluation of the use of solvent extraction for separation of hydrophobic organic contaminants from surfactant solutions during surfactant-enhanced aquifer remediation. Sep. Purif. Technol. 127, 53–60. doi:10.1016/j.seppur.2014.02.034
Zhao, Z., Wang, F., Xiang, L. Liu, Y., Harindintwali, J.D., Bian, Y., Jiang, X., Naidu, R., 2025. Synergistic degradation of polycyclic aromatic hydrocarbons using ferrate (VI) and periodate: Efficiency and mechanisms. Chem. Eng. J. 504, 158838. https://doi.org/10.1016/j.cej.2024.158838
Zheng, G.Y., Ting, L.W., Li, Z., Zhong, Z.B., Zheng, Q.S., Wei, 2007. Surfactant enhanced phytoremediation of soils contaminated with hydrophobic organic contaminants: potential and assessment. Pedosphere, 17, pp. 409-418
Zhong, H., Zhang, H., Liu, Z.F., Yang, X., Brusseau, M.L., Zeng, G., 2016. Sub-CMC solubilization of dodecane by rhamnolipid in saturated porous media. Sci. Rep. 6, 33266. https://doi.org/10.1038/srep33266.
Zhou, Q, Rosen, M, 2003. Molecular Interactions of Surfactants in Mixed Monolayers at the Air/Aqueous Solution Interface and in Mixed Micelles in Aqueous Media: The Regular Solution Approach. Lagmuir 19 (11), 4555–4562.
Zhou, R., Qin, X., Peng, S., Deng, S., 2014. Total petroleum hydrocarbons and heavy metals in the surface sediment of Bohai Bay, China: long-term variations in pollution status and adverse biological risk. Mar. Pollut. Bull. 83, 290–297.
Zoghi, P., Mafigholami, R., (2023). Optimisation of soil washing method for removal of petroleum hydrocarbons from contaminated soil around oil storage tanks using response surface methodology. Scientific Reports 13, 15457. https://doi.org/10.1038/s41598-023-42777-9.
L. Boszke, A. Kowalski, A. Astel, A. Barański, B. Gworek, J. Siepak. Mercury mobility and bioavailability in soil from contaminated area, Environmental Geology, 55, 1075–1087 (2008); https://doi.org/10.1007/s00254-007-1056-4
L. Craba, C. Brunori, M. Galletti, C. Cremisini, R. Morabito. Comparison of three sequential extraction procedures (original and modified 3 steps BCR procedure) applied to sediments of different origin, Annali di Chimica, 94, 409–419 (2004); https://doi.org/10.1002/adic.200490050
EP 0578925 B1 (1998); F.R. Döring, N. Döring, Verfahren zur Beseitigung von Schadstoffen, insbesondere im Erdbodenbereich [Method for the removal of contaminants, in particular from soil]; https://worldwide.espacenet.com/publicationDetails/biblio?FT=D&date=19940119&CC=EP&NR=0578925A1
EP 1123755 B1 (2005); F.R. Döring, N. Döring, Verfahren zur Entfernung anorganischer Verbindungen aus einem Erdbodenbereich [Method for removing inorganic compounds from soil]; https://worldwide.espacenet.com/publicationDetails/biblio?FT=D&date=20010816&CC=EP&NR=1123

755A1D.B. Gent, R.M. Bricka, A.N. Alshawabkeh, S.L. Larson, G. Fabian, S. Granade, Bench- and field-scale evaluation of chromium and cadmium extraction by electrokinetics, Journal of Hazardous Materials, 110(1-3), 53–62 (2004); https://doi.org/10.1016/j.jhazmat.2004.02.036

T.F. Jenkins, M.E. Walsh, P.G. Thorne, S. Thiboutot, G. Ampleman, T.A. Ranney, C.L. Grant, 1997. Assessment of sampling error associated with collection and analysis of soil samples at a firing range contaminated with HMX. CRREL technical publication – Special Report 97-22; https://apps.dtic.mil/sti/pdfs/ADA330661.pdf

B.-K. Kim, K. Baek, S.-H. Ko, J.-W. Yang, Research and field experiences on electrokinetic remediation in South Korea, Separation and Purification Technology, 79(2), 116–123 (2011); https://doi.org/10.1016/j.seppur.2011.03.002

R. Lageman, M.S. Godshalk, Electro-bioreclamation: A combination of in situ remediation techniques proves successful at a site in Zeist, the Netherlands, Electrochimica Acta, 52(10), 3449–3453 (2007); https://doi.org/10.1016/j.electacta.2006.01.089

H.K. Okoro, O.S. Fatoki, F.A. Adekola, B.J. Ximba, R.G. Snyman. A review of sequential extraction procedures for heavy metals speciation in soil and sediments, Soil & Sediments, 1, 181 (2012); https://www.omicsonline.org/scientific-reports/2161-0525-SR181.pdf

I. Outola, K. Inn, R. Ford, S. Markham, P. Outola. Optimizing standard sequential extraction protocol with lake and ocean sediments, Journal of Radioanalytical and Nuclear Chemistry, 282, 321–327 (2009); https://doi.org/10.1007/s10967-009-0183-7

M.K. Schultz, W.C. Burnett, K.G.W. Inn, J.W.L. Thomas, Z. Lin. NIST speciation workshop, Journal of Research of the National Institute of Standards and Technology, 101, 707–715 (1996); https://doi.org/10.6028/jres.101.069

M.K. Schultz, W. Burnett, K.G.W. Inn, G. Smith. Geochemical partitioning of actinides using sequential chemical extractions: Comparison to stable elements, Journal of Radioanalytical and Nuclear Chemistry, 234, 251–256 (1998); https://link.springer.com/article/10.1007/BF02389780

A. Tessier, P.G.C. Campbell, M. Bisson. Sequential extraction procedure for the speciation of particulate trace metals, Analytical Chemistry, 51, 844–851 (1979); https://doi.org/10.1021/ac50043a017

US 6,193,867 B1 (2001); G. Duncan Hitchens, Management of soil conditions and electroosmotic flow in electrokinetic remediation; https://worldwide.espacenet.com/publicationDetails/biblio?FT=D&date=20010227&CC=US&NR=6193867B1

US EPA, 2006. Data Quality Assessment: statistical methods for practitioners. EPA QA/G-9S, EPA/240/B-06/003, US EPA, Office of Environmental Information, Washington DC; https://nepis.epa.gov/Exe/ZyPURL.cgi?Dockey=900B0D00.TXT

S.H. Ward, D.C. Fraser, Conduction of electricity in rocks, in “Mining Geophysics”, Part B, Vol. II (eds. DA Hanson et al.). Tulsa, OK, Chapter 3, pp. 197–223. Society of Exploration Geophysicists, 1967; https://doi.org/10.1190/1.9781560802716.ch3

J.K. Wittle, S. Pamukcu, D. Bowman, L.M. Zanko, F. Doering, Field studies on sediment remediation, in K.R. Reddy, C. Cameselle, Eds., “Electrochemical remediation technologies for polluted soils, sediments and groundwater”, Chapter 32, pp. 661–696. John Wiley & Sons, Inc., 2009; https://doi.org/10.1002/9780470523650.ch32